

**PREPARATION, CHARACTERIZATION OF
ENZYME IMMOBILIZED MEMBRANES AND
MODELING OF THEIR PERFORMANCES**

**A Thesis Submitted to
the Graduate School of Engineering and Sciences of
İzmir Institute of Technology
in Partial Fulfillment of the Requirements for the Degree of**

DOCTOR OF PHILOSOPHY

in Chemical Engineering

**by
Yılmaz YÜREKLİ**

**December 2010
İZMİR**

We approve the thesis of **Yılmaz YÜREKLİ**

Prof. Dr. Sacide ALSOY ALTINKAYA
Supervisor

Prof. Dr. Ahmet YEMENİCİOĞLU
Co-Supervisor

Assoc. Prof. Dr. Oğuz BAYRAKTAR
Committee Member

Assoc. Prof. Dr. Erol AKYILMAZ
Committee Member

Assist. Prof. Dr. Gülşah ŞANLI
Committee Member

Assist. Prof. Dr. Ekrem ÖZDEMİR
Committee Member

22 December 2010

Prof. Dr. Mehmet POLAT
Head of the Department of
Chemical Engineering

Prof. Dr. Sedat AKKURT
Dean of the Graduate School of
Engineering and Sciences

ACKNOWLEDGMENTS

Acknowledgements are always difficult task. The words sometimes can never express what is in your heart to the extend you really want. First and foremost, I am especially grateful to my advisor Prof. Dr. Sacide Alsoy Altinkaya, who first introduced me to the art of membrane. She has provided me with every possible opportunity to succeed as a graduate student and beyond. I express my deepest appreciate to her for providing me the facility of studying abroad in one of the important membrane research center for a six months period. During seven years of study, she has also exerted effort as me. She has become a mentor She is largely responsible for my growth and development as a researcher. Her creativity and enthusiasm during the study has excited and motivated me especially in experimental and modeling difficulties. Thank you very much for your guidance regarding in research area and life as well.

I want to thank my co-advisor, Prof. Dr. Ahmet Yemenicioğlu for his contributions to the study. I wish to express my gratitude to my committee members, Assist. Prof. Dr. Ekrem Özdemir, Assist. Prof. Dr. Gülşah Şanlı, Assoc. Prof. Dr. Oğuz Bayraktar and Assoc. Prof. Dr. Erol Akyılmaz, for their insightful comments and constructive criticism, which helped to improve the overall quality of my thesis.

I would like to thank to Scientific and Technical Research Council of Turkey (TUBITAK) and the Ministry of Foreign Affairs of the Republic of France for partial funding. The Gambro-Hospal, Lyon, France is gratefully acknowledged for kindly providing the AN69 and AN69-PEI membranes.

During my six month study in France, I met with lovely and friendly people in Institut Europeen des Membranes (IEM). I would like to thank Dr. Andre Deratani, Dr. Christophe Innocent not only for their helpful discussions but also for their sincerity and cheerfully. I wish to express my gratitude to Dr. Sadika Guedidi for her technical assistance during the lab experiences and for her friendship and hospitality. I am also thankful to all Tunisian, Algerian researchers in IEM.

I am also thankful to the members of our group, Filiz Yaşar Mahlıçlı, Metin Uz, Başak Pekşen for their valuable discussions during meeting seminars and their help in lab experiences. I would like to thank to my officemate, İlker Polatoğlu, for his valuable discussions. Special thanks to my best friend Levent Aydın in Mechanical Engineering Department. During writing codes of the model equations in Mathematica (throughout

nights), I can never forget his help and support and I am thankful to him for opening a door to a new life in the world. Countless thanks go to Prof. Dr. Naci Kalay and his wife Mrs. Şadiye Kalay for their endless support and encouragement.

Lastly, I am eternally grateful for the unconditionally support and encouragement of my parents. I wish to express my endless love to my wife, Hanife, my son, Ahmet and my daughter, Aleyna, for their patience and their trust.

ABSTRACT

PREPARATION, CHARACTERIZATION OF ENZYME IMMOBILIZED MEMBRANES AND MODELING OF THEIR PERFORMANCES

The objective of this thesis study is to prepare active and stable urease (URE) immobilized membranes for the efficient removal of urea and to predict the performances of these membranes under pressure. Two commercially available ultrafiltration membranes namely Poly (acrylonitrile-co-sodium methallyl sulfonate) copolymer (AN69) and polyethyleneimine (PEI) deposited AN69 membranes (AN69-PEI) were used as supporting materials on which urease is immobilized by means of physical adsorption using layer-by-layer self assembly method or chemical attachment using N-ethyl-N'-(3-dimethylaminopropyl) carbodiimide hydrochloride (EDC) and N-hydroxysuccinimide (NHS) coupling agents as a zero crosslinker. During physical immobilization (pH 7.4), the effect of polyelectrolyte type on the activity of immobilized urease was compared between PEI and chitosan (CHI) cationic polyelectrolytes where urease was located either on top of the polyelectrolyte layer (AN69-PEI-URE or AN69-CHI-URE) or between two polyelectrolyte layers in a sandwiched form (AN69-PEI-URE-PEI or AN69-CHI-URE-CHI). The results reveal that the amount of urease immobilized on AN69 membranes are similar and slightly higher than the amount adsorbed on the activated AN69 surface by chemical attachment (AN69-C-URE). The maximum reaction rate was observed with AN69-PEI-URE membrane while the maximum retained activity during storage time was determined with AN69-C-URE membrane. Under dynamic conditions, the hydraulic permeabilities of the commercial and urease immobilized membranes were found similar and the highest urea conversion was achieved with the AN69-PEI-URE-PEI membrane. At the end of 450 minutes of filtration under pressure, the catalytic activity of AN69-C-URE membrane was completely preserved. The mathematical model developed can correlate the experimental filtration data quite well.

ÖZET

ENZİM İMMOBİLİZE EDİLMİŞ MEMBRANLARIN HAZIRLANMASI, KARAKTERİZASYONU VE PERFORMANSLARININ MODELLENMESİ

Bu tezin amacı, ürenin etkili bir şekilde uzaklaştırılması için aktif ve kararlı üreaz (URE) immobilize edilmiş membranlar hazırlamak ve performanslarını basınç altında tahmin etmektir. Üreaz enziminin kimyasal (N-etil-N'-(3-dimetilaminopropil) karbodiimid hidroklorür (EDC) ve N-hidroksisukkinimid (NHS) bağlayıcı çifti yardımı ile) ve fiziksel (layer-by-layer self assembly metodu ile) immobilizasyonu için ticari olarak ultrafiltrasyon amaçlı kullanılan isimleri Poly (akrilonitrile-co-sodyum metalil sulfonat) kopolimeri (AN69) ve polietilenimine (PEI) kaplanmış AN69 olan iki membran kullanılmıştır. Fiziksel immobilizasyon yönteminde (pH 7.4) polielektrolit (PEI ve CHI) tiplerinin üreaz immobilizasyon aktivitesine etkisi, üreazın polielektrolit üzerine (AN69-PEI-URE veya AN69-CHI-URE) veya bunların arasına (AN69-PEI-URE-PEI veya AN69-CHI-URE-CHI) sandvic formda tutturularak hazırlanmasıyla incelenmiştir. Sonuçlar, AN69 membranlarına immobilize edilen üreaz miktarlarının benzer olduğunu ve kimyasal yöntemle immobilize edilmiş üreaz (AN69-C-URE) miktarına göre daha yüksek olduğunu göstermiştir. Maksimum reaksiyon hızı AN69-PEI-URE membranıyla elde edilirken, depolama süresi boyunca maksimum kalıntı aktivite AN69-C-URE membranıyla elde edilmiştir. Dinamik koşullarda, ticari ve üreaz immobilize edilmiş membranların hidrolik geçirgenlikleri benzer değerlerde bulunmuştur ve en yüksek üre dönüşümü AN69-PEI-URE-PEI membranıyla elde edilmiştir. 450 dakika basınç altındaki filtrasyon sonunda AN69-C-URE membranının katalitik aktivitesi tamamen korunmuştur. Geliştirilen matematiksel model deneysel filtrasyon verilerini oldukça iyi bir şekilde doğrulayabilir.

3.2. Enzyme Adsorption Kinetics	30
3.3. Mass Transfer Resistances During Biocatalytic Membrane Processes.....	32
3.4. Activation Energy of Biocatalytic Reaction	36
3.5. Deactivation Kinetics During Storage of Enzyme.....	37
 CHAPTER 4. MODELING OF UREASE IMMOBILIZED MEMBRANES	 38
4.1. Introduction.....	38
4.2. Theory	39
4.3. Solution of Model Equations	45
 CHAPTER 5. OBJECTIVE	 46
 CHAPTER 6. EXPERIMENTAL.....	 48
6.1. Materials	48
6.2. Methods	49
6.2.1. Preparation of Urease Immobilized Membranes Using Layer-by- Layer Deposition (Physical Immobilization).....	49
6.2.2. Preparation of Urease Immobilized Membranes Using EDC/NHS Coupling Agent for Covalent Bonding (Chemical Immobilization)	50
6.2.2.1. Hydrolyzation reaction on AN69 surface	50
6.2.2.2. Activation of hydrolyzed AN69 surface	51
6.2.2.3. Immobilization of Urease onto modified AN69 surface	51
6.2.3. Determination of Free and Immobilized Urease Activity	52
6.2.4. Determination of Optimum pH and Temperature of Free and Immobilized Urease	53
6.2.5. Determination of Kinetic Parameters of Free and Immobilized Urease	53
6.2.6. Determination of Storage Stabilities of Free and Immobilized Urease	54
6.2.7. Filtration Studies.....	54
 CHAPTER 7. RESULTS AND DISCUSSION.....	 56

7.1. Studies with Native Urease.....	56
7.1.1. Determination of the Effect of Phosphate Buffer Concentration on the Activity of Native Urease	56
7.1.2. Determination of pH-Activity Profile of the Native Urease.....	60
7.1.3. Determination of Temperature-Activity Profile of the Native Urease.....	60
7.1.4. Determination of Kinetic Parameters of Native Urease	61
7.1.5. Determination of Storage Stability of Native Urease	62
7.2. Studies with Immobilized Urease	63
7.2.1. Studies with Urease Immobilized Membrane Prepared by Physical Immobilization Using Layer-by-Layer Technique	63
7.2.1.1. Determination of immobilized amount of urease onto AN69 and AN69-PEI membranes	63
7.2.1.2. Determination of pH-activity profiles of the urease immobilized membranes.....	67
7.2.1.3. Determination of Temperature-Activity Profiles of the Urease Immobilized Membranes.....	69
7.2.1.4. Determination of kinetic parameters of the urease immobilized membranes.....	70
7.2.1.5. Determination of storage stabilities of the urease immobilized membranes.....	74
7.2.2. Studies With Urease Immobilized Membrane Prepared by Chemical Immobilization Using EDC/NHS Coupling Agent	75
7.2.2.1. Effect of buffer concentration and its pH on the membrane activity	75
7.2.2.2. Effect of Crosslinking Time on the Membrane Activity ...	76
7.2.2.3. Effect of EDC Concentration on the Membrane Activity .	77
7.2.2.4. Effect of urease concentration on the membrane activity..	77
7.2.2.5. Effect of immobilization time on the membrane activity ..	78
7.2.2.6. Determination of the surface density	79
7.2.2.7. Determination of the pH-activity curve	80
7.2.2.8. Determination of the temperature-activity profile	81
7.2.2.9. Determination of the kinetic parameters of the immobilized urease	82

7.2.2.10. Determination of the storage stabilities of the native and the immobilized forms of the urease	83
7.3. Filtration Results.....	84
7.3.1. Permeability Studies	84
7.3.2. Catalytic Activity Studies	88
7.4. Model Results	96
7.4.1. Model Validation with the Experimental Filtration Data	96
7.4.2. Model Predictions	99
 CHAPTER 8. CONCLUSION.....	 104
 REFERENCES	 106
 APPENDIX A. DIMENSIONALIZED MODEL EQUATIONS.....	 116

LIST OF FIGURES

<u>Figure</u>	<u>Page</u>
Figure 2.1. Schematic representation of a) conventional wastewater treatment, b) membrane bioreactor	11
Figure 2.2. Schematic illustration of enzyme plus substrate.....	13
Figure 2.3. The reaction steps of urease-catalyzed hydrolysis of urea	16
Figure 2.4. The structural subunits of plant, fungal and bacterial origins of ureases	17
Figure 2.5. Three-dimensional structure of <i>Bacillus pasteurii</i> urease (BPU) represented as ribbon diagram of the $(\alpha\beta\gamma)_3$ heterotrimer. (a) View down the crystallographic threefold axis; (b) view from the side. The green, blue and red ribbons represent, respectively, the α , β and γ subunits. The magenta spheres in the α subunits are the nickel ions of the active center	19
Figure 2.6. Chemical structure of urease.....	20
Figure 2.7. Enzyme immobilization techniques: (a) entrapment, (b) adsorption, (c) Layer-by-layer self assembly, and (d) covalent immobilization. The blue spheres represent enzyme molecules.....	22
Figure 2.8. LbL protocol: dipping in 1. polyanion solution, 2. rinsing solution, 3. polycation solution, 4. rinsing solution.....	26
Figure 2.9. Structures of chitin, chitosan and cellulose	28
Figure 2.10. Chemical structure of AN69 membrane	29
Figure 2.11. Representation of AN69 membrane	29
Figure 3.1. Schematic representation of enzyme adsorption process	31
Figure 3.2. Concentration profiles of substrate and products at interface and in the immobilized enzyme system as a consequence of partition and mass transfer limitations	32
Figure 3.3. The variation of substrate concentration through an enzymatic membrane under dynamic condition.....	35
Figure 4.1. Schematic diagram of an enzyme immobilized membrane with substrate concentration profile.....	40
Figure 4.2. Regular packing of enzyme molecules	44

Figure 4.3.	Schematic illustration of pore size calculation procedure for the enzyme layer. (Pore size of the layer is determined by subtracting the area of four quarter circles from the area of square. The pore size is regressed by fitting a circle into the remaining area).....	44
Figure 6.1.	Preparation of two kinds of reactive urease immobilized membranes; the one allows directly contact with the environment (AN69-PE-URE) and the other is in sandwiched form (AN69-PE-URE-PE)	50
Figure 6.2.	Chemical reaction schemes (hydrolyzation, activation and immobilization) for preparing urease immobilized AN69 membrane.....	51
Figure 6.3.	Experimental protocol for the filtration of urea through URE immobilized membranes by means of chemical and physical attachment.....	55
Figure 7.1.	The change in activity as a function of urea concentration. Symbols represent pH of the reaction mixture at constant buffer concentration of 0.01M. Symbols: (\diamond) pH 5, (\square) pH 6, (\triangle) pH 7, (\circ) pH 7.4, ($*$) pH 8, (+) pH 9.....	57
Figure 7.2.	The change in pH as a function of urea concentration. Here, pHs represents the solution pH measured after 30 min reaction. Symbols represent pH of the reaction mixture at constant buffer concentration of 0.01M. Symbols: (\diamond) pH 5, (\square) pH 6, (\triangle) pH 7, (\circ) pH 7.4, ($*$) pH 8, (+) pH 9.....	57
Figure 7.3.	Activity change for the native urease as a function urea concentrations. Buffer concentrations: (\diamond) 0.01 M, (\square) 0.02 M, (\triangle) 0.05 M, (\circ) 0.08 M, ($*$) 0.1 M, (+) 0.15 M. Reactions were carried out at pH 6, 37°C for 30 min with 3.47 μ g/ml urease	58
Figure 7.4.	The change in pH at the end of 30 min reaction as a function of urea concentrations. Buffer concentrations: (\diamond) 0.01 M, (\square) 0.02 M, (\triangle) 0.05 M, (\circ) 0.08 M, ($*$) 0.1 M, (+) 0.15M. Reactions were carried out at pH 6, 37°C for 30 min with 3.47 μ g/ml urease	59
Figure 7.5.	The change in ammonium concentration during 30 min reaction. Reaction conditions; urea concentration 10 mM, buffer concentration 50 mM.....	59

Figure 7.6.	pH-activity profile of the native urease during 30 min reaction. Reaction conditions; urea concentration 0.01M, buffer concentration 0.05 M	60
Figure 7.7.	Temperature-activity profile of the native urease during 30 min reaction. Reaction conditions; urea concentration 0.01M, buffer concentration 0.05 M.	61
Figure 7.8.	The change in reaction rate of soluble urease as a function of urea concentration.....	62
Figure 7.9.	Storage stability of native urease. Urease was stored in water at 4°C	63
Figure 7.10.	Mass uptake curves (a) for AN69-URE, (b) for AN69-PEI-URE membranes; symbols; (◆) 34.7 µg/ml; (□) 52.1 µg/ml; (Δ) 69.4 µg/ml; (○) 138.8 µg/ml urease solutions. Lines are corresponding fits using Equation 3.3	64
Figure 7.11.	Mass uptake curves for AN69-CHI-URE; experiment was carried out in 69.4 µg/mL urease solution. Line is the corresponding fit using Equation 3.3	65
Figure 7.12.	Equilibrium sorption isotherm for (◆) AN69-URE and (□) AN69-PEI-URE membranes.....	66
Figure 7.13.	The change in relative activities of urease immobilized membranes as a function of pH. Symbols; (◇) AN69-URE. (□) AN69-CHI-URE. (Δ) AN69-PEI-URE.....	69
Figure 7.14.	The change in relative activities of urease immobilized membranes as a function of temperature. Symbols; (◇) AN69-URE, (□) AN69-CHI-URE, (Δ) AN69-PEI-URE	70
Figure 7.15.	The change in reaction rate of urease immobilized membranes as a function of urea concentration. Symbols; (◇) AN69-URE. (□) AN69-CHI-URE. (Δ) AN69-PEI-URE.....	71
Figure 7.16.	Variation of effectiveness parameters as a function of Damköhler number for the urease immobilized membranes. (◆) AN69-URE, (□) AN69-PEI-URE, (Δ) AN69-CHI-URE, (○) AN69-PEI-URE-PEI, (◇) AN69-CHI-URE-CHI.....	73

Figure 7.17. Effectiveness factors for immobilized urease as a function of substrate concentrations. (◆) AN69-URE, (□) AN69-PEI-URE, (Δ) AN69-CHI-URE, (○) AN69-PEI-URE-PEI, (◇) AN69-CHI-URE-CHI.....	73
Figure 7.18. Storage stabilities of urease immobilized membranes. Symbols; (◇) AN69-URE. (□) AN69-CHI-URE. (Δ) AN69-PEI-URE. (○) AN69-PEI-URE-PEI. (★) AN69-CHI-URE-CHI.....	74
Figure 7.19. Effect of buffer concentration and its pH on the membrane activity.....	75
Figure 7.20. Effect of crosslinking time on the membrane activity.....	76
Figure 7.21. Effect of EDC concentration on the membrane activity.....	77
Figure 7.22. Effect of urease concentration on the membrane activity.....	78
Figure 7.23. Effect of immobilization time on the membrane activity.....	79
Figure 7.24. Adsorption kinetics of urease immobilized AN69 modified membrane.....	80
Figure 7.25. pH-activity profiles of native (◆) and immobilized form of the urease (◇) prepared with 30 min. of rinsing and (□) 2 days of rinsing.....	81
Figure 7.26. Optimum temperature for the native (◆) and immobilized form of the urease (◇) for 30 min. of rinsing and (□) 2 days of rinsing.....	81
Figure 7.27. Reaction rate of urease immobilized PAN membrane as a function of substrate concentration; (◇) measured after 30 min and (□) 2 days of rinsing.....	82
Figure 7.28. Storage stabilities of (□) native and (◇) immobilized urease by means of chemical attachment onto AN69 membrane after 2 days of rinsing. Points are experimental data and the lines represent the deactivation model using Equation 3.20 and 3.21 for the immobilized and free forms of urease.....	83
Figure 7.29. Comparison of the two water permeation experiment carried out during compaction steps using AN69-PEI membrane.....	84
Figure 7.30. The change in permeate volume collected during water permeation through AN69-PEI membrane carried out at 0.5, 1.0 and 1.5 bar transmembrane pressure.....	85

Figure 7.31.	The change in water flux as a function of transmembrane pressure for AN69-PEI membrane.....	86
Figure 7.32.	Hydraulic permeabilities of water, buffer and urea solutions through (□) AN69-PEI, (⊙)AN69-PEI-URE, (≡)AN69-PEI-URE-PEI	87
Figure 7.33.	Hydraulic permeabilities of water, buffer and urea solutions through modified AN69 membrane on which urease was chemically immobilized.....	87
Figure 7.34.	Ammonia formation through catalytic decomposition of urea by AN69-PEI-URE membrane. Feed solution concentrations are (◇) 0.5 mM, (□) 5.0 mM, (Δ) 10 mM, (○) 50 mM.....	88
Figure 7.35.	Ammonia formation through catalytic decomposition of urea by AN69-PEI-URE-PEI membrane. Feed solution concentrations are (◇) 0.5 mM, (□) 5.0 mM, (Δ) 10 mM, (○) 50 mM.	89
Figure 7.36.	Ammonia formation through catalytic decomposition of urea by modified AN69 membrane on which urease was chemically immobilized. Feed solution concentrations are (◇) 0.5 mM, (□) 5.0 mM, (Δ) 10 mM, (○) 50 mM	90
Figure 7.37.	Reaction rate of AN69-PEI-URE membrane as a function of substrate concentration. Transmembrane pressures are, (◇) 0.5 bar, (□) 1.0 bar, (Δ) 1.5 bar	92
Figure 7.38.	Reaction rate of AN69-PEI-URE-PEI membrane as a function of substrate concentration. Transmembrane pressures are, (◇) 0.5 bar, (□) 1.0 bar, (Δ) 1.5 bar	93
Figure 7.39.	Reaction rate of chemically immobilized urease as a function of substrate concentration. Transmembrane pressures are, (◇) 0.5 bar, (□) 1.0 bar, (Δ) 1.5 bar	93
Figure 7.40.	The change of urea conversion with the solution flux through AN69-PEI-URE membrane. Symbols are, (◇) 0.5, (□) 5, (Δ) 10 and (○) 50 mM.....	94
Figure 7.41.	The change of urea conversion with the solution flux through AN69-PEI-URE-PEI membrane. Symbols are, (◇) 0.5, (□) 5, (Δ) 10 and (○) 50 mM.....	95

Figure 7.42.	The change of urea conversion with the solution flux through modified AN69 membrane on which urease was chemically immobilized. Symbols are, (\diamond) 0.5, (\square) 5, (Δ) 10 and (\circ) 50 mM.....	95
Figure 7.43.	Percentage retained activity of the catalytic membranes at the end of 450 min of filtration process. ($\textcircled{\cdot}$) AN69-PEI-URE, (\equiv) AN69-PEI-URE-PEI, (\square) AN69-URE.....	96
Figure 7.44.	Comparison of experimental data with the model estimations. The data were collected at a) 0.7, b) 1.1 and c)1.4 bar. Points represent experimental data and lines represent theoretical result. Symbols represent the feed concentrations: (\diamond) 1mM, (\square) 2.5mM, (Δ) 5mM and (\circ) 10 mM.....	97
Figure 7.45.	The change in dimensionless urea concentrations through enzymatic membrane layers as a function of Peclet numbers (0.006, 0.008, 0.013 and 0.026).....	100
Figure 7.46.	The change in urea concentrations through enzymatic membrane layers with respect to λ^2 / θ (3, 6, 9 and 30).....	101
Figure 7.47.	Urea conversions with respect to time. Lines represent Peclet numbers as 0.006, 0.008, 0.013 and 0.026.....	102
Figure 7.48.	Comparison of the urea conversion with respect to Peclet number. Symbols denote λ^2 / θ as, (\blacklozenge) 3, (\square) 6, (Δ) 9 and (\diamond) 15	102
Figure 7.49.	Effectiveness factor as a function of λ^2 / θ compared with the variation of Peclet number. Symbols denote as, (\blacklozenge) 0.006, (\square) 0.008, (Δ) 0.013 and (\diamond) 0.026.....	103

LIST OF TABLES

<u>Table</u>	<u>Page</u>
Table 2.1. Structure and properties of amino acid side chains (Source: Ratner et al.1996)	14
Table 2.2. The amino acid composition of jack bean urease (Source: Takishima et al. 1988)	18
Table 7.1. Effect of immobilization concentrations on equilibrium adsorbed amount per membrane surface area and the overall reaction rate constant for both AN69 and AN69-PEI membranes	63
Table 7.2. Equilibrium adsorption, initial and specific activity values of AN69 and polyelectrolyte deposited AN69 membranes	67
Table 7.3. Kinetic parameters of urease immobilized membranes	71
Table 7.4. Conditions used for crosslinking reaction and urease immobilization	76
Table 7.5. The change in effectiveness factors with respect to substrate concentrations under three different pressures (0.5, 1.0 and 1.5 bars) for the membranes on which urease is immobilized by means of covalent bonding (AN69-URE) and by means of electrostatic forces in the case of AN69-PEI-URE and AN69-PEI-URE-PEI	91
Table 7.6. The change in Damköhler numbers with respect to substrate concentrations under three different pressures (0.5, 1.0 and 1.5 bars) for the membranes on which urease is immobilized by means of covalent bonding (AN69-URE) and by means of electrostatic forces in the case of AN69-PEI-URE and AN69-PEI-URE-PEI	91
Table 7.7. Kinetic parameters of urease immobilized AN69 membranes	94
Table 7.8. Parameters used for the correlation and prediction of the experimental data carried out at 0.7, 1.1 and 1.4 bar transmembrane pressures respectively.....	98
Table 7.9. Kinetic parameters estimated from the model correlation and predictions with the experimental data carried out at 0.7, 1.1 and 1.4 bar transmembrane pressures respectively	99

LIST OF SYMBOLS

N_A	Solute flux, kmol/m ² .s
K_c	Hindrance factor for convection, dimensionless
K_D	Hindrance factor for diffusion, dimensionless
J_v	Solute flux, m/s
C	Solute concentration, kmol/m ³
$D_{i,\infty}$	Brownian diffusion coefficient of solute, m ² /s
m	Membrane mass, kg
A	Membrane area, m ²
k_1, k_2	Mass transfer coefficients for the feed and permeate sides, m/s
r_i	Radius of i th element, m
Re	Reynolds number, dimensionless
Sc	Schmidt number, dimensionless
M_w	Molecular weight of water, kg/kmol
D_p	Propeller diameter, m
N	Rotational speed, rate/s
T	Temperature, K
c_g	Gel layer concentration, kmol/m ³
V_{\max}	Maximum reaction rate possible if every enzyme molecule is saturated with substrate, kmol/m ³ .s
K_m	Substrate concentration for which the observed reaction rate is half of V_{\max} , kmol/m ³
V_f, V_p	Feed and permeate volume, m ³
ρ_i	Density of i th element, kg/m ³
μ_w	Viscosity of water, cP
δ_i	Thickness of i th element, m
ε_i	Porosity of i th element, dimensionless
λ_i	Effective solute to pore size ratio, dimensionless

φ	Association factor, dimensionless
v_A	Molar volume of urea at its normal boiling point temperature m^3/kmol
Φ_i	Partition coefficient of i^{th} component, dimensionless
α	Device geometry, dimensionless

CHAPTER 1

INTRODUCTION

The removal of urea from aqueous solutions in various industries ranging from chemical, biomedical to food industries is a major problem due to increased environmental and health concern. By the increase in environmental and health concern, the level of urea in the effluents of urea producing industries and in municipal waste water is pulled down to 1-10 ppm. The content of urea in alcoholic beverages should be eliminated to prevent the formation of carcinogenic compounds [1]. For long term human space flights, recycling of wastewater which includes urea coming mainly from human urine is crucial. A quick removal of urea is required through filtration of blood during hemodialysis therapy in which 100-300 L of dialysate solution is consumed. To reduce the cost of the treatment, regeneration of dialysate solution by removing urea is necessary [1]. Not only the removal of urea is but also determination of its amount through a fast and reliable method is also important since its application area is tremendously growing especially in the manufacturing of resins glues, solvents and some medicines [2].

Commonly used approaches for the removal of urea are nonenzymatic urea hydrolysis which requires high temperatures and pressures and biological conversion of urea nitrogen to dinitrogen which suffers from instabilities of microbial bed. Hence, both methods have high operating costs [3]. Adsorption is not considered as an alternative removal method since urea does not show high affinity to common adsorbents [4]. Urea rejection by reverse osmosis membranes is also not efficient [5, 6]. An attractive, alternative removal method is based on the enzymatic hydrolysis of urea by urease.

Use of enzymes, as green catalysts, is one of the promising strategies for meeting the requirements of decreasing energy costs and increasing safety. Enzymes exhibit high level of catalytic efficiency and specificity under mild conditions of temperature, pressure and pH with similar reaction rates achieved by chemical catalysts at extreme conditions. The enzymatic reactions offer the potential to greatly reduce the environmental impact of existing ,chemical processes. Mostly enzymes are

biodegradable and generally the reaction occurs in water which is nontoxic. Since no waste products are generated during biocatalytic reactions, product purification is simple and such reactions are less polluting than chemical synthesis routes. Enzymes are specific to certain substrates, enables eliminating side-reactions, yielding one required end-product resulting lower manufacturing costs. Therefore the practical use of enzymes is being expanded in fields such as fine-chemical and pharmaceuticals synthesis, food processing and detergent applications, biosensors fabrication, bioremediation and protein digestion in proteomic analysis, as well as in conventional industrial processes and products. Besides these advantageous, their instability, short operational lifetimes and impossibility for reuse limit their wide range of applications. Enzyme immobilization onto or within solid support has been accepted as one of the most successful methods in eliminating the limitations of the free enzyme [7, 8]. Immobilization enables easy recovery of enzymes and hence prevents product contamination, allows repetitive use of enzymes, continuous operation of enzymatic process, and rapid termination of reactions.

Various supports are used for enzyme immobilization. Among them, membranes are commonly used which allow to load high amounts of enzymes and integrate catalytic reaction and separation. In general enzymes are immobilized onto/into the membrane by physical adsorption, entrapment and covalent bonding. Each method has its advantages and disadvantages. In physical immobilization, ionic forces or weak interactions e.g., hydrophobic interactions, hydrogen bonding, and Van der Waals forces play significant roles [9, 10] while, in chemical immobilization, covalent bonding between substrate and enzyme exists [11-13]. Although physical adsorption is simple, cheap, environmentally benign and effective, it is frequently reversible. In contrast, chemical immobilization is effective and durable but it is expensive and lowers the enzyme performance. There are many factors affecting the performance of an immobilized enzyme, such as membrane material, membrane structure, immobilization method as well as enzyme characteristics, enzyme loading and reaction conditions. Besides, surface properties of the membrane also play a significant role. The properties of support materials required for a suitable covalent binding of enzymes include hydrophilic nature, sufficient amount of chemically active sites, resistance to biodegradation and high chemical and thermal resistance. In this work, polyacrylonitrile based membrane one of the most important polymeric materials used in biomedical field [11] was used as a support since its surface can be easily tailored [12] making this

support especially attractive for immobilization.

Urease is a highly efficient enzyme which is specific for converting urea to ammonia and carbon dioxide. The hydrolysis reaction of urea by means of urease is 10^{14} fold higher than the rate of uncatalyzed hydrolysis elimination reaction. Studies on urease immobilized membranes are important, since immobilized urease can be used in biomedical applications for the removal of urea from blood, in blood detoxication or in the dialysate regeneration system, in food industry, in waste water treatment and in analytical applications as urea sensor [14, 15].

Recently, a simple method has been reported for the attachment of macromolecules by means of electrostatic attraction between macro-molecules and charges on the surface of a membrane [16]. In this method, the basic process involves alternately dipping of a charged substrate into aqueous solutions of an anionic and a cationic polyelectrolyte. During the dipping stage, adsorption of polyelectrolyte leads to a charge inversion of surface due to an overcompensation phenomenon that enables subsequent adsorption by the oppositely charged polyelectrolyte [17, 18]. A large variety of polymers such as synthetic polyelectrolytes, proteins and nucleic acids have been employed to assemble multilayers [19]. The LbL method has recently received much attention in immobilizing biomolecules especially for biosensor applications [20, 21] and biocatalysis [22]. In the case of covalent binding of enzyme, recently, a well known coupling reaction of N-ethyl-N'-(3-dimethylaminopropyl) carbodiimide (EDC) and N-hydroxysuccinimide (NHS) has been used to construct enzyme layer on the carboxyl or amino-terminated surface [23-25]. EDC/NHS coupling agent has been reported non-cytotoxic in vitro [23] and biocompatibility is observed in animal studies [24].

There are several environmental factors affecting enzyme performance among which, the surface properties of the support material, pH and temperature are outstanding. These variables not only affect enzyme activity but also enzyme stability. Enzyme stability is regarded as the capacity of the enzyme to retain its activity. Measuring the activities of the immobilized enzyme with respect to pH, temperature, storage and operational stabilities with their apparent kinetic parameters are mostly pronounced in literature [11, 26-28].

Enzyme immobilized membranes are generally prepared for both reaction and separation purposes either in tubular form especially for cross-flow mode or flat sheet used in dead-end mode. In both cases, the amount of adsorbed enzyme, reduction in

water permeability, operational stability and catalytic conversion of substrate under variable temperature and pH are significantly important. The adjustment of operating conditions (transmembrane pressure, feed velocity and stirring rate) is performed such that external or diffusional mass transfer resistance can be negligible [29-32]. During ultrafiltration processes, the process efficiency is determined by surface properties of the membrane (surface charge, hydrophobicity and roughness), characteristics of the solute (particle size and charge), solution chemistry (solution pH and ionic strength), and system hydrodynamics (feed velocity and operating pressure). Modeling the transport rates of solutes during ultrafiltration processes is important for the determination of the system efficiency. Model equations allow optimizing structural characteristics of the membrane and operational conditions.

In this study, urease immobilized membranes were prepared using two different techniques and they were characterized under static and dynamic conditions. Commercial membranes, AN69 and AN69-PEI were selected as support materials. In the first method, urease was immobilized by means of alternating layer-by-layer polyelectrolyte deposition technique which refers to ionic immobilization. In the second method, urease was immobilized onto modified surface of AN69 through covalent bonding using EDC/NHS as a crosslinker. For the modification, NaOH was used to create carboxylic groups which can be activated by EDC easily. The optimum conditions (pH and temperature) with their kinetic parameters of the two types of urease immobilized membranes were determined. In addition, their storage stabilities during long time were also observed. By using the optimum conditions established from the static characterizations, the performance of those membranes were determined under dynamic conditions using dead-end ultrafiltration module.

To define the filtration of a substrate solution through an urease immobilized membrane, a mathematical model was also developed. The effects of pore size, thickness of the membrane and the catalytic layer if enzyme is available on the surface of the membrane, types of enzyme immobilization and also the effects of transmembrane pressure and concentration polarization on the solute flux were predicted by coupling convective and diffusive transport as well as enzymatic reaction. The mathematical model developed was tested with the experimental filtration data.

In the second chapter of this thesis, the main sources of urea as a pollutant are given. The conventional techniques which are inefficient in reducing the amount of discharged urea below the safety level determined by Environmental Protection Agency

and enzymatic hydrolysis of urea with urease under mild reaction conditions are explained. The drawbacks of the native enzyme in the application and methods for solving those problems are mentioned. The advantageous of urease immobilized membranes including type of immobilizations and the necessary support materials for the decomposition of urea is presented.

In the third chapter, equations used for estimating some kinetic properties of enzyme immobilized membranes are given. The effects of external mass transfer resistances on the observed kinetic parameters are discussed.

The fourth chapter includes the mathematical model equations derived to predict the performances of the enzyme immobilized membranes under dynamic conditions.

In the fifth chapter, the detailed experimental methods for preparing urease immobilized membranes by means of alternating layer-by-layer polyelectrolyte deposition technique and covalent bonding are given. In addition, all the methods used for characterizing the prepared membranes are explained. Chapter seven includes all the results and discussion of the studies completed and finally Chapter eight gives the main conclusion.

CHAPTER 2

MAIN SOURCES OF UREA AS A TOXIC COMPOUND AND ITS REMOVAL BY UREASE HYDROLYSIS

2.1. Introduction

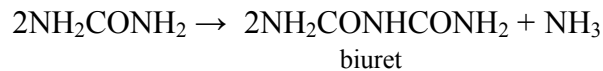
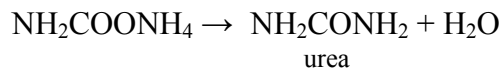
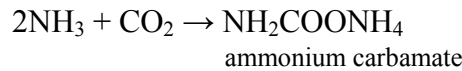
Urea is an important source of nitrogenous fertilizer containing 46.6 % nitrogen in its structure. It is an organic compound and synthesized in the body of many organisms as part of the urea cycle, either from the oxidation of amino acids or from ammonia. It is the first organic compound synthesized from inorganic material, cyanuric acid and ammonia by Wöhler in 1828 [30]. Since this invention, its production and consumption are in continuous rise and exceeds 100 million tones per year world wide, more than 90% of which is used as fertilizer [1]. The remaining part of urea is used for the manufacturing of resins, glues, solvents and some medicines [2]. In consumer products, urea is found in many liquid soaps, detergents and other cleaning products, and has been extensively used in the treatment of dry skin, both clinically and in cosmetics [2, 34]. Urea is also used as an animal-feed supplement. Although urea has generally low ecotoxicity to organisms, the indirect, longterm consequences of exposure to excessive levels of urea on ecosystems (eutrophication, groundwater pollution, soil acidification and ammonia emissions to air) are well documented [2] and hence effective removal or quantification of urea are important. Since, urea is mostly stable under normal conditions with a half life of 3.6 years, urease catalyzed hydrolysis reaction of urea into carbamate and ammonia is the most prominent alternative way. It is more economic and safe when urease is used in immobilized form.

In this chapter, the main sources of urea and its conventional removal processes from the industrial and municipal wastewater and its removal during hemodialysis therapy is presented. A brief introduction about the importance of enzymes and their structure is given. The functionality of urease as a complementary action to urea and its reaction route is discussed. Finally, enzyme immobilization techniques are discussed.

2.2. Urea Sources and Its Removal Processes

2.2.1. Urea Produced in Industry

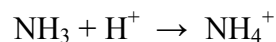
Urea is an important source of nitrogen based fertilizer which is synthesized in industrial scale by the reaction of CO₂ and NH₃ in the range of high temperatures and pressures. A series of reversible reactions are simultaneously occurred through the urea production. The first reaction produces ammonium carbamate which is then decomposed into urea. During urea synthesis, a side reaction that causes formation of biuret which does not only lower the yield but also burns of leaves of the plant should be minimized.



Urea production comprises 5 units; synthesis, recirculation, evaporation, prilling and wastewater treatment [35]. Conversion of ammonium carbamate to urea in the absence of ammonia increases with temperature. Common reaction temperatures 180-210°C and pressure 140-250 atm, NH₃:CO₂ mole ratio 3:1-4:1 and retention time 20-30 min are accepted for the process in optimum conditions [36].

Wastewater from synthesis, recirculation and evaporation units collected in a tank usually contains 3.1 mol% ammonium, 0.85 mol% dissolved CO₂ and 0.32 mol% urea [37]. The main source of wastewater comes from the reaction in which 0.3 tons of water is produced per every tons of urea generated. In addition, ejector steam, sealing, rinsing water and the process steam are used in wastewater treatment area, hence, all the total source generates 0.5 tons of wastewater per 1 ton of produced urea. According to environmental regulations, the level of these toxic compounds should be reduced before discharging into environment. In the past decade, the permitted discharge level of urea was 100 ppm, whereas, currently, the maximum allowable limit in the effluent has been

reduced to 10 ppm [38]. In the industry, the removal method of urea from the waste stream is based on hydrolysis (nonenzymatic) and biological conversion of urea nitrogen to dinitrogen. The first method requires high temperatures and pressures with complex technological equipments, while the latter suffers from the instability of microbial bed [1]. Both methods have high operating costs. One way to overcome these constraints might be using enzyme immobilized membranes either in tubular form or in flat sheet. While the membrane is utilized for selective separation in molecular size, the insoluble enzyme (urease) on the surface or in the matrix is used to catalyze the hydrolysis of urea into ammonia and carbon dioxide. Complete conversion can be achieved by adjusting the system parameters and the resulting ammonium ions are totally in soluble form depending on the solution pH based on the equilibrium relation given below. Below about pH 6.5 there is 100% NH_4^+ ; above about pH 11.5 is 100% NH_3 . Below pH 6.5, CO_2 is flash off. After removing CO_2 the pH of waste stream is readjusted to 12 and hence, complete removing of ammonia from the solution is achieved.



2.2.2. Urea Produced in Human Body

During protein digestions, nitrogen is produced which leads to the formation of ammonia. Since ammonia is a toxic compound, a stepwise series of reactions takes place in liver that convert it into urea which is less toxic and stable. The converted urea in blood is then transferred to kidney where it is filtrated and excreted as urine. Improper function of kidney interfere the normal formation and excretion of urea into urine which can lead to higher blood urea levels. Urea is more concentrated up to 50 fold in blood than in urine samples [39]. The increase in urea concentration in human body causes to denaturation of proteins. As a marker of liver and kidney functions, the determination of urea and small toxin molecules e.g, ammonia is essential. The reference intervals for serum or plasma urea are between 1 to 10 mM. Above this limit, the urea level in blood is needed to be reduced by hemodialyzer, in which small sized molecules, e.g, urea, creatinine are filtered through a semipermeable membrane by the contribution of both diffusive and convective transport. A typical hemodialyzer contains

as many as 10,000 of hollow fibers. While toxin blood is circulated inside the fibers, a dialysate solution is counter-currently flowing at the outside of the hollow fibers. In the past, a hemodialysis therapy lasted 24-30h/week, nowadays, by the improvement of blood and dialysate flow rates and membrane characteristics, the dialyzing time is reduced to 3x 2 h/week at the conditions in which the blood flow rate is 630 mL/min and dialysate flow rate is 1000 mL/min [40, 41]. During dialysis, the concentration of urea in the blood decreases from 20–50 mM to less than 10 mM [42]. In spite of those technological improvements, the conventional artificial kidneys based on hemodialysis are costly and inconvenient machines, difficult to handle and also largely limiting the mobility of the patient. In addition, they require as much as 100–300 L of dialysate solution per treatment. If those large volumes of dialysate solution would be reduced, the size of the machine could be smaller, mobile (easy to handle) and the cost of the therapy could be lower. To decrease the dialysate volume, a few attempts have been focused on the utilization of urease catalyzed hydrolysis of urea [43, 44]. In those studies, uremic toxins are hydrolyzed by the immobilized urease in a closed loop through which the same small amount of dialysate is recirculated and cleared. The resulting ammonium and carbonate ions are caught by ion exchangers, whereas the other toxins are eliminated by adsorption on activated charcoal. The commercialized dialysate regeneration systems require 5 L of dialysate or less. If half a million patients worldwide are being supported by hemodialysis [45], those huge differences in the dialysate volumes are significantly important in terms of cost minimization.

2.2.3. Urea in Municipal Wastewater

Although, human urine comprises less than 1% volume of municipal wastewater quantity (10 kg urea/year/adult excreted), it contributes 80% of nitrogen, 50% of phosphorus, and 90% of potassium in municipal wastewater [46]. The strict discharge standards to receive clean waters and recycling nutrients for the replenishing depleting resources has led to a need for enhanced treatment processes in wastewater treatment plants. Different techniques such as aerobic nitrification followed by anaerobic dinitrification and then phosphate precipitation, construction of wetlands [47] and membrane bioreactor with activated sludge process [48] are proposed.

The most popular method in wastewater treatment is membrane bioreactor. It is a combination of biological unit responsible for the biodegradation of waste compounds and membrane module for the physical separation of the treated water from the mixed liquor. Figure 2.1 summarizes the basic differences in wastewater treatment by membrane bioreactor and conventional technique. In a typical membrane bioreactor treatment, a preconditioned (if necessary) wastewater is fed to the reactor where suspended or soluble organic compounds are digested by means of inoculated activated sludge which are cultivated during 1 month before used. In activated sludge microorganisms use some components in wastewater such as urea, sugar etc, as nutrients for their growth. The oxygen demand for their respiratory is supplied by an air blower through a tube installed to the base of biological unit. The tube has many small holes through which air diffuses into system and drives the mixed liquor to upflow to scour the membrane surface. The resulting mixed liquor is separated through membrane and the effluent is discharged to surface water. If the membrane is outside the reactor the mixed liquor is pumped creating a high cross flow velocity along the membrane surface.

Membrane bioreactor system is currently applied to municipal wastewater treatment for small communities [49, 50] and for the treatment of industrial wastewater [51, 52] in various parts of the world. However, some drawbacks have to be overcome in order to achieve wide applicability area over the world. The main disadvantageous of this system is required high capital costs due to expensive membrane units and high energy costs due to the need for a pressure gradient. Membrane fouling problems can lead to frequent cleaning of the membranes, which stop operation and require clean water and chemicals. Another drawback can be problematic waste activated- sludge disposal. Since the MBR retains all suspended solids and most soluble organic matter, waste-activated-sludge may exhibit poor filterability and settleability properties [53].

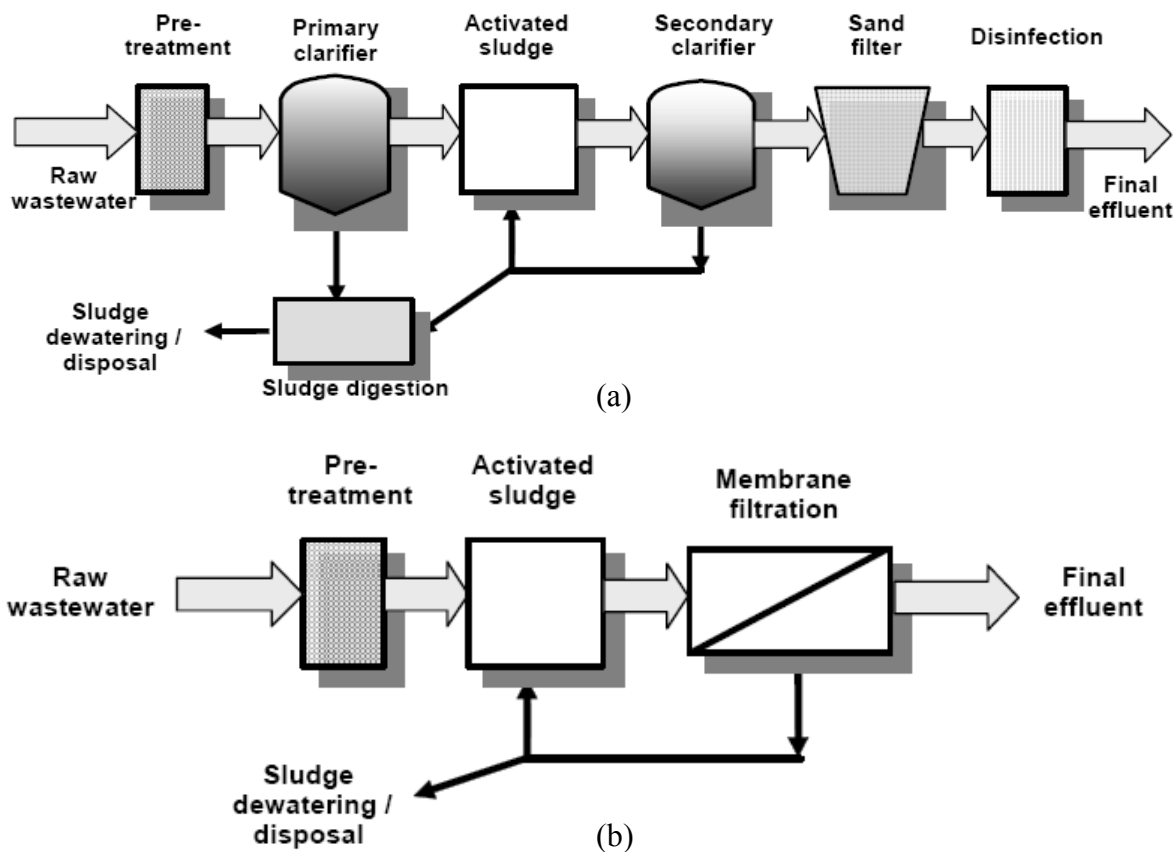


Figure 2.1. Schematic representation of a) conventional wastewater treatment, b) membrane bioreactor.

The activated sludge treatment takes a long time to complete decomposition of nitrogenous or carbonaceous components and utilization from microbial enhance solid mass at disposal need to be extra treatment. Instead of wastewater treatment by means of membrane bioreactor, enzymatic membrane reactor may serve a quick response to the problem of long duration time and excessive slurries.

2.3. Enzyme as a Green Catalyst

Enzymes are highly efficient biological catalysts that have evolved to perform efficiently under mild conditions required to preserve the functionality and integrity of the biological systems e.g., from viruses to man. With appropriate substrates, they can enhance reaction rates in excess of one million times over the corresponding uncatalysed reaction. Enzymes are highly selective towards specific substrates. They can differentiate the substrate molecules on the basis of positioning of target functional groups (regioselectivity), chemical functionality (chemoselectivity), and chirality

(stereoselectivity). High selectivities of enzymes provided by their unique amino acid sequence and three dimension structures eliminate side reactions that permit reaction efficiencies approach to 100%. The enzymatic reactions offer the potential to greatly reduce the environmental impact of existing chemical processes. Mostly enzymes are biodegradable and generally the reaction is occurred in water which is nontoxic and because no waste products generate during biocatalytic reactions, product purification is simple and such reactions are less polluting than chemical synthesis routes. Enzymes are most active under mild reaction conditions including near neutral pH, ambient temperatures and pressures thus decreasing energy costs and increasing safety.

Enzymes belong to a larger biochemical family of macromolecules known as proteins. The common feature of proteins is that they are polypeptides: their structure is made up of a linear sequence of α -amino acid building blocks joined together by amide linkages. This linear polypeptide chain then ‘folds’ to give a unique three-dimensional structure.

2.3.1. The Structures of the Amino Acids

Proteins are composed of a family of 20 α -amino acid structural units whose general structure is shown in Table 2.1. The differences between 20 α -amino acids lie in the nature of the side chain R. The simplest amino acids are glycine (Gly) involving no side chain, and alanine (Ala) which has a methyl group as a side chain. Some of side chains are hydrophobic in character, such as the thioether of methionine (Met); the branched aliphatic side chains of valine (Val), leucine (Leu) and isoleucine (Ile); and the aromatic side chains of phenylalanine (Phe) and tryptophan (Trp). The remainder of the amino acid side chains is hydrophilic in character. Aspartic acid (Asp) and glutamic acid (Glu) contain carboxylic acid side chains, and their corresponding primary amides are found as asparagine (Asn) and glutamine (Gln). There are three basic side chains consisting of the ϵ -amino group of lysine (Lys), the guanidine group of arginine (Arg), and the imidazole ring of histidine (His). The polar nucleophilic side chains responsible for the enzyme catalysis are the primary hydroxyl of serine (Ser), the secondary hydroxyl of threonine (Thr), the phenolic hydroxyl group of tyrosine (Tyr) and the thiol group of cysteine (Cys). The nature of the side chain confers certain physical and chemical properties upon the corresponding amino acid, and upon the polypeptide chain

in which it is located. The polypeptide chain is formed as a linear sequence composed of 100–1000 amino acids that are linked to the next via an amide bond. This is the primary structure of the protein. The sequence of amino acids in the polypeptide chain is important. In general, the polypeptide chain contains all the information to confer both the three-dimensional structure of proteins and the catalytic activity of enzymes.

2.3.2. Enzyme Structure and Function

The only difference between enzymes and proteins is that the former possess catalytic activity. The part of the enzyme tertiary structure which is responsible for the catalytic activity is called the ‘active site’ of the enzyme, and often makes up only 10–20% of the total volume of the enzyme [54]. The active site is usually a hydrophilic cleft or cavity containing an array of amino acid side chains which bind the substrate and carry out the enzymatic reaction, as shown in Figure 2.2.

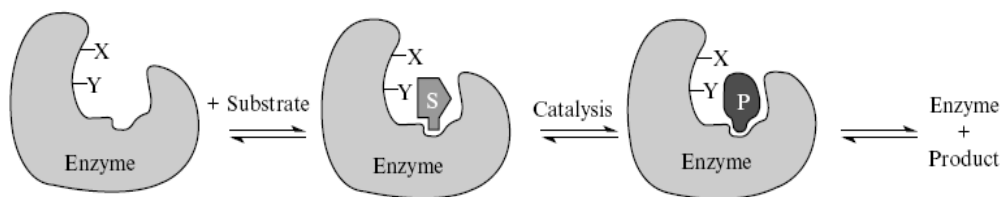


Figure 2.2. Schematic illustration of enzyme plus substrate

Table 2.1. Structure and properties of amino acid side chains.
(Source: Ratner et al. 1996)

Amino acid	Structure	Group and pK	Charge	Hydrophobicity ^a	Surface tension ^b
Isoleucine			Neutral	0.73	-15.2
Phenylalanine			Neutral	0.61	-17.3
Valine			Neutral	0.54	-3.74
Leucine			Neutral	0.53	-21.9
Tryptophane			Neutral	0.37	-9.6
Methionine			Neutral	0.26	-3.01
Alanine			Neutral	0.25	0.96
Glycine			Neutral	0.16	1.12
Cysteine		-SH: 8.3	0 to -1	0.04	0.69
Tyrosine		-OH: 10.9	0 to -1	0.02	-15.1
Proline			Neutral	-0.07	-0.49
Threonine			Neutral	-0.18	0.59
Serine			Neutral	-0.26	0.76
Histidine		-NH-: 6.0	0 to +1	-0.40	1.03
Glutamic acid		-CO2H: 4.3	0 to -1	-0.62	0.86
Asparagine			Neutral	-0.64	1.17
Glutamine			Neutral	-0.69	1.21
Aspartic acid		-CO2H: 3.9	0 to -1	-0.72	0.96
Lysine		-NH2: 10.8	0 to +1	-1.1	0.92
Arginine		-NH2: 12.5	0 to +1	-1.8	1.03

^a, More positive values are more hydrophobic.

^b, The values are the surface tension lowering of water solutions of the amino acids in units of erg/cm²/mole per liter [56].

One of the features of enzyme catalysis is its high substrate selectivity, which is due to a series of highly specific non-covalent enzyme–substrate binding interactions. Since the active site is chiral, it is naturally able to bind one enantiomer of the substrate over the other. There are four types of enzyme–substrate interactions used by enzymes, as follows: The first one is electrostatic interactions that take place between the substrate containing ionizable functional groups which are charged in aqueous solution at or near pH 7 and oppositely charged amino acid side chains at the enzyme active site. Hydrogen bonding usually occurs between a hydrogen bond donor containing a lone pair of electrons and a hydrogen-bond acceptor containing acidic hydrogen. These interactions are widely used for binding polar substrate functional groups. Van der Waals interactions arise from interatomic contacts between the substrate and the active site which are only significant in short range (2–4Å), since the strength of these interactions varies with $1/r^6$. If the substrate contains a hydrophobic group, then favorable binding interactions can be realized if this is bound in a hydrophobic part of the enzyme active site. These hydrophobic interactions may be very important for maintaining protein tertiary structure. Having bound the substrate, the enzyme then proceeds to catalyse its specific chemical reaction using active site catalytic groups, and finally releases its product back into solution.

2.3.3. Structural Characteristics of Native Ureases

Urease is the first crystallized enzyme from Jack bean by Sumner in 1926 [57]. After 50 years of his discovery in 1978, Dixon has showed jack bean urease possesses nickel ions in the active site, essential for activity [58]. From its discovery, extensive research have been carried out by focusing on its amino acid sequences, crystal structures, molecular basis of catalytic mechanism.

Ureases are enzymes widely occurring in nature. The significance of this enzyme is that it catalyzes the hydrolysis of urea to form ammonia and carbamate, which is then dissociated spontaneously into second mole of ammonia and carbonic acid with the reaction shown in Figure 2.3.

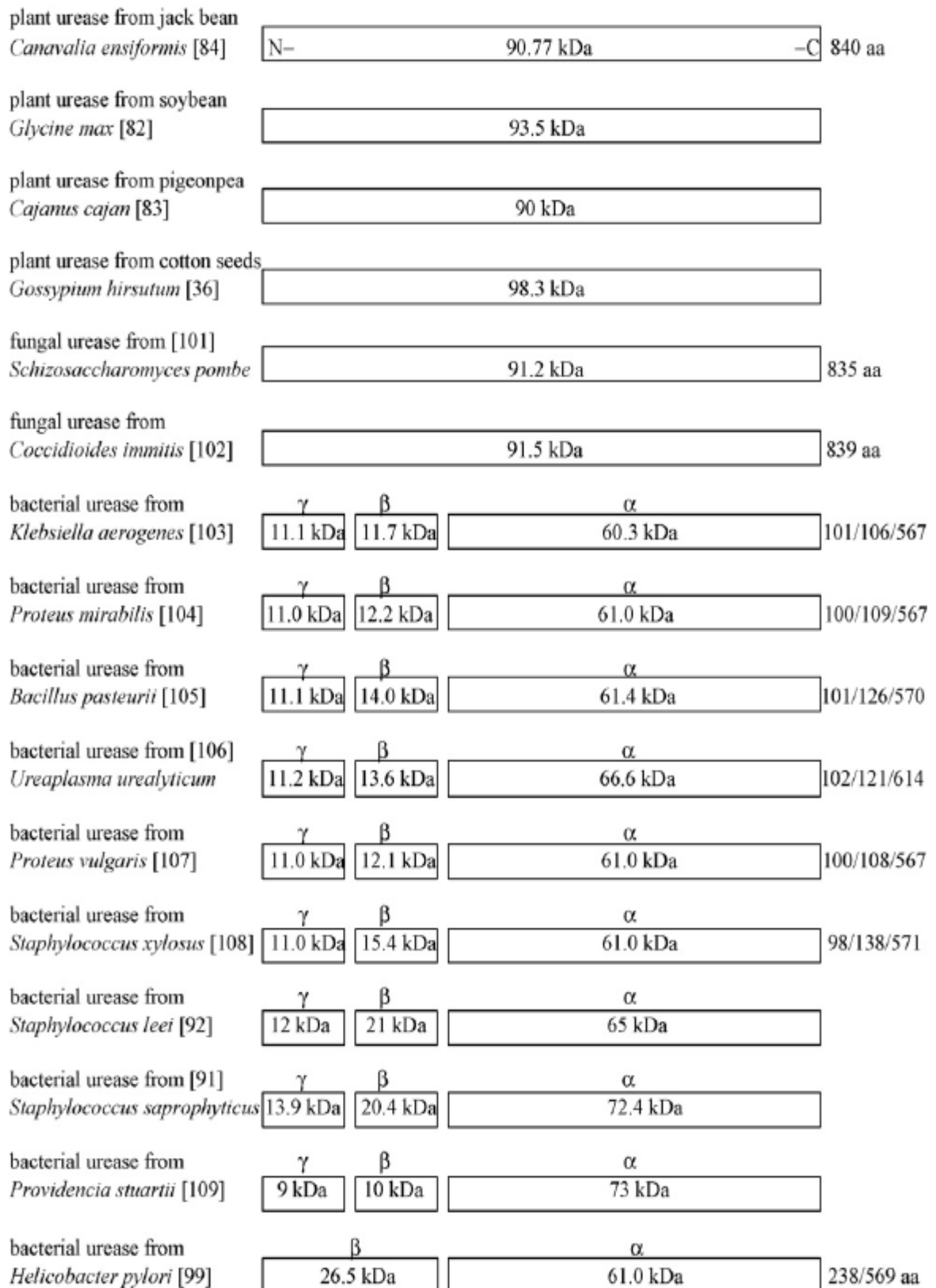


Figure 2.4. The structural subunits of plant, fungal and bacterial origins of ureases.
(Source: Krajewska B, 2009)

The complete amino acid sequences of jack bean urease have been determined by Takishima et al. [61]. They reported that the enzyme consists of single kind of polypeptide chain containing 840 amino acid residues whose compositions are tabulated in Table 2.2. The calculation of relative molecular mass of the subunit from the sequence give 90,770g/mol which indicates that urease is composed of six subunits.

Table 2.2. The amino acid composition of jack bean urease.
(Source: Takishima et al. 1988)

Met	21
Lys	49
Leu	69
Ser	46
Pro	42
Arg	38
Glu	50
Val	55
Gly	79
His	27
Asn	38
Ala	75
Tyr	21
Gln	18
Thr	54
Ile	65
Asp	50
Phe	24
Cys	15
Trp	4

The crystal structures of ureases from two bacteria, *Klebsiella aerogenes* [65, 66] and *Bacillus pasteurii* [67] have provided the knowledge on the urease active site. As shown in Figure 2.5, *B. pasteurii* urease (BPU) is a heteropolymeric molecule $(\alpha\beta\gamma)_3$ with exact threefold symmetry. The α subunit consists of an $(\alpha\beta)_8$ barrel domain

and a β -type domain. The β subunit, located on the external surface of the trimer, is predominantly β structure and has an additional C-terminal α helix of 12 amino acids which does not interact with the other subunits. The three γ subunits consist of $\alpha\beta$ domains located on top of each pair of α subunits, thereby favouring their association into a trimer.

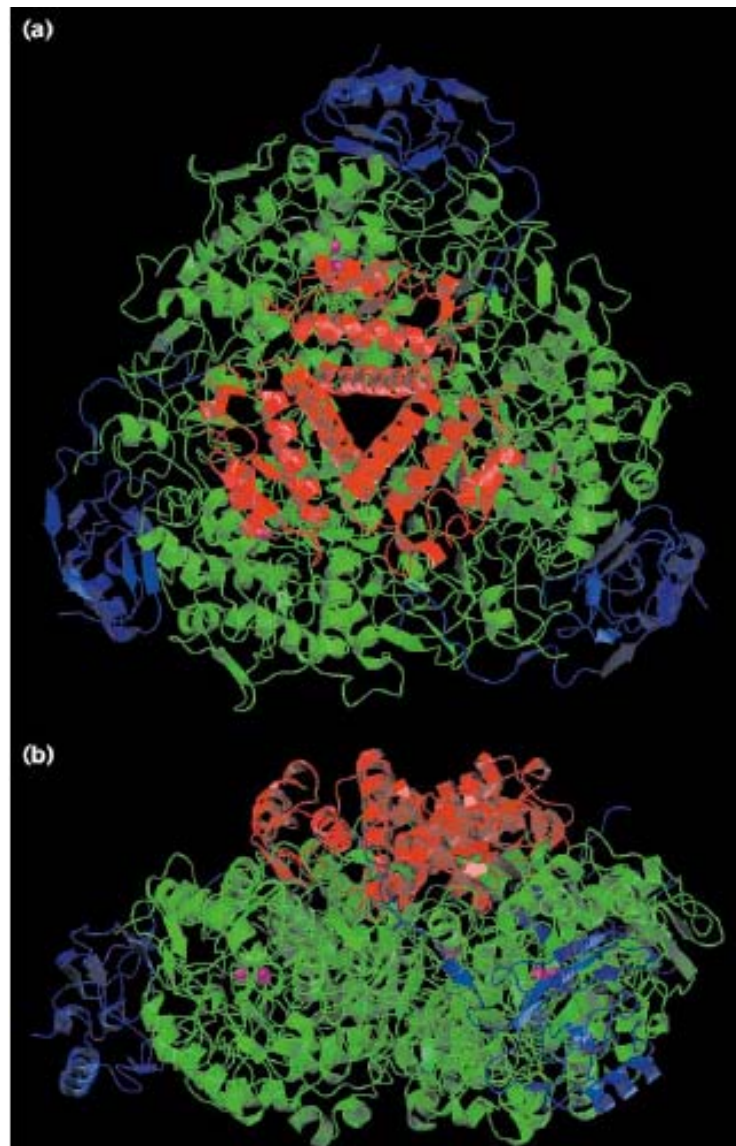


Figure 2.5. Three-dimensional structure of *Bacillus pasteurii* urease (BPU) represented as ribbon diagram of the $(\alpha\beta\gamma)_3$ heterotrimer. (a) View down the crystallographic threefold axis; (b) view from the side. The green, blue and red ribbons represent, respectively, the α , β and γ subunits. The magenta spheres in the α subunits are the nickel ions of the active center (Source: Benini et al. 1999).

The active site shown in Figure 2.6 contains a binuclear nickel centre. The Ni-Ni distances were found close in value, in *Bacillus pasteurii* and *Klebsiella aerogenes* urease as 3.7 and 3.5 Å, respectively. In the centre the nickel(II) ions are bridged by a carbamylated lysine through its O-atoms, with Ni1 further coordinated by two histidines through their N-atoms, and Ni2 by two histidines also through N-atoms and additionally by aspartic acid through its O atom. Besides, the Ni ions are bridged by a hydroxide ion (WB), which along with two terminal water molecules, W1 on Ni1, W2 on Ni2, and W3 located towards the opening of the active site, forms an H-bonded water tetrahedral cluster filling the active site cavity. It is this cluster that urea replaces when binding to the active site for the reaction. As a result of the above ligations, Ni1 is pentacoordinated and Ni2 hexacoordinated, and their coordination geometry is pseudo square pyramidal and pseudo octahedral, respectively. Crucially, the fact that the two ureases have a nearly superimposable active site implies that it is common to all ureases. Ureases are cysteine-rich enzymes. Jack bean urease was proven by disulfide titration in nondenaturing conditions to contain five other cysteine residues per subunit that are more reactive [68]. The overall number of cysteines per jack bean urease has been found as 90.

The mechanisms of urease-catalyzed hydrolysis of urea are first proposed by Benini et al. [67] and Karplus et al. [69]. Later on, binding of urea with the oxygen atom of its carbonyl group to the more electrophilic Ni1 ion in the active site of urease which is more susceptible to nucleophilic attack was shown by Dixon et al. [70]. Upon replacing W1–W3 waters, urea is further bound to Ni2 through the nitrogen of one of its amino groups (nonleaving-N), making its binding overall bidentate [67]. This binding is believed to facilitate the nucleophilic attack of water on the carbonyl carbon, resulting in the formation of a tetrahedral intermediate from which NH₃ and carbamate are released.

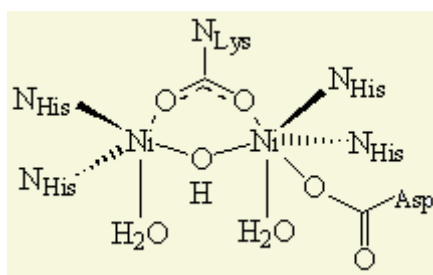


Figure 2.6. Chemical structure of urease

2.4. Strategies for Enzyme Stabilization

The unique catalytic properties of enzymes make them desirable in many chemical processes. They offer mild reaction conditions (physiological pH and temperature), a biodegradable catalyst which is derived from renewable resources and environmentally acceptable solvent (usually water), as well as high activities and chemo-, regio- and stereoselectivities. Furthermore, the use of enzymes do not require the need for functional group protection or activation affording synthetic routes which are shorter, generate less waste and hence are both environmentally and economically more attractive than traditional organic syntheses. However, poor thermostability, short operational lifetimes and impossibility for reuse restrict their wide range of application. Enzyme immobilization onto or within solid support has been accepted as one of the most successful methods in eliminating these limitations of the free enzyme [3, 7]. There are several reasons for using an enzyme in immobilized form. The stability under both operational and storage conditions are enhanced. Denaturation by heat or organic solvents is obviated. The enzyme can easily be handled and separated from the product, thereby eliminating protein contamination of the product. Immobilization also facilitates the efficient recovery and reuse of costly enzymes. Repeated re-use and enhanced stability increase the catalyst productivity (kg product/ kg enzyme) which in turn determines the enzyme costs per kg product.

2.4.1. Enzyme Immobilization Techniques

Immobilization involves the fixation of an enzyme to an insoluble matrix. The fixation may be physical or chemical in nature. The chemical techniques consist of covalent attachment and crosslinking either single or multifunctional groups. By contrast, the physical techniques include adsorption, entrapment, formation of Langmuir–Blodgett films, and layer-by-layer self assembly.

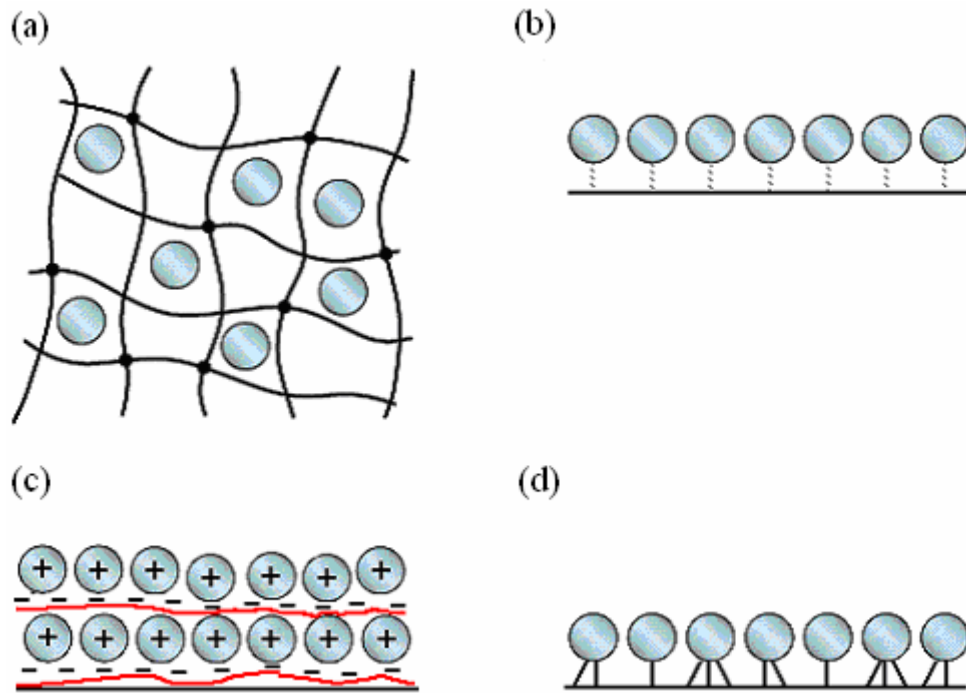


Figure 2.7. Enzyme immobilization techniques: (a) entrapment, (b) adsorption, (c) Layer-by-layer self assembly, and (d) covalent immobilization. The blue spheres represent enzyme molecules.

2.4.1.1. Entrapment

Enzyme immobilization by means of entrapment involves retention of an enzyme by a porous matrix, membrane or gel-like material based on differences between the size of the pores and the enzyme molecule [71, 72]. The enzyme cannot release into bulk reaction media because of having an effective radius greater than that of the pores, whereas substrates and products can diffuse freely in and out of framework of the support. As shown in Figure 2.7.a, the enzyme does not interact with the support directly, therefore, its conformational structure and hence activity is preserved. Enzyme immobilized in this way may be more stable than in free form due to the restricted conformational motion, in addition, entrapment may prevent thermal, pH, or chemical denaturation. Depending on the properties of the support, such as charge and hydrophobicity, the entrapment is feasible because of the partitioning effect which may provide exclusion of an inactivating agent from the vicinity of an enzyme. Similarly, the same partitioning effect is valid for substrate entrance and product output which constitutes a diffusional resistance causing lower activity observed than the free

enzyme. In literature, ureases have been entrapped into different types of polymer composite gels [73-78]. Kara F. et al. entrapped jack bean urease into chitosan–alginate polyelectrolyte complexes (C-A PEC) and poly(acrylamide-co-acrylic acid)/κ-carrageenan (P(AAm-co-AA)/carrageenan) hydrogels [73]. They examined the effects of pH, temperature, storage stability, reuse number, and thermal stability on the free and immobilized urease. Authors reported that the entrapment enhanced thermostability, storage stability and reusability of the urease. After 20 usage of entrapped urease in 5 days, it retained 89% of total activity. The storage value in the case of entrapped urease was reported such that 70% of initial activity was preserved at the end of 70 days, whereas the free enzyme lost its total activity after 20 days. In that study, catalytic reaction was carried out at 55°C at which diffusional limitations of substrate and product could be minimized.

2.4.1.2. Adsorption

In the case of physical adsorption, enzyme is bound on a support material by non-covalent, ionic, or affinity interactions (Figure 2.7.b). Any one or combination of hydrogen bonding, hydrophobic interactions, or Van der Waals forces are responsible for the adsorption. The strongest interactions are formed through electrostatic interactions between an enzyme and charged support [71]. Compared to other immobilization techniques, adsorption is relatively simple in practice and does not require sophisticated chemistries. Because of its simplicity, non-toxicity lower process cost, 90% of enzyme immobilization in industry, have been carried out by means of physical adsorption. Conformational rigidity particularly when there are multiple interactions between an enzyme molecule and the support may be increased. However, relative to chemical immobilization technique, the strength of interactions between an enzyme and support are relatively weak. The interaction can easily be disrupted by changing pH and ionic strength of the reaction medium that makes the enzyme prone to leaching. Generally, adsorption of an enzyme is based on non-specific bonding, interactions involving active site residues can lead to inactivation of an enzyme. Urease immobilizations by means of adsorption have been well documented by Krajewska [1]. Urease has been immobilized onto unmodified and modified acrylonitrile (AN) copolymer with 2-dimethylaminoethyl methacrylate (DMAEM) and diacrylamido-2-

methylpropanesulfonic acid (AMPSA) based on the method of physical adsorption and ionic interaction for the purpose of diagnostic test-strips to determine urea concentration in blood [79]. The best sensitivity of the test strip was found between the concentration interval (0.02-0.20 g/100 ml). The minimum concentration measured with these strips was 0.008 g/100 ml and authors reported that the prepared diagnostic test-strips are fully comparable to the well known 'Azostix' strips produced by AMES, USA [80]. In that study, the surface modification of the AN copolymer is very complex required too many steps which result in waste of chemicals and time. However, electrostatic interactions by means of layer-by-layer (LbL) self assembly eliminates those complex and time consuming protocols and offers simple and easy modification strategy which enables desired surface functionality of the support material through deposition of cationic or anionic polyelectrolytes (Figure 2.7.c).

2.4.1.2.1. Electrostatically Self-Assembly Technique and Layer-by-Layer Structure

Fabrication of thin films of functional organic materials is of interest in material science and in basic research and in technology. They are especially required in biosensor applications [16, 17, 81] owing fast response due to very thin layer which may reduce the diffusional resistance and in biocatalysis attachment [18] as they serve specific functional groups for the biomolecule while retaining the bulk properties of the respective support material. The basic process involves alternately dipping of a surface charged support material into oppositely charged of polyelectrolyte aqueous solutions. Polyelectrolytes can be defined as polymers with ionizable groups. In polar solvents, such as water, these groups can dissociate, leaving charges on polymer chains and releasing counterions in solution. Examples of polyelectrolytes include polystyrene sulfonate, polyacrylic and polymethacrylic acids and their salts, polyethyleneimine, chitosan, alginate, proteins and DNA.

The method first investigated by Decher [82] involves layer-by-layer deposition of oppositely charged polyelectrolytes by consecutive alternating immersion of a substrate in baths containing positively and negatively polyelectrolyte aqueous solutions. As shown in Figure 2.8, sequential adsorptions of anionic and cationic polyelectrolytes allow the buildup of multilayer film structures. The charge inversion occurs because the polyelectrolytes adsorb in excess over the surface charge. In

individual adsorption steps, this leads to charged surface in contact with a solution of a polyelectrolyte with the same charge and electrostatic repulsion limits the adsorption to a single polymer monolayer. Different surfaces can be modified similarly, but the assembly stoichiometry may vary and no limit to the number of layers deposited on any surfaces [83]. For example, Ramzi et al. [84] investigated the effect of a ultrathin polyelectrolyte multilayer (PEM) modification on the performance properties of salt rejection of the cellulose acetate (CA) nanofiltration membrane using chitosan (CHI) and alginate (ALG) as cationic and anionic polyelectrolytes respectively. The buildup layer pairs were reported as 35. The fabricated layer is extremely thin, average layer thickness from X-ray photoelectron spectroscopy (XPS) data was reported as 2.0, 2.8 and 4.1 Å for poly(ethylene terephthalate) (PET), PET-CO₂⁻, and PET-NH₃⁺ respectively [83]. It is possible to control the overall thickness of the multilayer obtained by controlling the number of deposition cycles and/or by changing the deposition conditions (e.g., pH, the polyelectrolyte concentrations and addition of salt in to deposition solution).

The electrostatic self-assembly technique usually uses water as the solvent, and no toxic solvent is involved. As such, this technique is environmentally friendly. The electrostatic self-assembly technique, in principle, can make a defect free nano structured layer-by-layer film on a porous surface because the defects formed in the previous layer, if any, could be self-repaired during the formation of the next layer.

In literature, LbL assembly have been extensively used for surface modification prior to biomacromolecule adsorption including protein and DNA, however, to our best knowledge, there are only few reports dealing with enzyme immobilization on membranes as support using LbL assembly. For instance Nguyen et al [85] have shown the feasibility of immobilizing glucose oxydase (GOx) by using adsorption of an intermediate polyelectrolyte layer on an oppositely charged membrane. The method has been demonstrated to offer a versatile route for preparing enzyme supported membranes, the activity of which depended on the support likely due to its pore size. Using the same approach, the Battacharyya's group [86, 87] has prepared catalytic membrane by enzyme immobilization within the pore domain of microfiltration (MF) membrane. As expected, supported enzyme stability was higher compared to the free GOx. On the other hand, the amount of immobilized enzyme and stability was found to be higher when the protein and the support are oppositely charged. In both of these studies, the outer layer consists of the enzyme layer and the LbL deposition acts as an

anchor for the biomacromolecule. Caruso et al [88, 89] have prepared enzyme modified membranes using alternative adsorption of peroxidase-poly(sodium 4-styrenesulfonate) complex and a positively charged polyelectrolyte within MF membrane pores. The membrane catalytic activity was found to increase up to a certain number of bilayers beyond which it is assumed that membrane pore blockage took place. In this case the enzyme is located within the successive layers and is an inner part of the LbL film. Urease was immobilized on polyacrylonitrile-chitosan (PAN-CHI) composite membrane activated with glutaraldehyde [22]. Author has concluded that PAN-CHI composite membrane had higher activity and it was more stable in the absence of glutaraldehyde which indicated the advantageous of LbL self assembly technique.

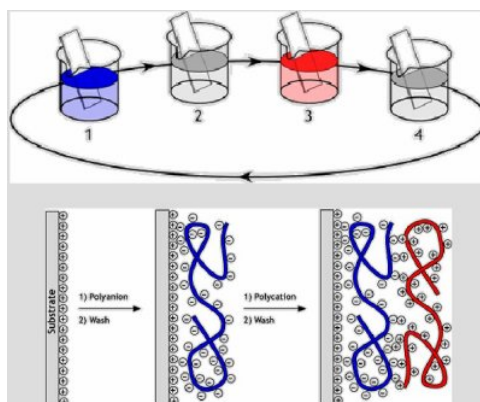


Figure 2.8. LbL protocol: dipping in 1. polyanion solution, 2. rinsing solution, 3. polycation solution, 4. rinsing solution.

2.4.1.3. Covalent immobilization

Covalent immobilization of an enzyme is achieved by the reaction of functional groups available on the enzyme and support (Figure 2.7.d). The reactive groups on the side chains of Lys, Cys, Arg, Asp, Glu, His, Tyr, Met, and Trp residues may be used. The groups of enzyme for covalent bonding are the amino group, carboxyl group, imidazole group, indole group while the reactive groups of support material include the hydroxyl group, carboxyl group, hydroxymethyl group, amino group, etc. Surface modification techniques such as radio frequency, plasma treatment, UV irradiation are required for the introduction of functional groups onto the surface of the support prior to enzyme immobilization. Functional groups can be also introduced to the support material without reactive groups, by grafting. Glutaraldehyde and carbodiimides are two

common coupling agents for chemical enzyme immobilization. In many studies, concerning covalent enzyme immobilization, glutaraldehyde has been selected as a crosslinking agent which acts on the Lys or Hyl residues [22, 90, 91]. However, cytotoxic reactions induced by the release of glutaraldehyde or glutaraldehyde derivatives have been reported during in vitro or in vivo degradation [92-95]. Recently, a well known coupling reaction of N-ethyl-N'-(3-dimethylaminopropyl) carbodiimide (EDC) and N-hydroxysuccinimide (NHS) has been used to construct enzyme layer on the carboxyl or amino-terminated surface [96-98]. EDC/NHS coupling agent has been reported non-cytotoxic in vitro [19] and biocompatibility is observed in animal studies [20]. Urease was immobilized onto silk clothe activated with EDC for the urease aided precipitation of hydroxyapatite [99].

Depending on the number of accessible reactive groups on the enzyme surface, an enzyme may be bound to the support at more than one site. The greater the number of covalent linkages between the enzyme and surface, the greater the extent to which the enzyme's rigidity is increased. Comparatively, covalent immobilization can lead to much greater thermostability enhancements than entrapment or adsorption [71]. As is to be expected anytime the structure of an enzyme is modified, covalent immobilization may have deleterious effects on enzyme activity.

2.4.2. Selection of a Suitable Support Material

In general, organic or inorganic, synthetic or natural matrixes can be selected as supports for the enzyme immobilization depending on the requirements for the application. Natural polymers such as chitin, chitosan and cellulose have many advantageous over many synthetic polymers in terms of biodegradability, nontoxicity, physiological inertness, hydrophilicity and remarkable affinity to proteins. The green properties of those materials make them attractive especially in such specific applications including food, pharmaceutical, medical and agricultural processing. Hydroxyl and amino groups in their structures (Figure 2.9) facilitate covalent immobilization of enzymes. Amino groups can be activated by glutaraldehyde and hydroxyl groups by cyanogen bromide, carbonyldiimidazole and 1-cyano-4-dimethylaminopyridinium tetrafluoroborate [100].

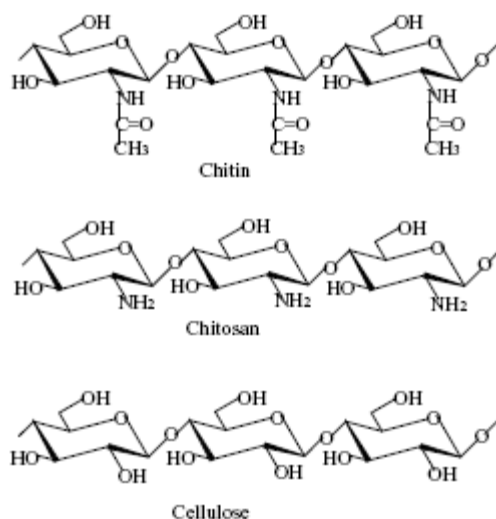


Figure 2.9. Structures of chitin, chitosan and cellulose

Although, the membranes from natural polymers have many advantageous, poor mechanical strength and chemical instability restrict their direct application in enzyme immobilization. For example, the abundance in hydrogen bonding among the polymer chains may result in a decrease in flexibility, the excellent affinity to proteins may make them easily eroded by bacteria and the high hydrophilicity may cause the membranes to swell in a wet atmosphere. However, these drawbacks are absent in membranes from many synthetic polymers. Therefore, membranes prepared by synthetic polymers have been much more preferred as enzyme carriers because of their low cost, easy surface modification, resistance to biodegradation and thermal and chemical stabilities. Polyethylene, nylon, acrylonitrile (AN) copolymer, polymethylmethacrylate (PMMA), polysulfone (PS), polyethylenethraphtalate (PTE), polytetrafluoreethylene (PTFE), polypropylene (PP) are some example of synthetic membranes extensively used as enzyme carriers. Because, many synthetic polymers are poor in biocompatibility, biodegradability, hydrophilicity and even cause damage to proteins, extensive research has been carried out to be able to meet the specific requirements for the enzymatic membrane. Copolymerization with a hydrophilic or reactive-group-contained comonomer has been accepted as the best solution and hence their commercially availability have been much more increased than homopolymers.

Polyacrylonitrile is a hydrophobic polymer and the hydrophobic interactions during enzyme immobilization lead to serious effect on the conformation of the enzyme which can be folded or denatured. To eliminate this, acrylonitrile monomer is copolymerized with sodium methallyl sulfonate (9% w/w) by the producer of Gambro-

Hospal Co.(Meyzieu, France) and Luokil Neftochim Bourgas (Spartak, Bulgaria) has been producing ternary copolymer including 91.3% acrylonitrile, 7.3% methylmethacrylate, 1.4% sodium vinylsulfonate). The copolymerized membranes have higher hydrophilicity. The degree of hydrophilicity of Lukoil product is %65 and its water flux is reported as 0.52 m³/m².h [22]. The chemical structure and dispersion of atoms in the commercial product (AN69) by Gambro-Hospal Co. are represented in Figure 2.10 and 2.11 respectively. AN69 membrane is negatively charged due to presence of sulfonate groups in its structure. This property makes it more hydrophilic and it is easy to modify the surface with cationic polyelectrolyte by simply self assembly technique. In addition, its nitrile (-CN) group can be converted into various functionalities to offer membranes better chemical bonding with enzyme molecules. For example, hydrolysis of AN69 membrane by aqueous NaOH solution converts some (-CN) groups into carboxylic groups that can easily be crosslinked by means of EDC/NHS coupling agent followed by enzyme immobilization.

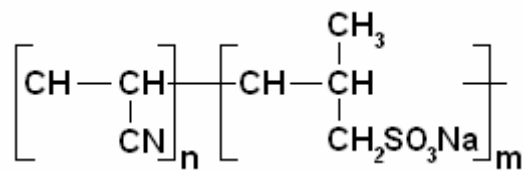


Figure 2.10. Chemical structure of AN69 membrane

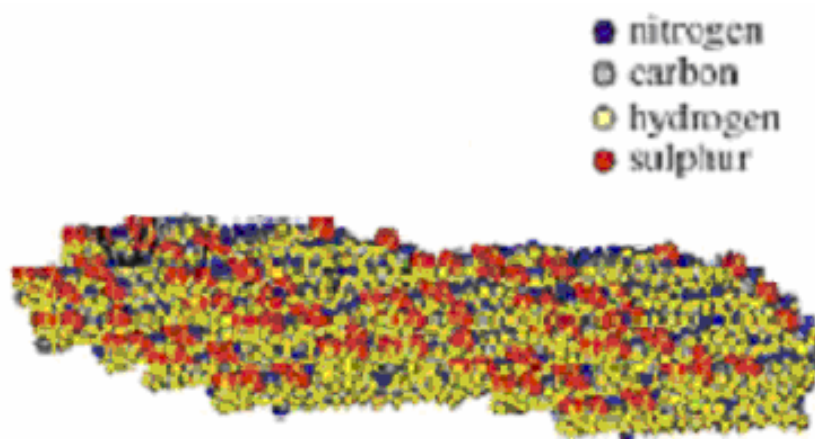


Figure 2.11. Representation of AN69 membrane

CHAPTER 3

THEORETICAL ESTIMATION OF SOME KINETIC PROPERTIES OF ENZYME IMMOBILIZED MEMBRANES

3.1. Introduction

Estimation of adsorption kinetics allows to determine optimum immobilization time and maximum allowable adsorbed amount of enzyme which may strongly influence its catalytic activity. The activity in operational modes of the enzyme immobilized membrane could be reduced due to a stagnant thin layer formation surrounded around the non-soluble enzyme molecules that prevents the free transport of substrate and products into or from the catalytic micro-environment. During enzymatic processes the external and internal mass transfer resistances should be minimized to apply the Michaelis-Menten kinetics which assumes that the system does not involve any mass transfer limitations. In general operating parameters are adjusted such that the mass transfer resistance is minimized. In this chapter, a theoretical approach for the estimation of some important kinetic properties of an enzyme immobilized membrane is discussed.

3.2. Enzyme Adsorption Kinetics

During preparation of an enzyme immobilized membrane in static conditions, there are mainly two distinctive processes that affect the overall rate of adsorption. Molecules first diffuse from the bulk solution to an area close to the membrane surface then transfer from this nearby position to the adsorbed state [101]. The adsorption process is said to be diffusion controlled if step 1 is much slower than step 2, and reaction controlled if the opposite is true. In general, protein concentration on the boundary layer is excessively higher than its bulk concentration which leads to molecules diffuse faster. A schematic representation of the enzyme adsorption onto a

membrane surface is illustrated in Figure 3.1. In cases where electrostatic interactions and post-adsorption conformational changes are important, reaction controlled model has been proposed [102]. The model assumes that the concentration of the macromolecules in the bulk solution is uniform and the same as that at the liquid/solid interface. No enzyme-enzyme interaction is taken into account. Every portion of the surface has the same energy of adsorption. Non-uniformity on a rough and porous membrane surface strongly influence the adsorption process so, the membrane surface is assumed to be smooth and each molecule is adsorbed on well defined sites. Langmuir isotherm is used to interpret adsorption at the solid-liquid interface. According to the model, there is a thin layer with a thickness of a few molecular diameters only, immediately adjacent to the surface. The reaction-controlled adsorption occurs within this layer and the rate of adsorption on the membrane surface is described by the following equation.

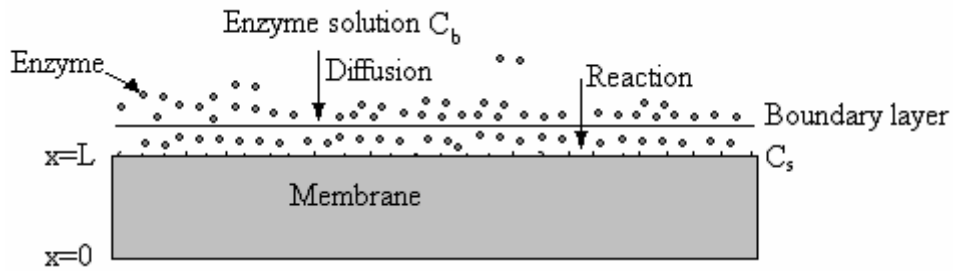


Figure 3.1. Schematic representation of enzyme adsorption process

$$\frac{d\Gamma}{dt} = k_1 C_s \left(1 - \frac{\Gamma}{\Gamma_{\max}}\right) \quad (3.1)$$

In this equation, the term $\left(1 - \frac{\Gamma}{\Gamma_{\max}}\right)$ accounts for the decrease in available membrane area and the surface concentration of the macromolecule, C_s , is equal to its bulk concentration ($C_s = C_b$). If Equation 3.1 is rearranged as

$$\frac{d\Gamma}{dt} = k_0 (\Gamma_{\max} - \Gamma) \quad (3.2)$$

and integrated between $t=0$ and $t=t$, then

$$\Gamma(t) = \Gamma_{\max} \left[1 - e^{-k_0 t}\right] \quad (3.3)$$

where, $k_0 = \frac{k_1 C_b}{\Gamma_{\max}}$.

Equation 3.3 was used to correlate urease adsorption kinetics with two fitting parameters, Γ_{\max} and k_0 .

3.3. Mass Transfer Resistances During Biocatalytic Membrane Processes

In the operational modes of the biocatalytic membranes, external and/or internal mass transfer resistances should be minimized in order to increase substrate conversion, and hence the efficiency of the process. External mass transfer resistance might be expected in the case of enzyme immobilized on the surface of the membrane since homogenous catalytic reaction becomes heterogeneous on which a stagnant liquid surrounding the solid enzyme hinders the transport of the substrate molecules. Figure 3.2 shows substrate and product profiles in the immobilized enzyme system as a consequence of partition and mass transfer limitations under static condition. Substrate conversion takes place in three steps; substrate transport from the bulk medium to the surface of the biocatalyst, enzymatic conversion into product and product transport back from the surface to the bulk medium. The substrate or product diffusion limits the catalytic efficiency of the enzyme in which any of these steps is the rate-limiting.

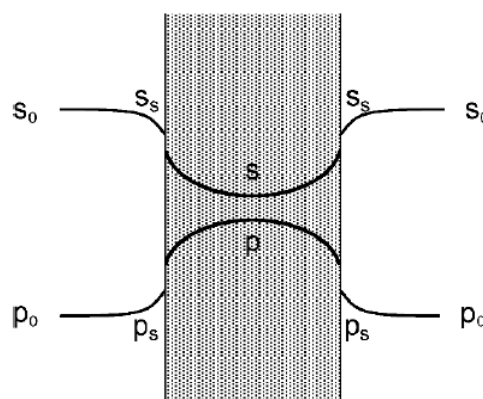


Figure 3.2. Concentration profiles of substrate and products at interface and in the immobilized enzyme system as a consequence of partition and mass transfer limitations.

At steady-state, the average rate of substrate transport from the bulk fluid to the membrane surface is balanced by the enzymatic reaction rate.

$$r = k_s (s_0 - s_s) = \frac{V_{\max} \cdot s_s}{K_m + s_s} \quad (3.4)$$

Here s_s and s_0 are the substrate concentrations at the interface and in the bulk fluid respectively, and k_s is the mass transfer coefficient of the substrate. The rate of reaction, r , can be determined by the substrate transport rate (diffusion limited) (Case I) or by catalytic potential of the enzyme (reaction limited) (Case II). In Case I, reaction rate is so fast with respect to substrate transport and its profile is steep, and can be negligible with respect to s_0 , while in Case II, substrate transport is so fast with respect to reaction rate, so there is no concentration profile which means that the substrate concentration at the catalytic surface is exactly the same as in the bulk medium. Equation 3.4 can be put in a dimensionless form as follows;

$$\beta_0 - \beta_s = \frac{\lambda \cdot \beta_s}{1 + \beta_s} \quad (3.5)$$

where, $\beta_0 = s_0 / K_m$, $\beta_s = s_s / K_m$, $\lambda = V_{\max} / k_s \cdot K_m$.

The influence of external mass transfer resistance on the overall enzymatic reaction is represented using the effectiveness factor, η , which is defined physically by

$$\eta = \frac{\text{Observed reaction rate}}{\text{Rate which would be obtained with no mass transfer resistance, i.e, } s_s = s_0}$$

Mathematically, η , is described by the following equation.

$$\eta = \frac{\frac{V_{\max} \cdot s_s}{K_m + s_s}}{\frac{V_{\max} \cdot s_0}{K_m + s_0}} = \frac{\beta_s (1 + \beta_0)}{\beta_0 (1 + \beta_s)} \quad (3.6)$$

β_s required in Equation 3.6 can be calculated from Equation 3.7 using measurable values of β_0 and λ . In Equation 3.7 only the positive root will give the positive value of β_s .

$$\beta_s = \frac{-(1 + \lambda - \beta_0) \pm \sqrt{[(1 + \lambda - \beta_0)^2 + 4\beta_0]}}{2} \quad (3.7)$$

The effectiveness factor can be calculated once λ and β_0 are known. λ value is evaluated using V_{\max} and K_m values determined from Lineweaver-Burk plot and the mass transfer coefficient during reaction can be calculated using the empirical correlation developed by Smith [103].

$$\frac{k_s \cdot r_{mem}}{D_{i,\infty}} = \alpha Re^{0.567} \cdot Sc^{0.33} \quad (3.8)$$

The definitions of Re and Sc numbers are given below.

$$Re = \frac{D_p^2 N \rho_w}{\mu_w} \quad (3.9)$$

$$Sc = \frac{\mu_w}{\rho_w D_{i,\infty}} \quad (3.10)$$

The free diffusivity of urea can be obtained from the empirical correlation of Wilke-Chang.

$$D_{i,\infty} = \frac{117.3 \cdot 10^{-18} (\varphi M_w)^{1/2} T}{\eta_w \nu_A^{0.6}} \quad (3.11)$$

Here, in this equation the association factor, φ , for water is taken as 2.6 [104].

Under dynamic conditions, mass transfer resistances present during the transfer of the substrate from the feed side to the permeate side are shown in Figure 3.3. The relative importance of the mass transfer compared to the enzymatic reaction is determined by a dimensionless number called Damköhler number, D_a . The Damköhler number can be interpreted as the ratio of the maximum reaction rate to the maximum mass transfer rate.

$$D_a = \frac{V_{\max}}{K_0 S_0} \quad (3.12)$$

If $Da \ll 1$, the maximum mass-transfer rate is much larger than the maximum rate of reaction and the process is said to be in the reaction-limited regime. On the other hand, when the mass-transfer resistance is large, mass transfer is the limiting process and $Da \gg 1$. K_0 in Equation 3.12 corresponds to the overall mass transfer coefficient and it is obtained from the sum of all resistances shown in Figure 3.3

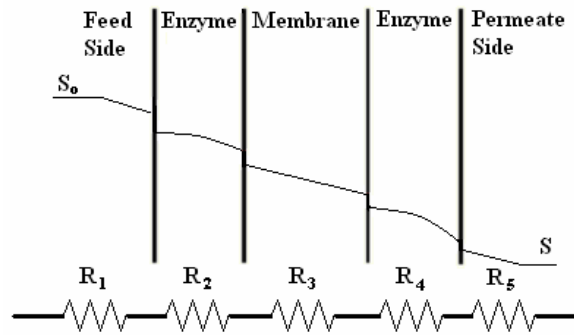


Figure 3.3. The variation of substrate concentration through an enzymatic membrane under dynamic condition.

$$R_T = R_1 + R_2 + R_3 + R_4 + R_5 = \frac{1}{K_0} = \frac{1}{k_s} + \frac{L_{enz}}{D_e} + \frac{L_{mem}}{D_m} + \frac{L_{enz}}{D_e} + \frac{1}{k_p} \quad (3.13)$$

In Equation 3.13 the mass transfer coefficient on the feed side, k_s , is calculated from Equation 3.8 and on the permeate side from the thickness of the boundary layer, δ_p , and free solution diffusivity as follows;

$$k_p = \frac{D_{i,\infty}}{\delta_p} \quad (3.14)$$

The effective solute diffusivities in the enzyme layers and in the membrane are calculated by multiplying the free solution diffusion coefficients with the partition coefficient, porosity and diffusive hindrance factor.

$$D_{eff,i} = \varepsilon_i \Phi_i K_{i,D} D_{i,\infty} \quad (3.15)$$

The solute diffusive hindrance factor, $K_{i,D}$, is a function of the ratio between the solute and the pore diameters ($\lambda_i = d_{i,s} / d_p$) [105]. If parabolic fully developed solute flow within the pore is assumed, the diffusive hindrance factor can be defined as [106]:

$$K_{i,D} = 1.0 - 2.30\lambda_i + 1.154\lambda_i^2 + 0.224\lambda_i^3 \quad (3.16)$$

The partition coefficient in Equation 3.15 is calculated by assuming spherical solutes in cylindrical pores and the expression is given below.

$$\Phi_i = (1 - \lambda_i)^2 \quad (3.17)$$

During filtration of substrate solution through enzymatic membrane layers, internal mass transfer resistance may also be considered. One of other important dimensionless numbers called Thiele modulus, κ , can be used to identify the transport mechanism by comparing enzyme catalytic potential and substrate mass transfer rate with the expression given below.

$$\kappa = \left(\frac{V_{\max}}{D_{\infty m} C_{Feed}} \right)^{1/2} L_{mem} \quad (3.18)$$

A high value of κ , say $V_{\max} / C_{Feed} \gg D_{\infty m}$ implies that the system is mass transfer limited while in the case of small values of κ , the process is controlled by catalytic reaction.

3.4. Activation Energy of Biocatalytic Reaction

The activation energy or energy barrier of the reaction, E_a (kcal/mol) may be different in free and immobilized form of an enzyme due to conformational changes occurred during immobilization. The activation energies of free and immobilized urease can be an indication of immobilization efficiency. The relationship between the rate of an enzymatic reaction, V , and the activation energy, E_a , is given by the Arrhenius equation:

$$V = Ae^{-E_a/RT} \quad (3.19)$$

The activation energy, E_a , can be determined from the slope of $\ln V$ plotted as a function of $1/T$.

3.5. Deactivation Kinetics during Storage of Enzyme

During storage of an enzyme both in free or immobilized forms in water or in buffer solution, deactivation may occur from the conformational and micro-environmental effects involving structural changes of enzyme and the interactions between enzyme-enzyme molecules or enzyme and ionic components available in solution. In addition, the release of weakly adsorbed enzymes into the bulk solution may also lower the activity. There are usually two models accepted to describe the deactivation kinetics during storage test for the free and immobilized forms of enzymes; exponential model and linear model which are expressed below.

$$\ln \left[\frac{V(t)}{V(0)} \right] = -k_d t \quad (3.20)$$

$$V(t) = V(0) - k_d t \quad (3.21)$$

In those equations, $V(0)$ and $V(t)$ represent initial reaction rate and the reaction rate at any time of storage respectively while k_d is the deactivation constant.

CHAPTER 4

MODELING OF UREASE IMMOBILIZED MEMBRANES

4.1. Introduction

Enzyme immobilized membranes combine biocatalytic conversion and separation and recently have been advanced in pharmaceutical industries, food industries, waste-water treatments and biomedical therapies for concentration, purification, fractionation and reaction mediation purposes [14, 15]. The process efficiency is increased while using immobilized form of enzymes which enables easy recovery and hence prevents product contamination, repetitive use, continuous operation of enzymatic process, and rapid termination of reactions under soft operating conditions.

During ultrafiltration processes, the process efficiency is determined by surface properties of membrane (surface charge, hydrophobicity and roughness), characteristics of solute (particle size and charge), solution chemistry (solution pH and ionic strength), and system hydrodynamics (feed velocity and operating pressure).

Modeling of transport rates of solutes during ultrafiltration processes is important for the determination of the system efficiency. Model equations allow optimizing transport characteristics of membrane and operational conditions. The effects of pore size, thickness of the skin layer and the catalytic layer if enzyme is available on the surface of the membrane, types of enzyme immobilization and also the effects of transmembrane pressure and concentration polarization on the solute flux can be predicted by coupling convective and diffusive transport.

In literature, there are two distinct physical models, solution diffusion and hydrodynamic (pore) models that describe solute diffusion through membranes. The solution diffusion model does not take into account the presence of a porous layer, only considers the diffusion of species without interaction with the assumption of no pressure drop across the separating layer. The pore model assumes the membranes have pores as bundles of capillary tubes. Toh et al.[2007] studied the effect of membrane formation parameters on transport through integrally skinned asymmetric polyimide organic

solvent nanofiltration membranes [107]. The experimental data was interpreted both by solution diffusion and pore flow models. Authors concluded that both models can adequately describe the performance of the membranes. In reference [108], solute transfer through a catalytic membrane has been analyzed based on solution diffusion model.

In this chapter, a mathematical model was developed to predict solute transport rates through enzyme immobilized membranes. The model is fully predictive and the model predictions were compared with the experimental data. For this purpose urease was immobilized onto polyethyleneimine (PEI) modified AN69 membrane (AN69-PEI-URE). Ultrafiltration experiments were conducted under different transmembrane pressures and urea concentrations using dead-end ultrafiltration module.

4.2. Theory

The schematic diagram of an enzyme immobilized membrane is shown in Figure 4.1. The enzyme is immobilized on both surface of the membrane. Transport phenomena across such a membrane are described as follows: Penetrant flows from feed side into enzyme layer-1, in which hydrolytic reaction is subsequently generated by the enzyme. The products and unreacted solute are then transported from the membrane into enzyme layer-2 where further conversion of unreacted solute occurs.

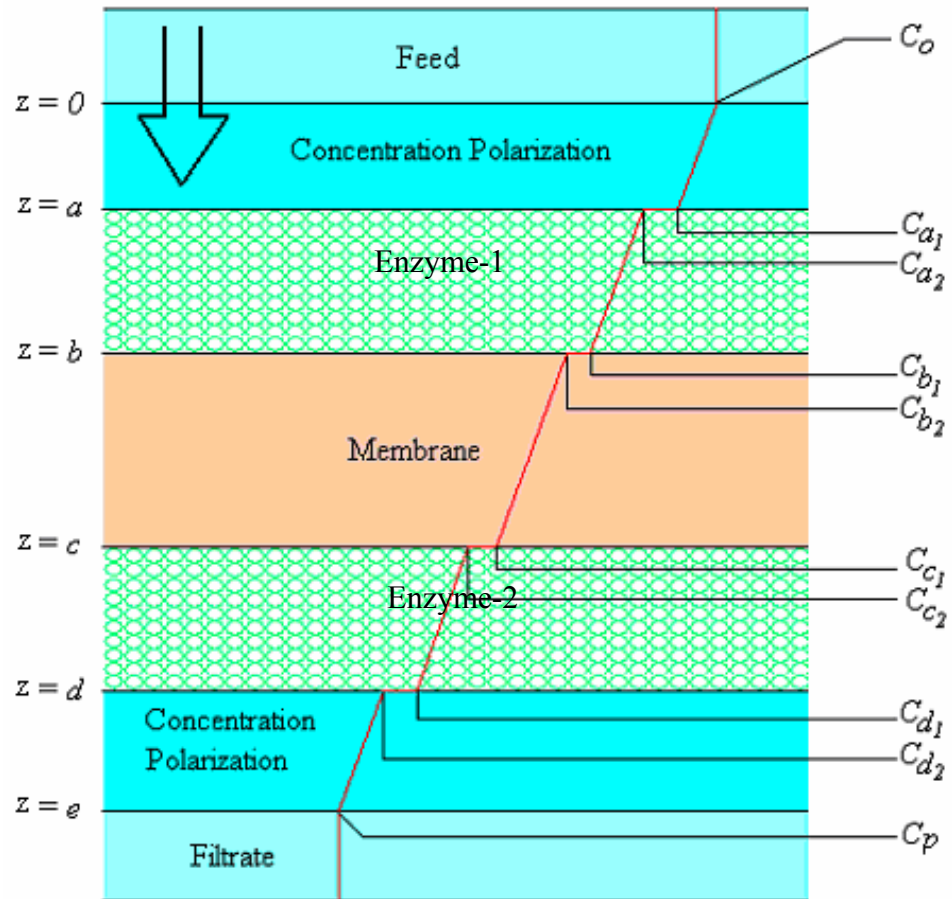


Figure 4.1. Schematic diagram of an enzyme immobilized membrane with substrate concentration profile

The following assumptions were utilized to develop the model equations:

- Substrate and products flowing across membrane immediately attain the steady-state.
- Substrate transport across the membrane can be described by Nernst-Planck equation.
- The enzyme kinetic rate obeys the simplest Michaelis-Menten equation.
- The reaction takes place only in the catalytic layer.
- The enzyme activity does not change along the filtration process.
- Substrate diffusivity through enzyme and membrane layers is independent of substrate concentration
- Mass transfer is one dimensional and takes place under isothermal conditions.

Substrate solution whose initial volume and concentration is V_0 and C_0 is filtrated by the application of a constant pressure through an enzymatic membrane. The difference in transmembrane pressure causes to move the substrate molecules through enzyme and membrane layers. The filtrated solution is collected in a beaker. An unsteady-state equation is appropriate to identify the change in feed and permeate concentrations as a function of time. The overall mass balance by considering volume change occurred in feed and permeate sides are defined as follows;

$$\frac{d(C_F V_F)}{dt} = -k_{mF} A_0 (C_F - C_{a,1}) \quad (4.1)$$

$$\frac{d(C_P V_P)}{dt} = -k_{mP} A_0 (C_{d,2} - C_P) \quad (4.2)$$

If we transform Equations 4.1 and 4.2 into dimensionless form using dimensionless parameters given in Appendix-A, Equations 4.3 and 4.4 were obtained

$$-(Pe)C_F^* + \delta V_F^* \frac{dC_F^*}{dt^*} = -Bi_F [C_F^* - C_{F,i}^*] \quad (4.3)$$

$$(Pe)C_R^* + \delta V_R^* \frac{dC_R^*}{dt^*} = Bi_P [C_{P,i}^* - C_R^*] \quad (4.4)$$

The dimensionless volume change during filtration can be calculated by the following equations;

$$V_F^*(t) = (V_{F0} - J_v A_0 t) / V_{F0} \quad (4.5)$$

$$V_R^*(t) = J_v A_0 t / V_{F0} \quad (4.6)$$

In equations 4.1 and 4.2 the interfacial solute concentrations (e.g. $C_{a,1}$, $C_{d,2}$) are related to the solute concentrations in the enzyme or membrane layers. Partition coefficient reflects the ratio of the solute concentrations at each interface of the layers

through linear equilibrium relationships as follows;

$$\Phi_i = C_{i2} / C_{i1} \quad (4.7)$$

where, $i=a, b, c, d$ and Φ_i is the partition coefficient.

Substrate transport through each layer is described by the extended Nernst-Planck equation which is given below. This equation consists of flux terms due to diffusive, convective and electric field gradient under steady state conditions. To simplify, the flux term due to electric field gradient is ignored and the remaining terms are given in Equation 4.8.

$$N_i = K_{i,C} C_i J_i - \varepsilon K_{i,D} D_{i,\infty} \frac{dC_i}{dx} \quad (4.8)$$

The species continuity equations through the enzyme and membrane layers are given below;

$$\frac{\partial N_i}{\partial x} + r = 0 \quad (4.9)$$

$$\frac{\partial N_i}{\partial x} = 0 \quad (4.10)$$

The reaction term, r , is determined assuming the reaction obeys Michaelis-Menten kinetic which can be calculated by the following equation;

$$r = \frac{V_{\max} C_i}{K_m + C_i} \quad (4.11)$$

In the dimensionless form, the species continuity equations for the enzyme and membrane layers can be written below

$$(K_{e,C} Pe) \frac{dC_e^*}{dz^*} - (K_{e,D} \varepsilon_e D_{Re}) \frac{d^2 C_e^*}{dz^{*2}} = \frac{\lambda^2 C_e^*}{\theta + C_e^*} \quad (4.12)$$

$$(K_{m,C} Pe) \frac{dC_m^*}{dz^*} - (K_{m,D} \varepsilon_m) \frac{d^2 C_m^*}{dz^{*2}} = 0 \quad (4.13)$$

To solve these equations, 4 boundary conditions are required which are given below.

$$B.C.I \text{ at } z = a \quad N_A|_{Enzyme-I} = N_A|_{feed} = k_{mF} A_0 (C_F - C_{a,1})$$

$$B.C.II \text{ at } z = b \quad N_A|_{Enzyme-I} = N_A|_{membrane}$$

$$B.C.III \text{ at } z = c \quad N_A|_{Membrane} = N_A|_{Enzyme-II}$$

$$B.C.IV \text{ at } z = d \quad N_A|_{Enzyme-II} = N_A|_{fpermeate} = k_{mP} A_0 (C_{d,2} - C_P)$$

These conditions are simply obtained from the continuity of the fluxes at the boundaries. The solution flux, J_i , required in Equation 4.8 is obtained by the use of Hagen-Poiseuille equation [109].

$$J_i = \frac{n\pi r_p^4 \Delta P}{8\mu_w \delta_i} \quad (4.14)$$

where, $n\pi r_p^2$ is the membrane porosity and Equation 4.14 changes to $J_i = (\varepsilon_i r_p^2 \Delta P / 8\mu_w \delta_i)$.

The solute diffusive hindrance factors for the enzyme and membrane layers $K_{e,D}$ and $K_{m,D}$ in Equation 4.12 and 4.13 can be calculated from Equation 3.14. For the convective hindrance factors $K_{i,D}$, $K_{i,c}$, Equation 4.15 is used.

$$K_{i,c} = (2 - \Phi_i) (1.0 + 0.054\lambda_i - 0.988\lambda_i^2 + 0.441\lambda_i^3) \quad (4.15)$$

The partition coefficients for the enzyme and membrane layers are already given in Equation 3.17. Stokes Einstein equation is used to find the solute radius,

$$r_s = \frac{k_1 T}{6\pi\mu D_{i,\infty}} \quad (4.16)$$

The membrane porosity is obtained from Equation 4.17,

$$\varepsilon = 1 - \frac{m}{\rho_p A \delta_m} \quad (4.17)$$

where, ρ_p is the density of the membrane (1,170 kg/m³).

In this model enzyme molecules are considered to be spheres. The porosity of enzyme layer depends on the way in which the spheres are distributed. For a regular packing of enzyme molecules shown in Figure 4.2, the porosity corresponds to 0.48 [108].

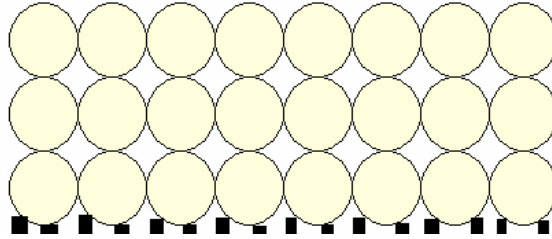


Figure 4.2. Regular packing of enzyme molecules

In order to calculate enzymatic gel layer thickness, δ_e , the enzyme surface concentration is divided to the protein concentration, c_g , in the gel layer. The surface concentration is determined from the protein balance before and after immobilization while concentration in the gel layer is given as follows considering enzymatic gel layer as system of a monodisperse spheres.

$$c_g = (1 - \varepsilon)\rho_g \quad (4.18)$$

Gel density, ρ_g , was assumed to be 1000 kg/m^3 in the calculations. Pore size of the enzyme layer is calculated from the radius of the circle of the remaining area among four spheres which is schematically shown in Figure 4.3.

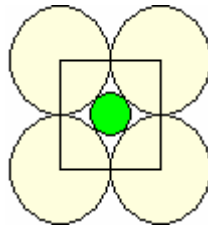


Figure 4.3. Schematic illustration of pore size calculation procedure for the enzyme layer. (Pore size of the layer is determined by subtracting the area of four quarter circles from the area of square. The pore size is regressed by fitting a circle into the remaining area).

Mass transfer coefficient on the permeate side and the solute diffusivities (effective diffusivity) in the enzyme layers and in the membrane can be evaluated using Equation 3.14 and 3.15 respectively given in Chapter 3.

4.3. Solution of Model Equations

Before simulation all parameters were introduced numerically to the program. For the simulation, the following parameters are introduced: Initial feed concentration, partition coefficients of substrate at the phase boundaries, mass transfer coefficients of the substrate on the feed and permeate sides, diffusion coefficients of substrate in solution, in the enzyme layers and in the membrane, enzyme kinetic constants, enzyme layer and membrane thicknesses, porosities, pore sizes, molecular size of the substrate, the area of the membrane, feed side volume, stirring rate and transmembrane pressure.

To solve equations, they were first discretized using finite difference approximation. The 12 algebraic equations were simultaneously solved for each node using FindRoot command in Mathematica which is capable to solve nonlinear equation systems. Before simulation, one starting value was specified (e.g. 0.01) in which case Newton methods are applicable. AccuracyGoal is selected as Automatic. The time and position intervals (Δt and Δx) were defined in changeable mode which allow to make stability easily. The simulation calculates the concentration profiles in the feed and permeate side and along the enzymatic membrane by generating 5000 data which correspond 25 minutes.

CHAPTER 5

OBJECTIVE

The main objective of this study is to prepare an active and stable biocatalytic ultrafiltration membrane for combining separation and catalytic abilities. Urease was selected as a model enzyme because of its extremely high reaction rate against urea which is among the hazardous toxic chemicals for human body in cases of renal insufficiency and for environment when it is discharged without treatment. The urease immobilized membrane can be adapted for the removal of urea if stable and active enzymatic membrane reactor is fabricated. In addition, urease immobilized membranes can be used as diagnostic test-strips for the quantification and qualification purposes. These two applications require successive research about the stability and activity of immobilized urease under static and dynamic conditions. To immobilize urease, commercially available poly (acrylonitrile-co-methallyl sulfonate) AN69 (commercial name) membrane was used as a support material. It is a flat sheet ultrafiltration membrane with a molecular weight cut off value of 30 kDa. The sulfonate groups in its structure not only give hydrophilicity but also provide negative charges. Urease was immobilized on AN69 membrane both through physical and chemical methods. For physical immobilization; negatively charged surface of the support membrane was modified with two types of cationic polyelectrolytes, polyethyleneimine (PEI) and high molecular weight chitosan (CHI). Urease which is negatively charged above its isoelectric point was then easily deposited on the polyelectrolyte layers through electrostatic interactions. Finally, the layer-by-layer self assembly method allowed to cover the enzyme surface with a new polyelectrolyte layer. The last layer was applied to preserve the urease conformation during long time of storage. The advantageous of this method is such that, even urease completely loses its activity, the surface can then be reactivated by adding fresh urease, since the deposition of polyelectrolyte onto surface of a membrane is irreversible. Another advantageous of this method is that the kinetic parameters of immobilized urease are as similar as the parameters of the soluble urease, since immobilized urease does not contact with the support. In addition, the active site of urease is open to substrate because the ionic interaction takes place between the

charged groups on the urease (any active site binding) and the charges available on the polyelectrolyte.

As a second immobilization method, urease was immobilized on AN69 via chemical bonding using EDC/NHS coupling agent. The performances of the urease immobilized by chemical attachment and ionic interactions were evaluated in terms of storage stabilities, pH and temperature profiles as well as the kinetic parameters.

In addition to static conditions, the filtration and catalytic performance of the membranes prepared by means of covalent attachment and layer-by-layer self assembly of urease were also tested under dynamic conditions using a dead-end ultrafiltration cell. The influences of transmembrane pressure and feed concentration on the conversion of urea were investigated. In addition, operational stability of urease was determined.

Finally, a mathematical model was developed to predict the catalytic performance of urease immobilized membrane. Model consists of both the contribution of diffusive and convective transport and enzymatic reaction as well. The model can be used to investigate the effects of the operating conditions (transmembrane pressure, stirring rate, feed composition), membrane properties (pore size, porosity, thickness) and enzyme properties (kinetic parameters) on the filtrate flux and conversion of the substrate.

CHAPTER 6

EXPERIMENTAL

6.1. Materials

Native (AN69) and polyethyleneimine modified polyacrylonitrile (AN69-PEI) membranes of 25 μm in thickness are already used commercially in hemodialysis applications and were kindly provided by Gambro-Hospal Co.(Meyzieu, France). AN69 membrane is produced by copolymerization of acrylonitrile with sodium methallyl sulfonate. The weight percentage of sodium methallyl sulfonate in the copolymer is adjusted to %9 w/w. AN69 membrane is negatively charged due to presence of sulfonate groups. It has been further modified by adsorption of PEI yielding a positively charged membrane. This modified membrane was denoted as AN69-PEI. For surface modification using layer-by-layer deposition technique, polyethyleneimine 50% v/v and high molecular weight chitosan (CHI) as cationic polyelectrolytes (PE) were used and supplied by Sigma . Jack bean urease (URE) type III (EC 3.5.1.5 and U1500-20KU, 1.18 G solid, 17,000 units/G solid) and Bradford reagent (B 6916) for the determination of enzyme amount were purchased from Sigma-Aldrich. Protein content in urease was determined by Bradford method and was found as 0.0347 mg in 1mg of product [110]. N-ethyl-N'-(3-dimethylaminopropyl) carbodiimide hydrochloride (EDC) used as a zero-length crosslinker was purchased from Sigma. N-hydroxysuccinimide (NHS) used for the prevention of side reactions and inhibition of EDC during activation of membrane surface was obtained from Fluka. Urea was obtained from Labosi. For activity measurement, Weatherburn method was used [111]. According to the method, two reagents were prepared. Reagent A consists of phenol (Rectabur >99%) and sodium nitroprusside dihydrate (Fluka) while reagent B contains sodium hydroxide anhydrous pellets (Carlo Erba >97%) sodium hypochlorite (Riedel, 6-14% Cl active). Sodium phosphate buffer solutions (NaH_2PO_4 , Na_2HPO_4) and acetic acid were purchased from Fluka. All aqueous solutions were prepared with milli-Q water (>18M Ωcm).

6.2. Methods

6.2.1. Preparation of Urease Immobilized Membranes Using Layer-by-Layer Deposition (Physical Immobilization)

Two types of membranes made of native (AN69) and polyethyleneimine modified polyacrylonitrile (AN69-PEI) were used as supports for urease immobilization. URE was prepared in 0.01 M sodium-phosphate buffer at pH 7.4 above its isoelectric point (IP 4.9), hence it was applied as negatively charged enzyme. As depicted in Figure 6.1, a small piece of AN69 or polyelectrolyte (PE) deposited AN69-PE membranes were immersed into predetermined concentration of urease solution. Immobilization was carried out under moderate stirring at 4°C during 24 hours. The amount of urease adsorbed onto the surface of the membrane was determined from the decrease in enzyme concentration in solution. Throughout the immobilization, 1x3 ml samples were withdrawn from the solution at predetermined times and analyzed based on Bradford method. At the end, the urease-immobilized membrane was washed twice with 15 ml of water for 15 min. The prepared membrane is denoted as AN69-PE-URE and preserved in water at 4°C. In order to prevent desorption of immobilized urease and hence increase the stability the top layer was further coated with PE by immersing the AN69-PE-URE membrane in PE (either PEI or CHI) solution for 30 min. At this time the prepared membrane is denoted as AN69-PE-URE-PE. To determine the influence of polyelectrolyte type on the efficiency of urease immobilization, CHI has also been used as an alternative to PEI. The membranes involving CHI as a PE were prepared by first immersing the native membranes, AN69, into CHI solution for a period of 30 min at room temperature. Next, the CHI modified AN69 membrane (AN69-CHI) was first immersed into URE solution and then CHI solution to prepare two types of URE immobilized membranes, AN69-CHI-URE and AN69-CHI-URE-CHI, respectively. The conditions for URE immobilizations, washing and CHI deposition were maintained the same as those applied during the preparation of PEI including membranes. PEI and CHI solutions were prepared by continuous stirring overnight maintaining their concentrations as 1g/L and pH values as 8 and 5 respectively using 0.1 M HCl and 0.1 M NaOH.

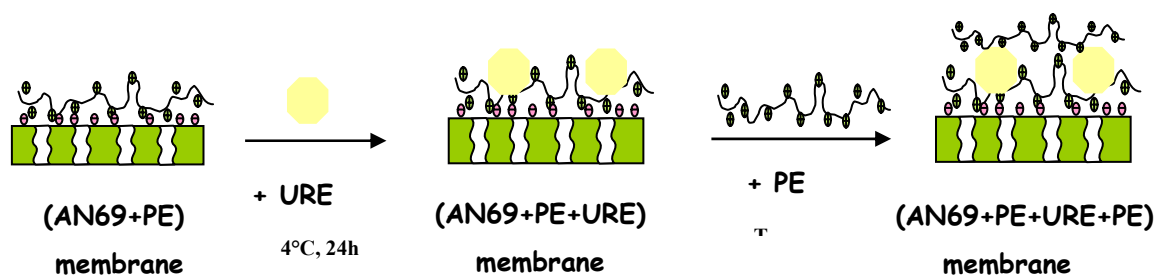


Figure 6.1. Preparation of two kinds of reactive urease immobilized membranes; the one allows directly contact with the environment (AN69-PE-URE) and the other is in sandwiched form (AN69-PE-URE-PE).

6.2.2. Preparation of Urease Immobilized Membranes Using EDC/NHS Coupling Agent for Covalent Bonding (Chemical Immobilization)

6.2.2.1. Hydrolyzation Reaction on AN69 Surface

For the introduction of carboxylic groups onto surface of the AN69 membrane, hydrolysis reaction which is described in Figure 6.2 was carried out using 1M of NaOH. The reaction condition was selected as 50°C and 20 min which is usually reported in literature [91]. During the reaction, cyanide groups (-CN) are partially converted into amide (-CONH₂) and carboxylic groups (-COOH). The reaction temperature and the time are the key parameters that affect the end product, i.e., the proportions of amide, carboxylic and cyanide groups. Modification of amide group leads to change in membrane's mechanical and physical properties such that extending the reaction time results in loss of mechanical strength of the membrane due to the continuous modification of -NH groups in the bulk and increase in hydrophilicity cause a reduction in water permeability because of the swelling. The condition selected in this study is believed to be creating enough surface functional groups without altering the membrane bulk property. At the end of the reaction, the membrane was successively rinsed three times in 50 ml of water each for 15 min and then rinsed again 2 times in 50 ml of phosphate buffer for another 15 min. During rinsing, the color of the hydrolyzed yellowish red AN69 membrane was turned into white.

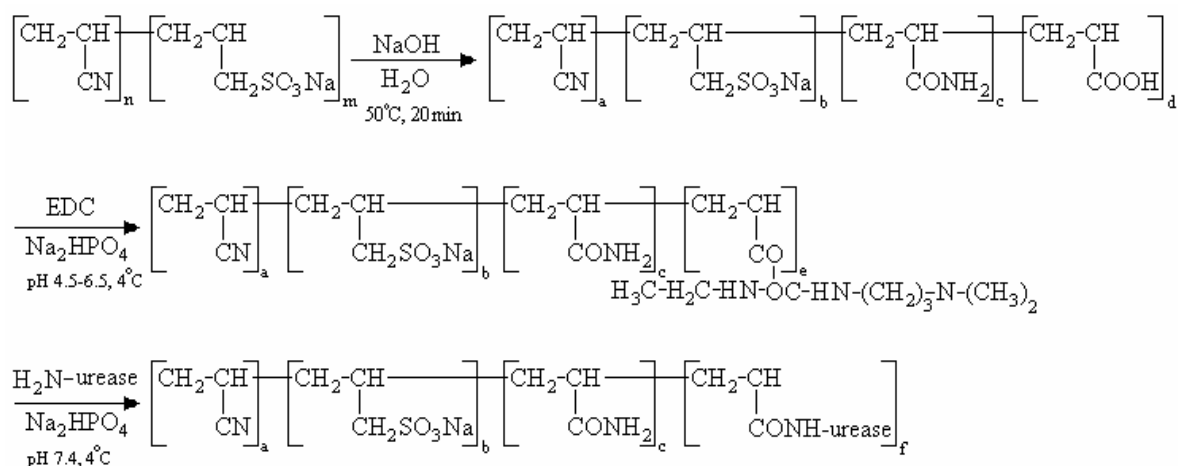


Figure 6.2. Chemical reaction schemes (hydrolyzation, activation and immobilization) for preparing urease immobilized AN69 membrane.

6.2.2.2. Activation of Hydrolyzed AN69 Surface

Rinsed membrane was subsequently put into reaction mixture containing 10 ml of EDC/NHS coupling agent dissolved in phosphate buffer. The concentration of buffer solution and its pH were selected between the intervals of 0.01-0.1M and 4.5-6.5 respectively. Different reaction time from 1 to 24 hours and the concentration of coupling agent from 0 to 0.5 M were examined in order to determine their influences on the final activity. During crosslinking reaction, EDC is covalently bonded to the carboxylic group on the membrane surface as described in Figure 6.2. Then, the membrane was intensely rinsed 3 times with 25 ml of water for 15 min and 2 times in 25 ml of phosphate buffer for 15 min in order to clean the surface from the undesired side products and from the unreacted EDC.

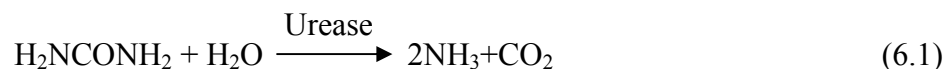
6.2.2.3. Immobilization of Urease onto Modified AN69 Surface

The surface treated membrane was put into 10 ml of predetermined concentration of urease solution (dissolved in 0.01M phosphate buffer at pH 7.4) maintained at 4°C. Optimization during immobilization was performed by changing the urease concentrations from 0.002 to 0.07 mg/ml and immobilization time between the interval from 1 to 24 hours. Based on the mechanism of the displacement between CO

group in the O-acylisourea and NH₂ group in the enzyme structure, urease molecules are covalently bonded to the acetate group remained on the surface of modified AN69 membrane (Figure 6.2). Followed by immobilization, the membrane was rinsed twice in 25 ml of 0.022 M phosphate buffer at pH 7.4. During optimization, the final product was rinsed twice in 25 ml of 0.022 M phosphate buffer at pH 7.4 for 30 min. After the optimization part, the final product was characterized into two groups; one washed only 30 min and the others washed 2 days with water at 4°C. The different rinsing times may affect the stability of the membranes due to release of weakly bonded URE. The amount of URE immobilized onto surface modified AN69 membrane was also determined in the same manner as followed during its physical immobilization.

6.2.3. Determination of Free and Immobilized Urease Activity

Urease catalyzes the hydrolysis of urea to ammonium and carbon dioxide according to the reaction given below.



In the form of free urease, the reaction was carried out by mixing 0.5 ml enzyme (1mg/ml dissolved in water) and 4.5 ml urea solution (10mM prepared in 50 mM and 22 mM Na-phosphate buffer at pH 7.4 for physical and chemical immobilization, respectively) which was already conditioned to reaction temperature of 37°C. At the end of 30 min, reaction was stopped by adding 2.5 ml of acetic acid solution (10%v/v).

In the case of immobilized form of urease, the reaction was started by immersing a small piece of catalytic membrane into 5 ml of urea solution whose temperature was maintained at 37°C. After 30 min reaction, 1 ml of sample was withdrawn and mixed with 0.5 ml of 10% acetic acid solution. In both cases, the reaction mixtures were stirred at a constant rate of 100 rpm.

The concentration of ammonia formed during catalytic reaction was determined by Weatherburn method. Based on the method, 20 µl of the final reaction mixture was poured into a tube which consists of 5 ml of reagent-A (5g of phenol with 25 mg of sodium nitroprusside diluted to 500 ml with water). After shaking gently, 5 ml of reagent-B (2.5 g of sodium hydroxide and 4.2 ml of sodium hypochlorite diluted to 500

ml with water) was added. The mixture was then incubated at 37°C for 20 min. At the end, the color change during incubation which gives a relation to the liberated ammonium concentration was detected at a wavelength of 625 nm using Perkin Elmer UV/VIS Spectrophotometer. The activity of urease was defined as,

$$\text{Activity} = \frac{\text{Number of moles of NH}_3 \text{ produced in 30 min}}{(30 \text{ min}) \times (\text{cm}^2)} \quad (6.2)$$

6.2.4. Determination of Optimum pH and Temperature of Free and Immobilized Urease

Enzyme is a PE carrying both positive and negative charges distributed around the exterior of it. It is thus, depending on the pH and ionic strength of the media, charge interactions between enzyme and surroundings can be expected which may alter the catalytic activity. In general, enzymes can protect their structural singularity under at least physiological conditions, i.e., in the range of 0 to 45°C, pH 5 to 8 and in aqueous solutions of about 0.15 M ionic strength. Beyond these conditions they lose their normal nature or structure which is known as the phenomena of denaturation. Based on this fact, the optimum pH and temperature of free and immobilized URE were determined in the pH ranges between 5-9 and temperature ranges of 10-60°C using the same reaction conditions mentioned above.

6.2.5. Determination of Kinetic Parameters of Free and Immobilized Urease

The kinetic parameters of free and immobilized forms of urease were determined by measuring the initial rate of reaction (V_i) with increased urea concentrations ($[S]$). They were then obtained from the intercept and slope of the Lineweaver and Burk plot which uses the linear transformation of the Michaelis-Menten expression.

$$\frac{1}{V_i} = \left(\frac{K_m}{V_{\max}} \right) \frac{1}{[S]} + \frac{1}{V_{\max}} \quad (6.3)$$

6.2.6. Determination of Storage Stabilities of Free and Immobilized Urease

Free and immobilized URE were stored in water at 4°C. Their storage stabilities were determined by measuring the residual activities after a given time of storage.

6.2.7. Filtration Studies

Filtration studies were performed using a dead-end stirred cell filtration system (Model 8050, Millipore Corp, Bedford, MA) with a total internal volume of 10 ml and an active surface area of 4.1 cm². The feed side pressure was maintained by nitrogen. To avoid concentration polarization the feed solution was continuously stirred with a speed of 300 rpm. Filtrate samples were collected at several transmembrane pressures measuring the filtrate flux by means of an analytical balance (Sartorius) and in all permeation experiments system temperature was maintained at 23±2°C.

Throughout the permeation experiments, following protocol was applied. First, the native membrane AN69-URE in the case chemical immobilization and AN69-PEI-URE and AN69-PEI-URE-PEI membranes prepared with physical immobilization was placed into the cell and compacted twice with water at 2 bar for 10 min. After observing almost the same water permeability between those two compaction tests, the permeation of water solutions with increasing pressure was measured. Then, the similar permeability experiments were carried out using buffer solution. Buffer permeation experiment was repeated after the commercial membrane was immobilized with urease. The latter was aimed for comparison. This was the reference for the permeation of urea solution prepared in the concentration of 0.5, 5, 10 and 50 mM. During a set of an experiment, the membrane was exposed to urea solution from 0.5 to 50 mM under constant pressure. The same procedure was followed for different transmembrane pressures (0.5, 1.0, and 1.5 bar) and the protocol is illustrated in Figure 6.3. At the lowest pressure, 30 min was required to attain stable flux and the permeability of the solution was calculated by collecting permeate after stabilization was achieved. For the whole membranes, urea analysis of retentate and permeate sides were performed at the end of 10 min filtrations.

In order to determine the ammonia concentration which is related to the catalytic efficiency during filtration experiment, 100 μl of sample was withdrawn from the permeate side at each 10 min time intervals for the AN69-PEI-URE membrane at three different transmembrane pressures (0.7, 1.1 and 1.4 bar).

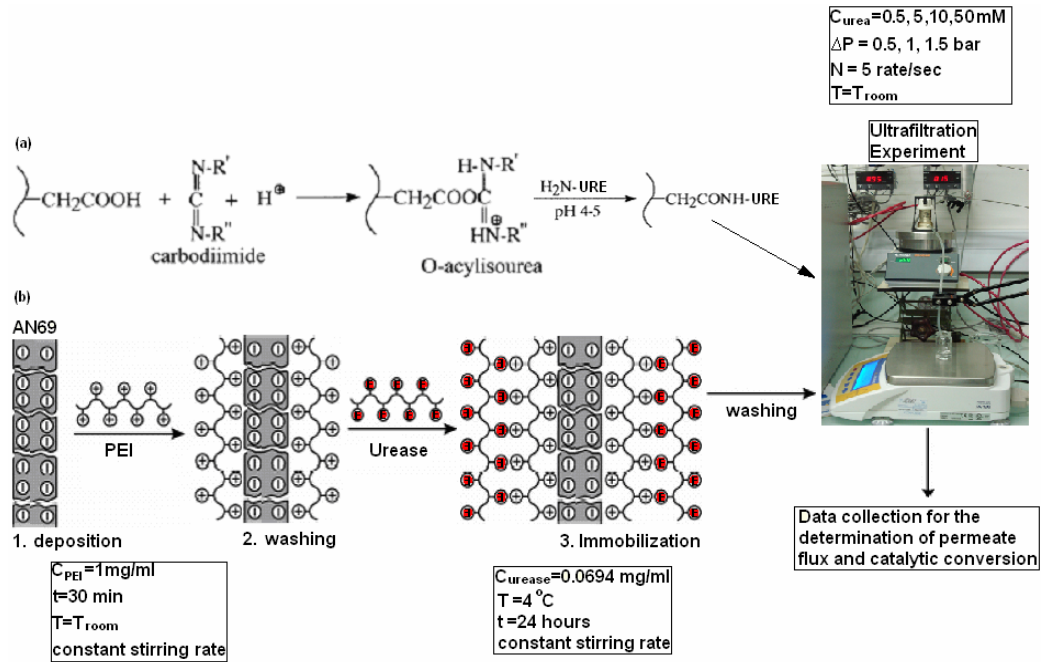


Figure 6.3. Experimental protocol for the filtration of urea through URE immobilized membranes by means of chemical and physical attachment.

40 μl of this sample was mixed with 20 μl of 10% acetic acid solution for determining ammonia content by Weatherburn method (C_1). Total amount of urea in filtrate and retentate solutions were determined by decomposing all urea enzymatically. For this purpose 60 μl of urea solution was reacted with 10 μl of urease (0.347 mg urease/ml solution was used in 22 mM buffer at pH 7). The enzymatic reaction was carried out at 37 $^\circ\text{C}$ for 60 min. Then, the reaction was stopped with 35 μl of 10% acetic acid. During 60 min, urea was totally converted to ammonia and its concentration was determined following the same procedure given above (C_2). Finally, unreacted urea concentration was calculated by subtracting C_2 from C_1 and then dividing this value to 2.

CHAPTER 7

RESULTS AND DISCUSSION

7.1. Studies with Native Urease

7.1.1. Determination of the Effect of Phosphate Buffer Concentration on the Activity of Native Urease

In aqueous solution, ammonia and carbon dioxide produced from the reaction of urease-catalyzed hydrolysis of urea generate a net increase in pH. In general the reaction has been studied in buffers to eliminate the change in pH. However, an optimization should be performed by the adjustment of ionic strength and pH of the buffer solution that may cause inhibitory action by protonating or deprotonating of the enzyme functional groups. To clarify this, urease activity was measured at different buffer concentrations between 10-100 mM from pH 5 to 9. Figure 7.1 shows the activity versus urea concentration. It is well known from the literature that the activity of urease is strongly altered in acidic media because of competitive action of H_2PO_4^- ions with respect to urea molecules [112]. The ions come from the sodium-phosphate buffer. However, from Figure 7.1, one can conclude that there is no considerable change in the activities for the measured pH range. This may be explained by the rapid increase of the pH after a few second of the reaction, so that enzyme can maintain its stability during reaction time.

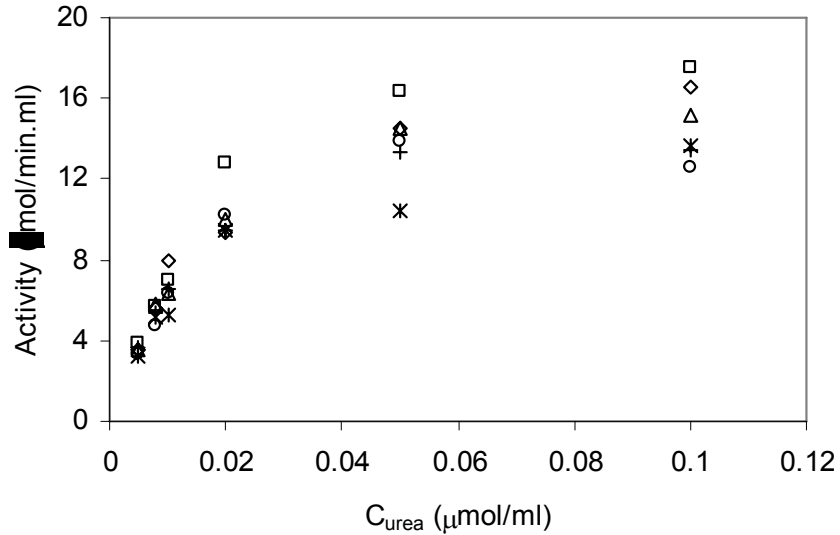


Figure 7.1. The change in activity as a function of urea concentration. Symbols represent pH of the reaction mixture at constant buffer concentration of 0.01M. Symbols: (\diamond) pH 5, (\square) pH 6, (\triangle) pH 7, (\circ) pH 7.4, ($*$) pH 8, ($+$) pH 9.

The pHs of all the samples reported in Figure 7.1 was measured at the end of 30 min reaction and their variations are illustrated in Figure 7.2. The pHs of all enzymatic reactions reached to similar value around 9 which indicated that buffering power (10 mM) was not sufficient.

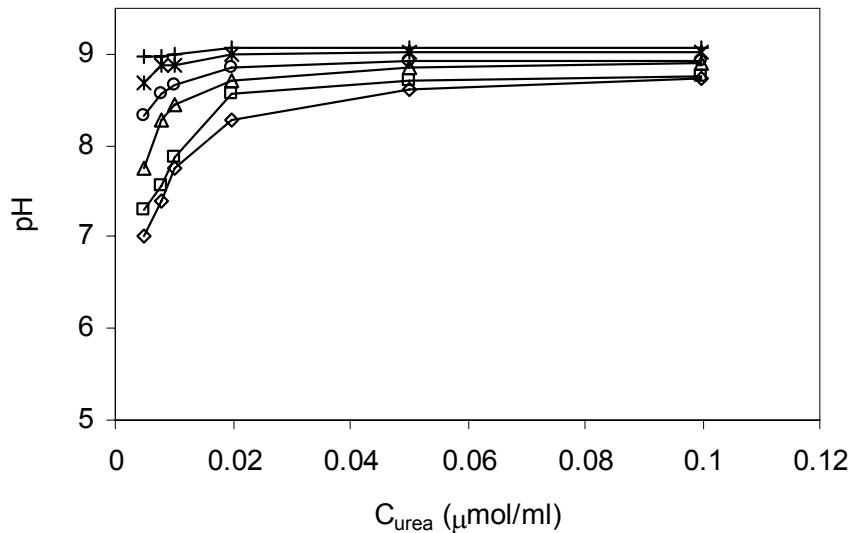


Figure 7.2. The change in pH as a function of urea concentration. Here, pHs represents the solution pH measured after 30 min reaction. Symbols represent pH of the reaction mixture at constant buffer concentration of 0.01M. Symbols: (\diamond) pH 5, (\square) pH 6, (\triangle) pH 7, (\circ) pH 7.4, ($*$) pH 8, ($+$) pH 9.

In order to see the buffer effect on the activity of the native enzyme, urea solutions in different buffer concentrations were prepared and their activities were measured. Figure 7.3 illustrates the variation of the activities of the native urease as a function of urea concentrations at pH 6. The enzymatic activity increased inversely with the buffer concentration. Above the buffer concentration of 0.02 M, it has a competitive inhibitory action on the enzyme performance. In reference [112], competitive inhibitory action induced by the H_2PO_4^- ion is reported and increase in buffer concentration decreased the urease activity.

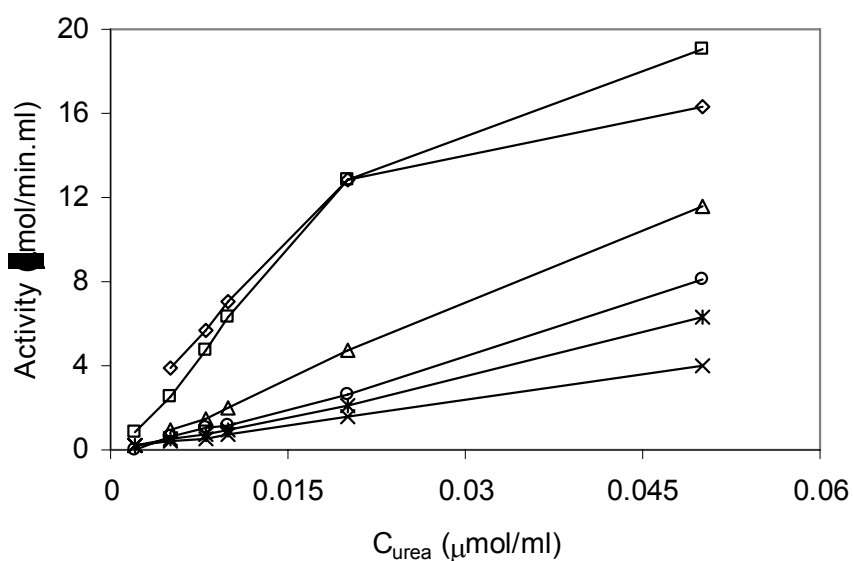


Figure 7.3. Activity change for the native urease as a function urea concentrations. Buffer concentrations: (\diamond) 0.01 M, (\square) 0.02 M, (\triangle) 0.05 M, (\circ) 0.08 M, ($*$) 0.1 M, ($+$) 0.15 M. Reactions were carried out at pH 6, 37°C for 30 min with 3.47 $\mu\text{g/ml}$ urease.

Figure 7.4 illustrates the change in pH obtained from the same experiments shown in Figure 7.3. The activity increase of native urease is proportional to formation of ammonia which then leads to excessive increase in pH especially at lower ionic strength of solution. Increasing buffer concentration increases H_2PO_4^- concentration that inhibits the liberation of ammonia by the action of protonation of active site group of enzyme (catalytic histidine).

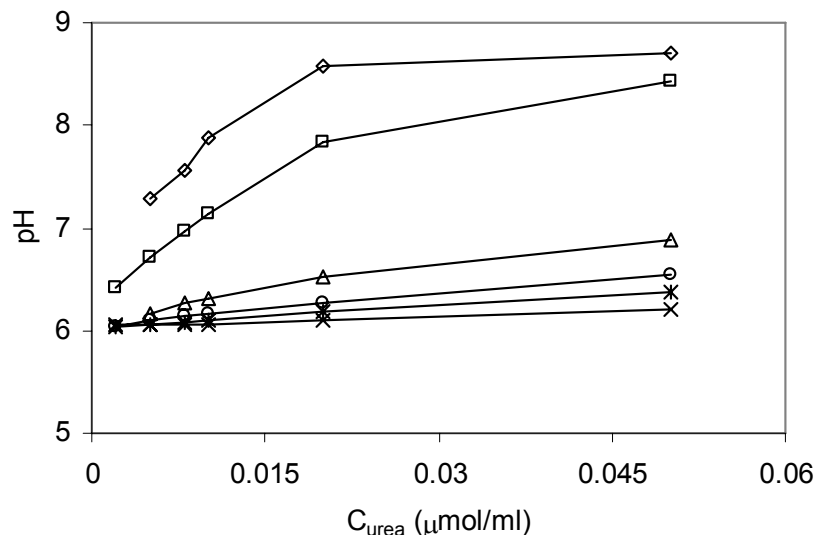


Figure 7.4. The change in pH at the end of 30 min reaction as a function of urea concentrations. Buffer concentrations: (\diamond) 0.01 M, (\square) 0.02 M, (\triangle) 0.05 M, (\circ) 0.08 M, ($*$) 0.1 M, (+) 0.15M. Reactions were carried out at pH 6, 37°C for 30 min with 3.47 $\mu\text{g/ml}$ urease.

From Figure 7.3 and 7.4, one can conclude that even though there is a small inhibition effect of 50 mM sodium phosphate buffer on the activity of urease especially at lower substrate concentrations (less than 10 mM urea solution), negligible pH variation during 30 min reaction was observed. The change in ammonium concentration during 30 min. reaction is shown in Figure 7.5. The linear increase in absorbance values indicates that urease does not lose its activity during 30 min. reaction.

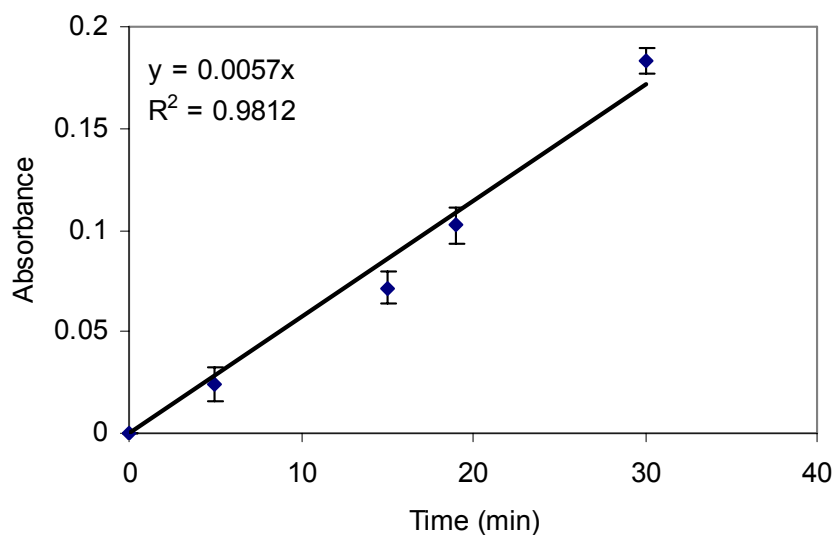


Figure 7.5. The change in ammonium concentration during 30 min reaction. Reaction conditions; urea concentration 10 mM, buffer concentration 50 mM.

7.1.2. Determination of pH-Activity Profile of the Native Urease

Ionic strength of the solution as well as its pH has a significant influence on an enzyme performance, since enzymes contain many positively and negatively charged groups which may be protonated or deprotonated at any given pH. The enzyme activity, Michaelis constant and activation energy can be changed resulting from the inhibitory action of buffer, for example, phosphate buffer competitive at pH 7.0 [91]. In Figure 7.6 the pH-activity profile of the native urease is shown. Optimum pH of the native urease was found as 7 which is almost around the reported values in literature (7- 7.5) [11]. The sudden reduction in activity at acidic medium can be explained by the protonation of active site group of the urease (catalytic histidine) and hence has free access to the site and inhibition attains its strongest stage. However, above pH 6.5, His 320 is deprotonated and repulses H_2PO_4^- ion which results in weak inhibition.

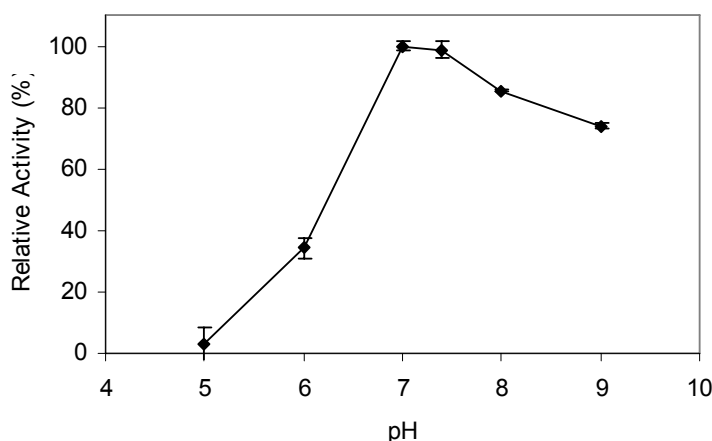


Figure 7.6. pH-activity profile of the native urease during 30 min reaction. Reaction conditions; urea concentration 0.01M, buffer concentration 0.05 M.

7.1.3. Determination of Temperature-Activity Profile of the Native Urease

In Figure 7.7, relative activities of native urease are reported as a function of temperature. Free urease shows an optimum at 30°C. Beyond 37°C, it was suddenly denatured. The activity values increasing with temperature ranging from 10°C up to 30°C were used in Equation 3.19 to determine the activation energy of the enzymatic reaction. From the Arrhenius plot, the value was determined as 5.6 kcal/mol which is in accordance with the result reported in literature [12].

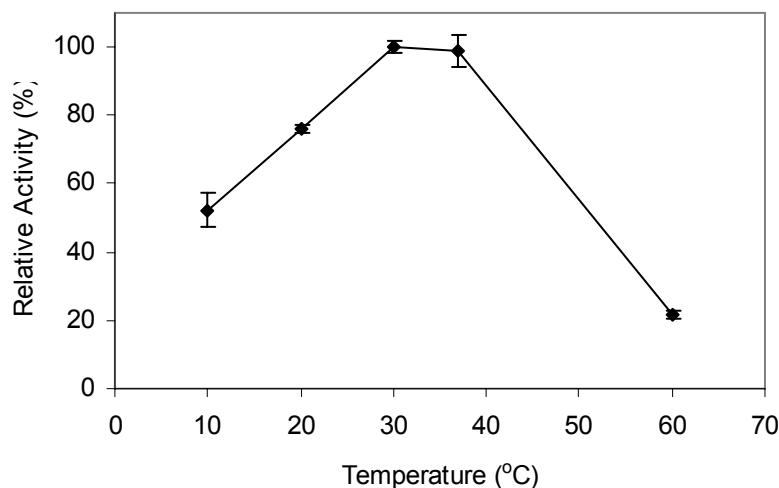


Figure 7.7. Temperature-activity profile of the native urease during 30 min reaction. Reaction conditions; urea concentration 0.01M, buffer concentration 0.05 M.

7.1.4. Determination of Kinetic Parameters of Native Urease

The kinetic parameters K_m and V_{max} are useful to characterize an enzyme. K_m , the so called Michaelis constant, is defined as the substrate concentration for which the observed reaction rate is half of V_{max} , and that of V_{max} is the maximal reaction rate possible if every enzyme molecule present is saturated with substrate. These parameters were calculated from measurement of urease activity within different substrate (urea) concentrations. The kinetic constants of urease were determined using Lineweaver-Burk plot and the results are depicted in Figure 7.8. Based on the figure, V_{max} and K_m were estimated as 94.34 $\mu\text{mol}/\text{min}\cdot\text{mg}$ and 10.37 mM respectively. In reference [90], K_m for native urease was reported as 5.01 mM within 10 mg urease. V_{max} value was determined as 45,400 $\mu\text{mol}/\text{mg}\cdot\text{min}$ which is much higher than the value reported here. The maximum reaction rate $V_{max} = k_{cat} [E_0]$ depends on the amount of total enzyme in the reaction mixture. While 0.5 mg/ml urease was used in this study, 10 mg/ml was used in that study. This difference may also come from the source of urease used in that reference whose activity value (33.6 units per mg protein) was 2 times greater than the activity used in this study. In another reference, [113] the kinetic parameters of urease isolated from dehusked pigeonpeas were reported as 3 mM and 6,200 $\mu\text{mol}/\text{min}\cdot\text{mg}$ for K_m and V_{max} respectively. Similar values were reported in a detailed review by Krajewska [64].

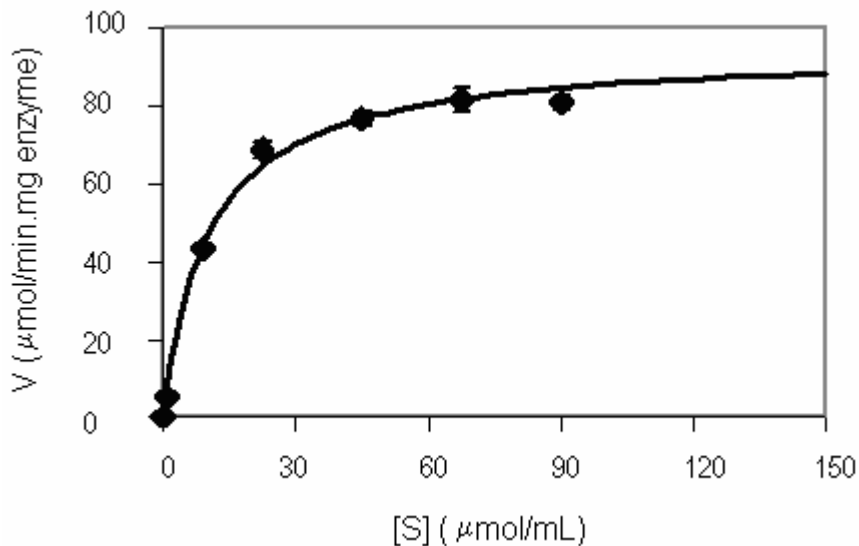


Figure 7.8. The change in reaction rate of soluble urease as a function of urea concentration

7.1.5. Determination of Storage Stability of Native Urease

In general if an enzyme is stored in solution, it is not stable during storage. Its activity gradually decreases. In Figure 7.9, urease storage in water at 4°C with respect to time is shown. At the beginning of the storage up to 7th day, it preserves almost 80% of its initial activity, further storage leads to reduction in activity seriously. The deactivation kinetics during storage test for the free urease was correlated using linear model (Equation 3.21). Based on the model, the deactivation rate constant, k_d , was estimated as $8 \times 10^{-5} \text{ min}^{-1}$.

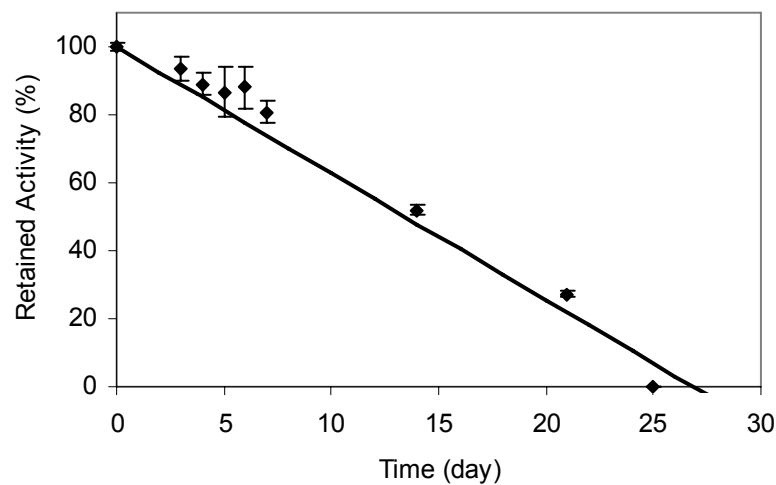


Figure 7.9. Storage stability of native urease. Urease was stored in water at 4°C.

7.2. Studies with Immobilized Urease

7.2.1. Studies with Urease Immobilized Membrane Prepared by Physical Immobilization Using Layer-by-Layer Technique

7.2.1.1. Determination of Immobilized Amount of Urease onto AN69 and AN69-PEI Membranes

To optimize the immobilization conditions, AN69 and AN69-PEI commercial membranes were placed into different concentrations of urease solutions. The protein concentration of the enzyme solution was monitored and curves showing change of surface density of immobilized urease vs. time in different membranes was obtained. According to mass uptake curves shown in Figure 7.10, both membranes show similar trends in terms of adsorption characteristics. In this figure, one can consider two regions during the immobilization process. The first six hours, in which the electrostatic interactions between enzyme molecules and the surface charge groups are dominant, is responsible for monolayer coverage and further adsorption takes place between enzyme molecules at boundary and on the surface which are already adsorbed [114]. When the concentration gradient between bulk and surface of the membrane is high, adsorption takes place immediately even within a short period of time (1 hour).

Table 7.1. Effect of immobilization concentrations on equilibrium adsorbed amount per membrane surface area and the overall reaction rate constant for both AN69 and AN69-PEI membranes.

Type of membrane	Concentration		
	($\mu\text{g}/\text{ml}$)	Γ_e ($\mu\text{g}/\text{cm}^2$)	$k_o \cdot 10^5$ (1/s)
AN69-URE	34.7	7.8	5.7
	52.1	7.7	7.1
	69.4	12	7
	138.8	11.5	9
AN69-PEI-URE	34.7	7.8	6.9
	52.1	9.6	8
	69.4	10.8	6.5
	138.8	10.1	8.8
AN69-CHI-URE	69.4	10.9	5.5

The data in Figure 7.10 were correlated with the adsorption model given by Equation 3.3. Two fitting parameters, Γ_e ($\mu\text{g}/\text{cm}^2$), the equilibrium amount adsorbed per membrane surface area and k_0 (s^{-1}), the overall reaction rate constant determined from nonlinear least-square fit are tabulated in Table 7.1. Consistent with the experimental data, the correlated Γ_e values indicate that maximum surface coverage by the enzyme molecules on both AN69 and AN69-PEI membranes takes place at the urease concentration of $69.4 \mu\text{g}/\text{mL}$. Therefore, this value was used for further experiments.

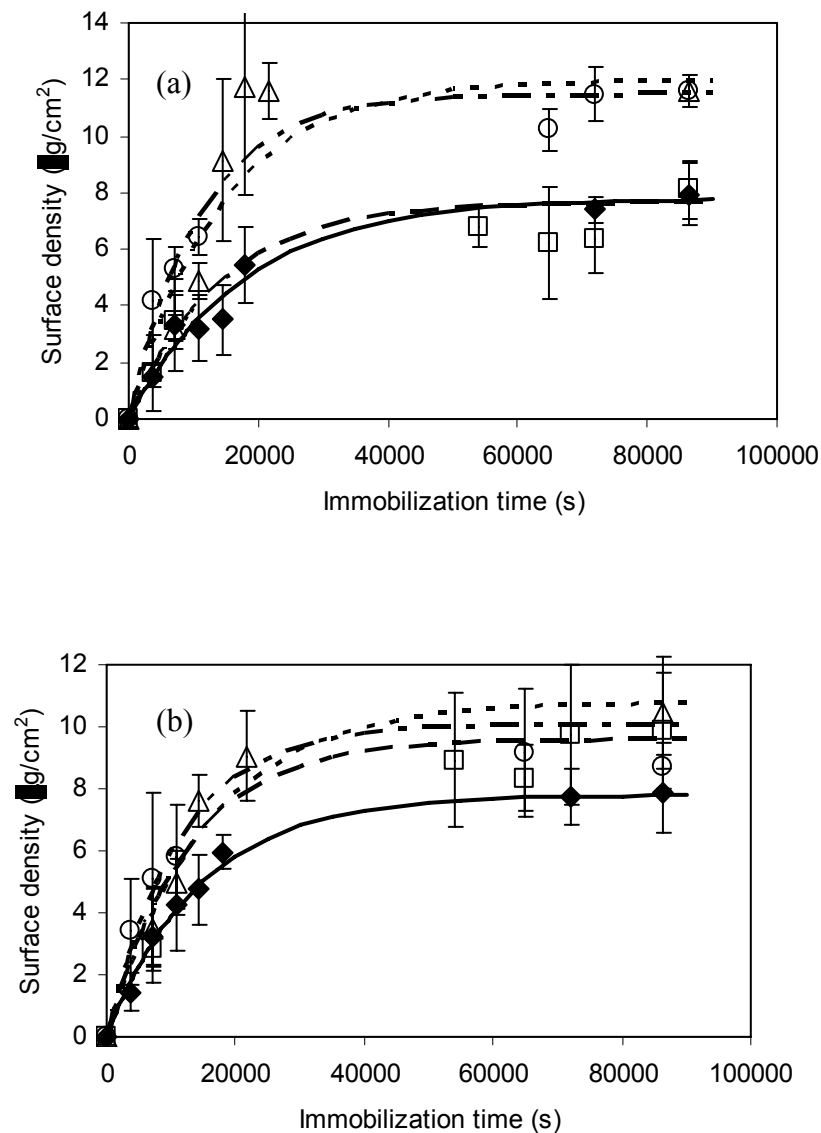


Figure 7.10. Mass uptake curves (a) for AN69-URE, (b) for AN69-PEI-URE membranes; symbols; (\blacklozenge) $34.7 \mu\text{g}/\text{mL}$; (\square) $52.1 \mu\text{g}/\text{mL}$; (Δ) $69.4 \mu\text{g}/\text{mL}$; (\circ) $138.8 \mu\text{g}/\text{mL}$ urease solutions. Lines are corresponding fits using Equation 3.3.

In Figure 7.11, the adsorption kinetic for the urease adsorption onto AN69-CHI membrane is illustrated. Equilibrium rate constant for urease adsorption onto AN69-CHI membrane was found lower than those on AN69 or AN69-PEI membranes. This may be due to branched structure of chitosan and its higher molecular weight which cause significant diffusional resistance and reconfiguration during adsorption.

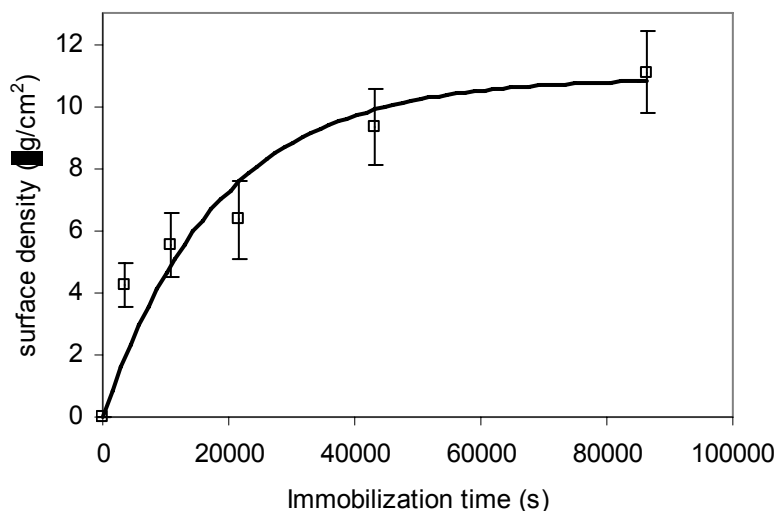


Figure 7.11. Mass uptake curves for AN69-CHI-URE; experiment was carried out in 69.4 $\mu\text{g/mL}$ urease solution. Line is the corresponding fit using Equation 3.3.

Figure 7.12 shows equilibrium isotherm for AN69-URE and AN69-PEI-URE membranes. For both membranes equilibrium was achieved at the end of 24 hours of immobilization. The amount of urease adsorbed on AN69-PEI membrane is increased with increasing urease concentration up to 69.4 $\mu\text{g/mL}$ beyond which no significant change was observed. This behavior exhibits little variation in the case of urease immobilized on AN69. The surface density in this case first increased then remained constant and further increase in immobilization concentration lead to increase in surface adsorption. The S type adsorption estimated for AN69 membrane might be explained by non-specific adsorption, since the surface charge of the membrane is identical with the urease at the immobilization condition that may cause folding (variation of three-dimensional structure) the urease molecules due to repulsive forces between charged groups available on the membrane and in the urease. Consequently, enzyme molecules may interact with each other forming larger aggregates. Depending on the sizes of those aggregates the surface adsorbed amount may change. The results of adsorption kinetics also revealed that urease can be adsorbed on any surface (hydrophobic/hydrophilic,

similar/dissimilar charges) independently. Such kind of observation has been reported in the case of albumin adsorption on both negatively and positively charged multilayer surfaces [115]. Maximum surface adsorptions attained at the end of immobilizations are given in Table 7.1 for the urease immobilized AN69 membranes. The maximum adsorbed amount of urease immobilized on PAN membrane via glutaraldehyde treatment has been reported as $0.25 \mu\text{g}/\text{cm}^2$ [30]. The large variation might be due to the difference in immobilization method, surface charge density, and also the characteristics of enzyme.

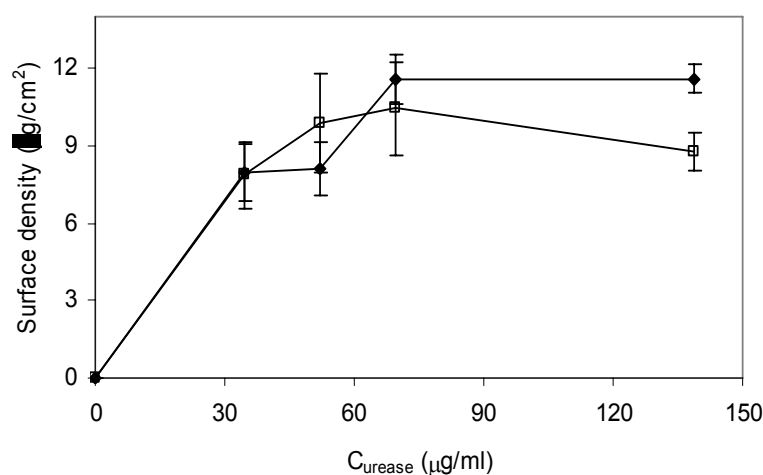


Figure 7.12. Equilibrium sorption isotherm for (◆) AN69-URE and (□) AN69-PEI-URE membranes.

In Table 7.2, equilibrium adsorbed amount, initial and specific activities of urease with and without polyelectrolyte deposited AN69 membranes are given. As it was mentioned, maximum adsorbed amount of urease has been observed on AN69 membrane due to non-specific weak forces. Slightly reduced amount was adsorbed on chitosan deposited AN69 membrane. Chitosan has a high molecular weight ($750000\text{g}/\text{mol}$) which might lead to open structure on the surface of the membrane which causes urease to penetrate inside the pores. Consequently there might be internal adsorption that allows more urease adsorbed not only on the surface but also in the pores. In this case, reaction rate can be reduced by internal diffusional resistance. In the case of urease immobilized onto PEI deposited AN69 membrane, the lowest adsorbed amount was obtained however, the initial activity was the highest. PEI is known to have a more linear structure than CHI, and urease attached on that surface experiences less diffusional resistance due to its direct contact with the substrate [116]. One can

conclude from the results in Table 7.2 such that orientation of the enzyme on the surface when adsorbed is more important than the amount of enzyme adsorbed.

Table 7.2. Equilibrium adsorption, initial and specific activity values of AN69 and polyelectrolyte deposited AN69 membranes

Membrane	Surface density $\mu\text{g}/\text{cm}^2$	Initial Activity $\mu\text{mol}/\text{min}\cdot\text{cm}^2$	Specific Activity $\mu\text{mol}/\text{min}\cdot\text{mg enzyme}$
AN69	11.57 ± 0.99	0.10 ± 0.0084	8.64
AN69-CHI	11.09 ± 1.33	0.14 ± 0.0088	12.62
AN69-PEI	10.43 ± 1.81	0.21 ± 0.0223	20.13

7.2.1.2. Determination of pH-activity Profiles of the Urease Immobilized Membranes

It is well known that the pH-activity profile depends on the nature of the enzyme, carrier and the immobilization method. Synergetic action of the partitioning effect and the increased stability of enzyme particularly when multipoint bonding is obtained affects the pH-activity profile [116]. While partitioning affects the optimum pH value, that of the modified stability affects the shape of the pH-activity profile. Depending on the electrostatic or hydrophobic interaction of the enzyme with the support and low molecular charged species such as hydrogen and hydroxyl ions present in solution, the position of the optimum pH displaces to higher or lower pH values or is not influenced since, the low molecular charged species exhibits different concentrations between the microenvironment around the catalytic site and the bulk solution. The shape of pH-activity curve of the enzyme-immobilized membrane may be broader, narrower, more asymmetrical than or identical to that of soluble enzyme.

To characterize immobilized form of urease, their activities were measured as a function of pH ranging from 5 to 9. Figure 7.13 represents the change in relative activities of urease immobilized membranes with respect to reaction pH. For the native urease, optimum pH in which the relative activity is higher than 95% was found in the range between 6.9-7.5. While pH optimum was not changed in the case of AN69-URE and AN69-PEI-URE, significant shift in pH to acidic site have been observed for the CHI deposited AN69 membrane.

In heterogeneous biphasic systems where enzyme is in one phase, while the substrates and/or products are in the other, partition effects are important. For an immobilized enzyme, partition at the biocatalyst interface can be the result of the different physicochemical properties of the bulk medium and the enzyme environment on the support. Mostly, partition occurs due to electric charges available on the carrier matrix and it always occurs with respect to protons. Therefore, partition has an effect on the pH dependence of the immobilized enzyme proven by the proton displacement with the expressions given below [117].

$$K_{ph^+} = \frac{h^+}{h_0^+} = \exp\left(\frac{-\varepsilon \cdot \varphi}{k_B \cdot T}\right) \quad (7.1)$$

$$pH - pH_0 = 0.43 \frac{\varepsilon \cdot \varphi}{k_B \cdot T} \quad (7.2)$$

Where, ε , is electron charge, φ is electrostatic potential of support, k_B is Boltzman universal constant, T is absolute temperature h^+ and h_0^+ proton molar concentrations (mol/l) at interface and in the bulk respectively. Equation 7.2 can be used for predicting the displacement of the pH profile of an enzyme immobilized on a charged support. When the support is positively charged ($\varphi > 0$), then $pH > pH_0$; when negatively charged ($\varphi < 0$), then $pH < pH_0$. The magnitude of that displacement ($0.43 \cdot \varepsilon \cdot \varphi / k_B \cdot T$) represents the difference with respect to the pH profile of the free enzyme; if there is no other effects occurred as a consequence of immobilization. The magnitude of that displacement can be reduced by increasing the ionic strength of the medium since in that case other ions will compete with hydrogen ions for partition. This displacement in the activity versus pH curve should be to the left in the case of cationic supports. The range of optimum pH where relative activities are higher than 95% were found as 5.8-7.05 for AN69-CHI-URE, 6.85-7.2 for AN69-PEI and 6.9-7.1 for AN69. This result suggests that the CHI deposited AN69 membranes should be selected in the application in which acidic medium is required.

Similar pH range (5.86-6.22) has been reported in reference [116]. In the case of urease immobilized on AN69-PEI membrane, there is no significant difference obtained for the optimum pH value which suggests that no partitioning effect exists. At higher

pH, urease immobilized onto AN69-PEI membrane retains higher activity than the soluble counterpart, which reflects that the stability of urease could be enhanced in the immobilized form. However, in the case of urease immobilized onto AN69 membrane, the shape of pH-activity curve was narrower than the soluble urease. This lower stability might be attributed to the hydrophobic interaction between urease and AN69 membrane. Similar findings have been reported for positively charged supports. Liang et al. [118] have reported that pH-activity curve was shifted toward low pH while for membranes charged negatively toward high pH. In another study [79], a pH shift in acidic direction was obtained which was attributed to attraction of quaternary amino groups on the carrier with the hydroxylic groups in the solution. In the same study, optimum pH of the urease immobilized on the negatively charged membrane was found to shift in basic direction. This has been explained by the attraction of the protons in the space surrounding the urease by the sulfonate groups not bounded to urease.

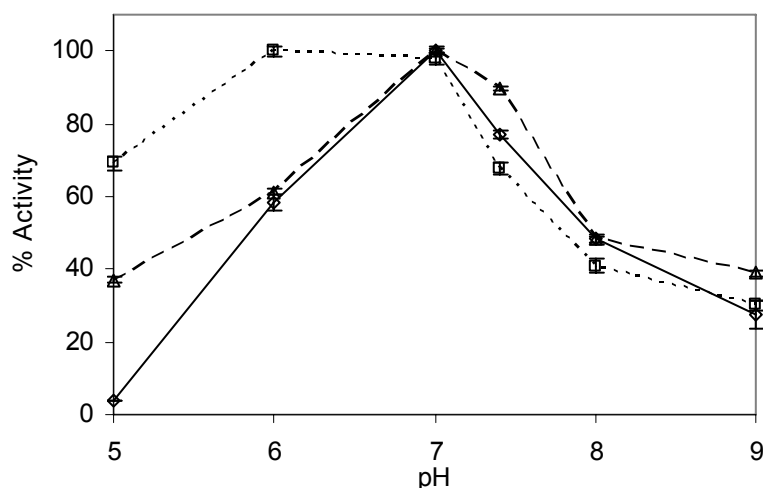


Figure 7.13. The change in relative activities of urease immobilized membranes as a function of pH. Symbols; (\diamond) AN69-URE. (\square) AN69-CHI-URE. (Δ) AN69-PEI-URE.

7.2.1.3. Determination of Temperature-Activity Profiles of the Urease Immobilized Membranes

The optimum temperatures (T_{opt}) of urease immobilized membranes were determined and are illustrated in Figure 7.14. While T_{opt} for the native urease was found to be around 30°C, immobilization caused to increase the stability of urease through a wide range of temperature. For urease bound AN69 membranes, T_{opt} was nearly two times higher than that of free urease. This indicates that the immobilized forms of

urease resisted against denaturation due to temperature rise. Similar results have been reported for the immobilized urease on different supports using different immobilization method [119]. Using the same approach as in the case of native urease, the activity data of urease immobilized membranes increasing with temperature were used in Equation 3.19. From Arrhenius plots the activation energies necessary to react urease molecule with urea were determined as 9.1, 10.8, and 5.4 kcal/mol for AN69-URE, AN69-PEI-URE and AN69-CHI-URE respectively. The values found for the immobilized forms of the urease are higher than that obtained for the soluble urease, which reflects that the conformational changes in the enzyme structure occurred. In addition, a homogenous reaction is turned into heterogeneous one while enzyme is immobilized onto AN69 membrane whose molecular structure becomes more rigid and its free motion is restricted. They might lead to reduction in affinity to urea.

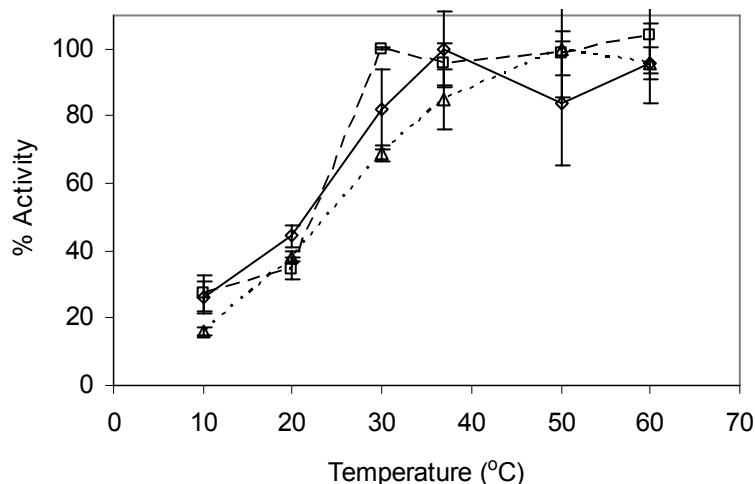


Figure 7.14. The change in relative activities of urease immobilized membranes as a function of temperature. Symbols; (\diamond) AN69-URE, (\square) AN69-CHI-URE, (Δ) AN69-PEI-URE.

7.2.1.4. Determination of Kinetic Parameters of the Urease Immobilized Membranes

Comparison of the results in Figure 7.8 and 7.15 indicates that the reaction rate of the native urease is nearly 5 to 10 times higher than the immobilized form of ureases. This could be attributed to the inactivation of urease during immobilization process, changes in the enzyme structure due to interaction between enzyme and the support and to the increased diffusional resistance encountered by the substrate while it approaches to the catalytic site of the urease and by the reaction products while it removes from the

same site. The kinetic constants for the urease immobilized on AN69 and polyelectrolyte deposited AN69 membranes are given in Table 7.3.

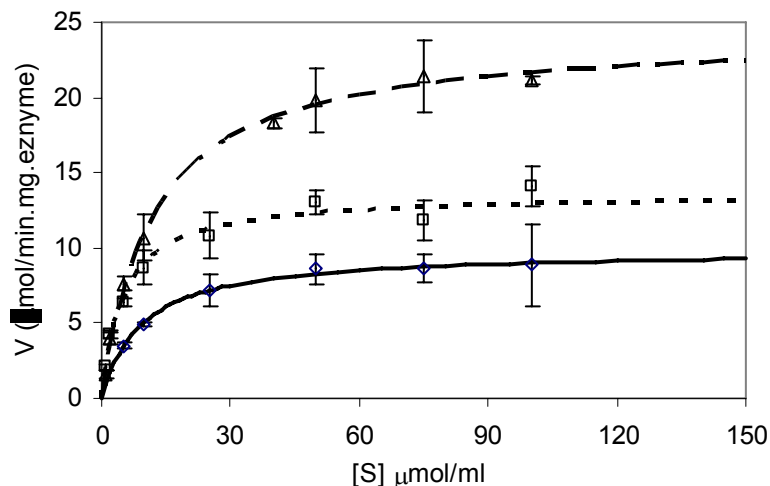


Figure 7.15. The change in reaction rate of urease immobilized membranes as a function of urea concentration. Symbols; (\diamond) AN69-URE. (\square) AN69-CHI-URE. (Δ) AN69-PEI-URE.

The differences in K_m values for the immobilized form of urease might be due to different interaction between urease and the supports. It is known that electrostatic interaction is favoured through immobilization of urease onto polyelectrolyte deposited AN69 membranes because of existing positively charged groups which allows binding of negatively charged urease without causing significant change in its structure. In contrast hydrophobic AN69 membrane having negatively surface charged groups (SO^{-3}) which are not responsible for specific adsorption may cause conformational changes of urease while immobilization takes place. Therefore the enzyme molecules may assume in part an inactive conformation.

Table 7.3. Kinetic parameters of urease immobilized membranes

	K_m	V_{max}
	$\mu\text{mol/mL}$	$\mu\text{mol/min.mg protein}$
AN69	8.81	9.83
AN69-CHI	6.66	14.83
AN69-PEI	10.65	23.50

In literature, the influence of functional groups introduced on the surface of Poly (acrylonitrile-methylmethacrylate-sodium vinylsulfonate) using seven different

chemical modifications on the immobilization performance of urease has been studied [79]. The kinetic parameters of the native urease ($K_m=3.2$ mM and $V_{max}=0.0454$ mmol/min.mg) with the immobilized counterparts were compared and the results show that the rate of enzyme reaction is higher on negatively charged membranes. In another study, temperature effects on the kinetic parameters of urease immobilized membrane have been reported [116]. Michaelis constant for immobilized urease is increased from 7.81 to 52.3 mM with the increase in temperature from 20 to 40°C compared with the native enzyme which is increased from 2.84 to 17.4. The difference between K_m values for native and immobilized urease is attributed to mass transfer limitation of substrate and the reaction products. As oppositely the decrease in K_m values for both soluble and insoluble urease with increasing temperature has been reported in literature [116]. Authors explained this behavior such that the diffusional fluxes of the substrate and the reaction products increase with increasing temperature.

In this study, to be able to increase the stability of immobilized urease which is directly exposed to substrate solution, it was sandwiched between two polyelectrolyte layers. The produced membranes are so called AN69-CHI-URE-CHI and AN69-PEI-URE-PEI. It is thought that the polyelectrolyte on the top layer keeps the urease molecules more stable and reduces its release rate into solution. The so called Michaelis-Menten constants were determined as 5.34 $\mu\text{mol}/\text{min.mg}$ protein and 1.93 $\mu\text{mol}/\text{ml}$ for the former and 8.45 $\mu\text{mol}/\text{min.mg}$ protein and 4.08 $\mu\text{mol}/\text{ml}$ for the latter. The reductions in reaction rate would be diffusional effect encountered during a passage of molecules through the extra layer.

In the case of immobilized form of urease, substrate conversion takes place in three steps; substrate transport from the bulk medium to the surface of the biocatalyst, enzymatic conversion into product and product transport back from the surface to the bulk medium. The substrate or product diffusion limits the catalytic efficiency of the enzyme in which any of these steps is the rate-limiting. The influence of external mass transfer resistance on the overall enzymatic reaction is represented using the effectiveness factor. In addition to the effectiveness factor, η , the relative importance of mass transfer compared to the enzymatic reaction is determined by a dimensionless number called Damköhler number, D_a . Figure 7.16 shows the change of effectiveness factor as a function of Damköhler number for different urease immobilized membranes. At low values of D_a number ($D_a < 0.1$), which indicates reaction controlled region, the

effectiveness factor approaches to 1 which guarantees that the enzyme kinetic parameters are measured in the absence of external mass transfer resistance. As Da number becomes larger, the effectiveness factor deviates from 1. In other words, as the transport of substrate is controlled by mass transfer rather than enzymatic reaction, the kinetic parameters determined by neglecting external mass transfer resistance will be approximate. Figure 7.17 shows effectiveness factors for immobilized urease as a function of substrate concentrations. Except at the lowest urea concentration (1 mM), the effectiveness factors all approach to one which confirm that experimental conditions were chosen properly, thus, the kinetics of the immobilized urease corresponds to that observed in the absence of partition and mass transfer limitations.

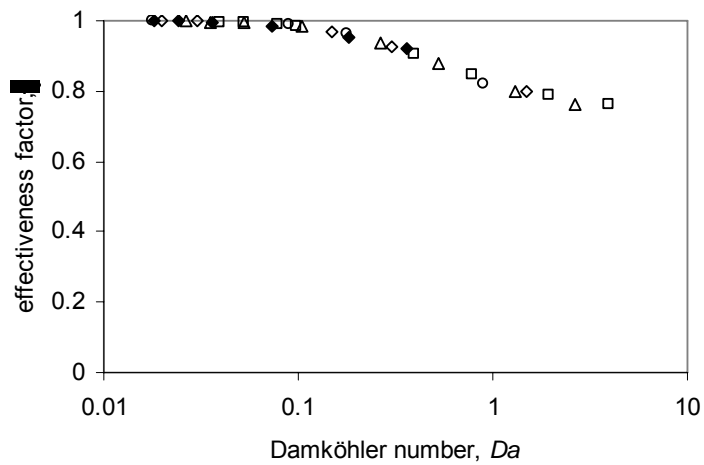


Figure 7.16. Variation of effectiveness parameters as a function of Damköhler number for the urease immobilized membranes. (\blacklozenge) AN69-URE, (\square) AN69-PEI-URE, (\triangle) AN69-CHI-URE, (\circ) AN69-PEI-URE-PEI, (\diamond) AN69-CHI-URE-CHI.

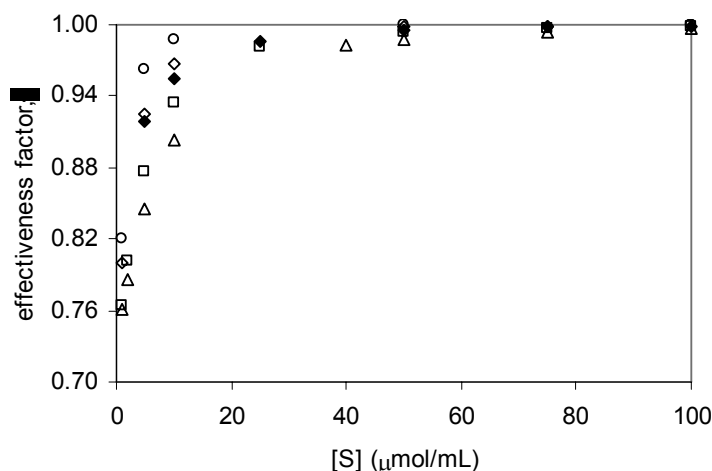


Figure 7.17. Effectiveness factors for immobilized urease as a function of substrate concentrations. (\blacklozenge) AN69-URE, (\square) AN69-PEI-URE, (\triangle) AN69-CHI-URE, (\circ) AN69-PEI-URE-PEI, (\diamond) AN69-CHI-URE-CHI.

7.2.1.5. Determination of Storage Stabilities of the Urease Immobilized Membranes

The main objective of this study was to find a way that could be efficient to immobilize an enzyme onto a membrane and maintain its activity during a sufficient time. That's why the activities of catalytic membranes stored in water were measured at predetermined time intervals and the percentage retained activities are illustrated in Figure 7.18 as a function of time. Relative activities were calculated by taking the highest activity as reference. From Figure 7.18 one can conclude that the membranes having opposite charges with the enzyme show better stabilities than the membranes with identical charges. While 30% of the initial activity was maintained in the case of AN69-PEI-URE at the end of 28th days, 50% of initial activities were preserved for the urease immobilized membranes in sandwiched form.

The deactivation kinetics during storage tests for the immobilized urease was correlated using exponential model represented by Equation 3.20. According to the findings, the deactivation constants are in the order of AN69-URE > AN69-CHI-URE > AN69-PEI-URE > AN69-CHI-URE-CHI > AN69-PEI-UR-PEI. Based on the model observation, a quick inactivation will occur for the urease immobilized on AN69 membrane and the most stable one among them is the membrane in which urease is sandwiched between PEI layers.

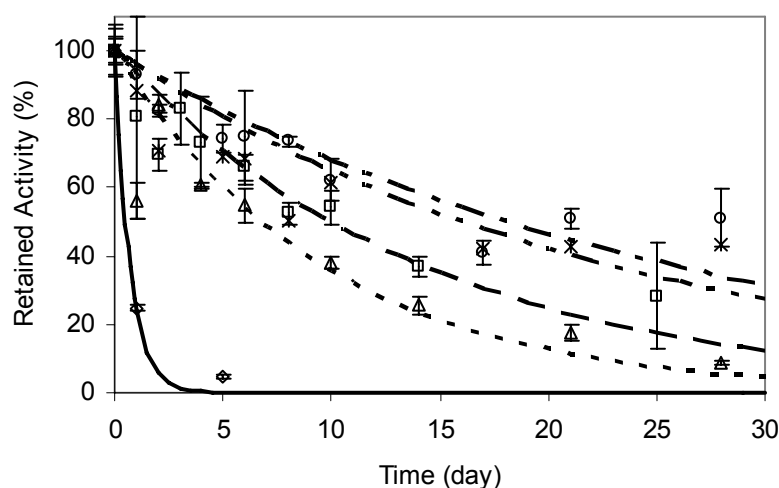


Figure 7.18. Storage stabilities of urease immobilized membranes. Symbols; (\diamond) AN69-URE. (\square) AN69-CHI-URE. (Δ) AN69-PEI-URE. (\circ) AN69-PEI-URE-PEI. (\star) AN69-CHI-URE-CHI

7.2.2. Studies With Urease Immobilized Membrane Prepared by Chemical Immobilization Using EDC/NHS Coupling Agent

7.2.2.1. Effect of Buffer Concentration and its pH on the Membrane Activity

The effects of buffer concentration and its pH used for crosslinking reaction were examined and the activity of the membranes prepared with these conditions are comparatively illustrated in Figure 7.19. For three cases of pH examined here the highest activity is obtained at the lowest buffer concentration. The higher buffer concentration may reduce the ionization of EDC to hydrogen and chlorine ions which may cause an active site reduction or the concentrations of the free ions of sodium phosphate buffer in the crosslinking solution may have competitive blocking affect that prevents the access of (chemical bonding) EDC molecules to the acetate group. In literature 0.05 M buffer of 2-morpholinoethane sulfonic acid (MES) at pH 5.4 was selected as appropriate in order to minimize hydrolysis of EDC [96].

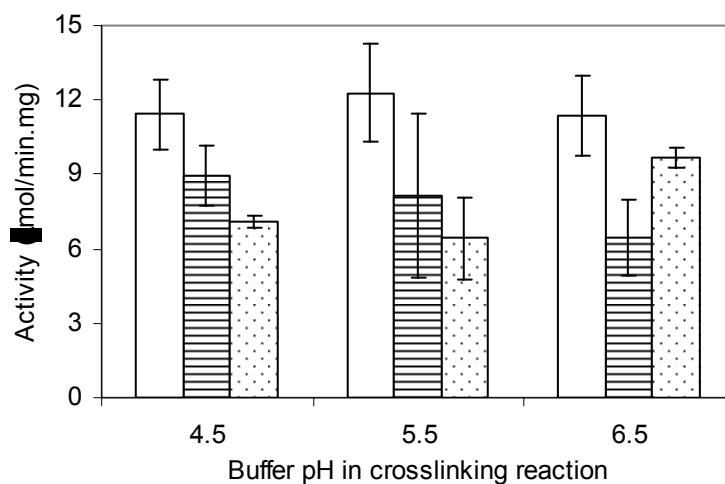


Figure 7.19. Effect of buffer concentration and its pH on the membrane activity. (□) 0.01M, (≡) 0.05M, (⊙) 0.1M.

Other parameters used for crosslinking reaction and immobilization are given in Table 7.4. Based on the results in Figure 7.19 the buffer concentration and its pH were chosen as 0.01 M and 5.5 respectively for further experiments.

Table 7.4. Conditions used for crosslinking reaction and urease immobilization

	Fixed	Variable
Concentration of buffer (M)		0.01 0.05 0.1
Buffer pH		4.5 5.5 6.5
Crosslinking time (h)		1 2 3 4 20 24
Immobilization time (h)	24	
Concentration of EDC (M)	0.05	
Concentration of urease (mg/ml)	0.5	

7.2.2.2. Effect of Crosslinking Time on the Membrane Activity

Crosslinking reactions were performed at 4°C to be able to control the reaction. The reaction is slow at lower temperature and side reactions due to instability or inactivation of EDC can be prevented by this manner. Figure 7.20 represents the change in activity as a function of crosslinking time. At the end of 3 hours, the surface functional groups (COO⁻) are believed to be saturated with EDC molecules. At the end of long reaction time, hydrolysis of EDC might occur which may result in a reduced activity. From Figure 7.20, it was decided to fix the crosslinking time as 3 hours for further experiments.

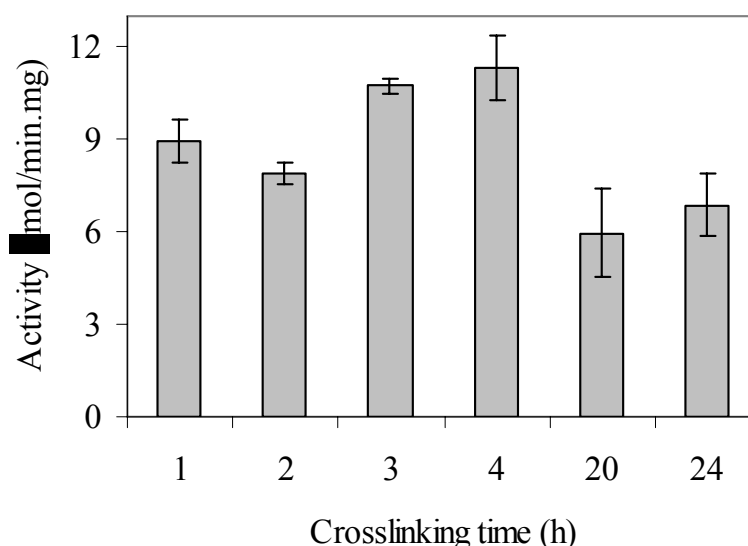


Figure 7.20. Effect of crosslinking time on the membrane activity

7.2.2.3. Effect of EDC Concentration on the Membrane Activity

The effect of EDC concentration is investigated in Figure 7.21. The increase in EDC concentration gives an increase in activity up to certain point of 0.05 M and then a gradual decrease is obtained beyond that point. This is explained again as a saturation limit; beyond that point inactivation may occur. Since the maximum activity was obtained at 0.05 M EDC concentration, it was used for further experiment.

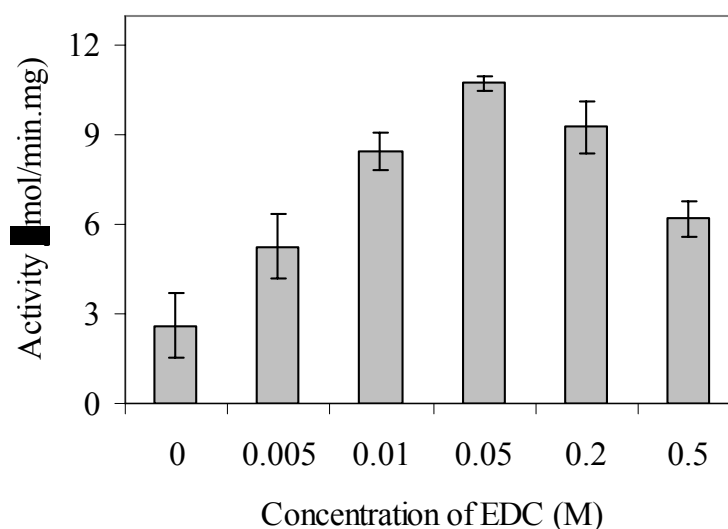


Figure 7.21. Effect of EDC concentration on the membrane activity

7.2.2.4. Effect of Urease Concentration on the Membrane Activity

In order to determine the saturation concentration of the urease, immobilization solutions were prepared in different urease concentrations. Figure 7.22 shows the equilibrium sorption isotherm of urease immobilized membrane. The saturation limit was achieved around 0.0347 mg/ml urease concentration. This value was used for further experiments.

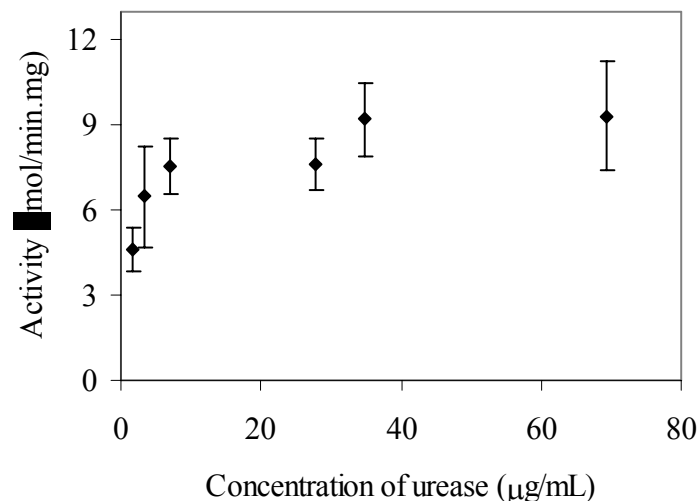


Figure 7.22. Effect of urease concentration on the membrane activity

7.2.2.5. Effect of Immobilization Time on the Membrane Activity

The effect of immobilization time on the activity of the membrane is studied between 1 and 24 hours of interval and the results are illustrated in Figure 7.23. The lowest activity was observed for the case of 1 hour immobilization. This might be assigned to the randomly distributed urease molecules due to much more empty spaces available on the membrane surface which results in active site binding of urease molecules. However, at a longer time, steric effects between urease molecules could be dominant that provide correct alignment of the urease molecules through multipoint attachment. A gradual increase in specific activity for 24 hour immobilization compared to that obtained at 20 h of immobilization could be explained by an increase in the amount of immobilized urease which can be clearly estimated from Figure 7.24. During last 4 hours of immobilization $0.6 \mu\text{g}/\text{cm}^2$ increase in adsorbed amount of urease was obtained. Measurements of retained activity during storage of urease immobilized membrane prepared with 2 hours of immobilization indicated that, only 10% of initial activity was preserved at the end of 20 days of storage while activity lost was much slower in the case of 24 hour immobilization. Consequently, immobilization time was selected as 24 hours.

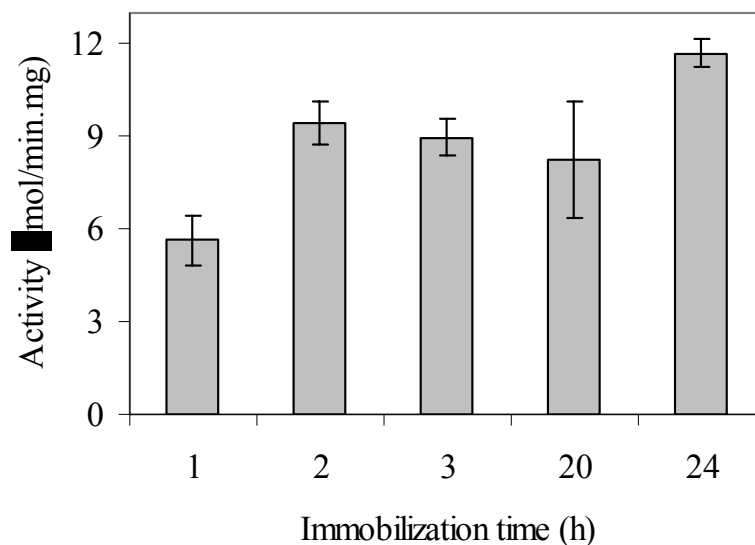


Figure 7.23. Effect of immobilization time on the membrane activity

7.2.2.6. Determination of the Surface Density

During immobilization, 1x3 ml samples at predetermined time intervals were withdrawn from immobilization solution to follow the decrease in the amount of urease which corresponds to the amount adsorbed onto AN69 membrane. Figure 7.24 represents the adsorbed amount of urease on a unit surface of the AN69 membrane. A rapid adsorption occurred and it is almost completed within 2 hours of immobilization. At the end of 1 day of immobilization, 8.3 μg urease was adsorbed on a unit surface. In reference [26] urease was covalently immobilized onto PAN membrane using glutaraldehyde as a crosslinker and the amount of adsorbed urease was reported between 21-48 $\mu\text{g}/\text{cm}^2$. This large difference may come from the difference in immobilization procedures and purity of the urease. In addition, the support membrane in that reference has a pore size of around 10 to 40 nm that brings about the enzyme adsorption on the surface and within the pores. In our case the membrane has a pore size of 2 to 4 nm which allows surface adsorption only. The static adsorption model represented by Equation 6 fits the kinetic data well. Using nonlinear least-square fit, the two model constants, Γ_{max} and k_0 , were determined as 8.1 $\mu\text{g}/\text{cm}^2$ and $15 \times 10^{-5} \text{ s}^{-1}$, respectively.

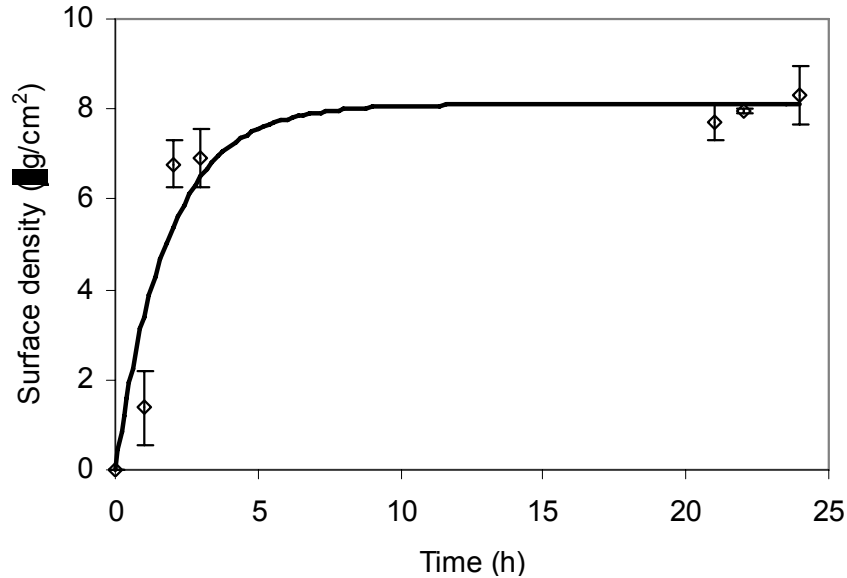


Figure 7.24. Adsorption kinetics of urease immobilized AN69 modified membrane

7.2.2.7. Determination of the pH-Activity Curve

The effect of pH on the activity of free and immobilized enzyme on the modified AN69 membrane was investigated within the range of 5.0 to 9.0. Relative activity as a function of pH is depicted in Figure 7.25. The urease immobilized membranes in Figure 7.25 were prepared by two different washing steps. The one is washed with water for 30 min and the other is washed in water for 2 days. The optimum pH of the native and immobilized urease was found similar. The pH-activity curve of the latter was narrower which would be due to the low molecular weight charged species that exhibit different concentrations between the microenvironment around the catalytic site and the bulk solution. There is negligible variation in the pH-activity profiles of the two forms of the urease immobilized membrane. When the pH-activity profiles of chemically immobilized urease is compared with physically immobilized one, no shift in optimum pH occurred and narrower profile for the former might result in the pH of catalytic micro-environment the same as in the bulk medium so no partition is expected and it is more sensitive to pH.

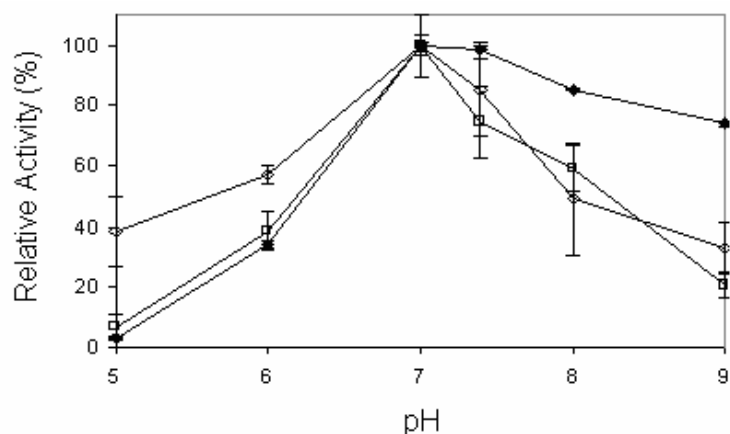


Figure 7.25. pH-activity profiles of native (◆) and immobilized form of the urease (◇) prepared with 30 min. of rinsing and (□) 2 days of rinsing.

7.2.2.8. Determination of the Temperature-Activity Profile

The optimum temperatures (T_{opt}) for native and immobilized forms of the urease were determined and are illustrated in Figure 7.26. For native urease T_{opt} was found to be around 30°C. For urease bound onto PAN membrane, T_{opt} was nearly two times higher than that of free urease. This indicates that the immobilized urease resisted denaturation due to temperature rise. Similar results have been reported for the immobilized urease on different supports with different methods [26, 90, 116]. The change in urease activity with temperature was found similar for both types of membranes.

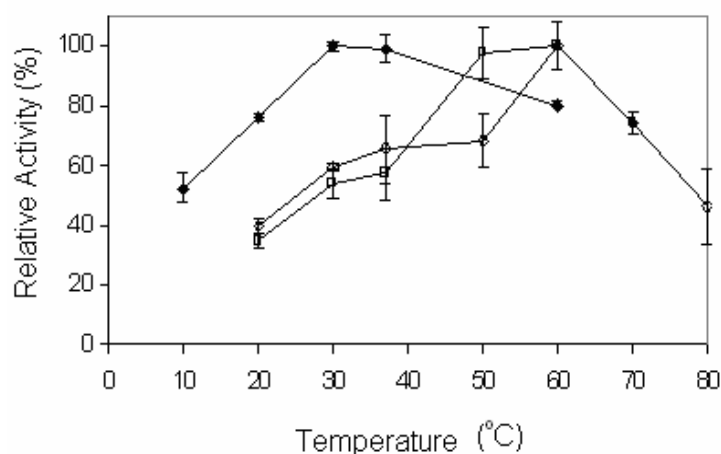


Figure 7.26. Optimum temperature for the native (◆) and immobilized form of the urease (◇) for 30 min. of rinsing and (□) 2 days of rinsing.

7.2.2.9. Determination of the Kinetic Parameters of the Immobilized Urease

The effects of immobilization on kinetic properties of urease were also investigated by determining the kinetic parameters of the enzyme from Lineweaver-Burk plots. Using Figure 7.27, V_{\max} and K_m values of the urease immobilized AN69 membrane prepared with 30 min and 2 days of rinsing have been calculated as 25.77 $\mu\text{mol}/\text{min}\cdot\text{mg}$ and 17.9 mM and 12.42 $\mu\text{mol}/\text{min}\cdot\text{mg}$ and 7.5 mM, respectively. The observed V_{\max} is around 10 times lower than the value obtained for the native urease. As expected, the immobilization reduced the affinity and kinetic capacity of urease to urea considerably. Structural change of enzyme after immobilization which will bring about a mass transfer limitation may influence the affinity between substrate and enzyme. The large difference in the V_{\max} value determined for the two cases of immobilized forms of the membrane comes from the amount of the released urease during 2 days of washing. However, it shows a better fit to Michaelis-Menten kinetics which indicates that it is more stable than the sample obtained by the 30 min rinsing. The continuous increase in activity for the sample obtained by the 30 min rinsing might be due to the release of urease into reaction mixture during activity measurement which might enhance the liberated ammonia exponentially.

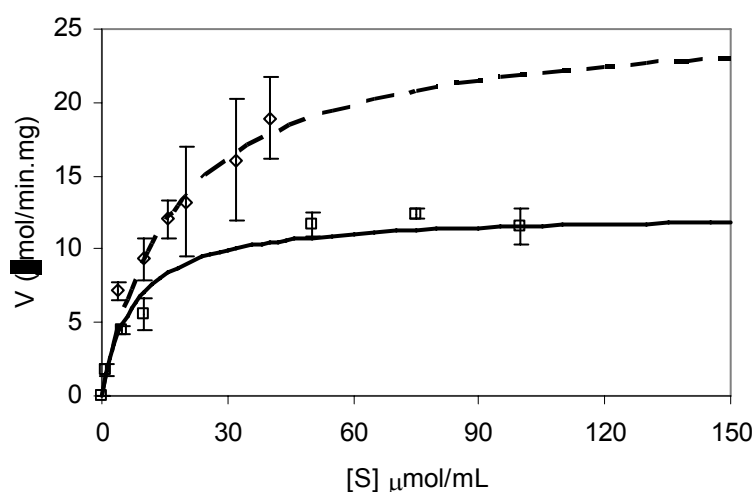


Figure 7.27. Reaction rate of urease immobilized PAN membrane as a function of substrate concentration; (\diamond) measured after 30 min and (\square) 2 days of rinsing.

7.2.2.10. Determination of the Storage Stabilities of the Native and the Immobilized Forms of the Urease

Figure 7.28 represents the comparison of the retained activities of the native and chemically immobilized urease after 2 days of rinsing. A linear decrease in activation was observed in the case of native urease which lost its activity within 25 days of storage. However, 90% of initial activity in immobilized form of urease was retained at the end of 20 days of storage. This result showed that immobilization enhances the stability due to restriction of mobility of the enzyme molecules. The storage stability data were correlated using Equation 3.20 and 3.21 in order to determine deactivation constants which were found as $1.1 \cdot 10^{-5}$ and $8 \cdot 10^{-5} \text{ min}^{-1}$ for the immobilized and native forms of urease respectively. When the stabilities of urease immobilized membranes prepared by means of layer-by-layer self assembly and chemical attachment, the increase in stability for the latter might be attributed to strong interaction of enzyme molecules with the EDC/NHS activated surface which might prevent release of urease molecules during a prolonged time.

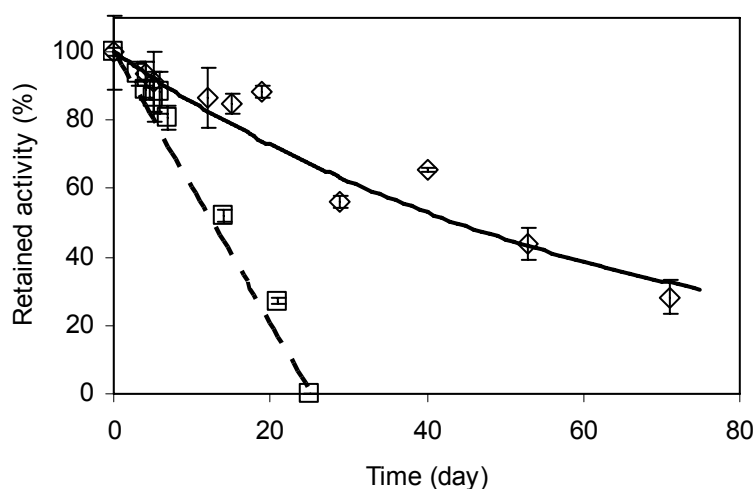


Figure 7.28. Storage stabilities of (\square) native and (\diamond) immobilized urease by means of chemical attachment onto AN69 membrane after 2 days of rinsing. Points are experimental data and the lines represent the deactivation model using Equation 3.20 and 3.21 for the immobilized and free forms of urease.

7.3. Filtration Studies

7.3.1. Permeability Studies

The volumetric flowrate of solution through the membrane was measured directly from the volume collected with respect to time. Figure 7.29 shows the comparison of the change in water filtrate as a function of time collected twice during compaction of water for the commercial AN69-PEI membrane. Two sets of data overlap with each other which indicate that there is no leakage or broken part, filtration experiment is said to be continued.

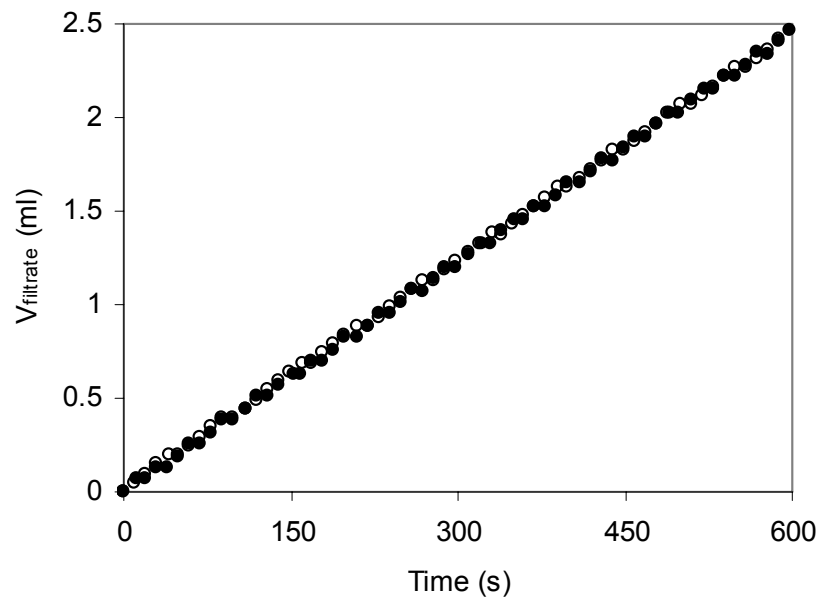


Figure 7.29. Comparison of the two water permeation experiment carried out during compaction steps using AN69-PEI membrane.

The changes in permeate volume collected during water permeation through AN69-PEI membrane as a function of time for three different pressures are illustrated in Figure 7.30. Points denote experimental data and the lines are the best fit to a linear equation with the regression coefficients above 0.99. During filtration, permeate volume increases linearly. The slopes of the lines give the volumetric flowrate of the solution;

$$J_A = \frac{\Delta V_{filtrate}}{\Delta t} \quad (7.3)$$

Dividing this value to the membrane surface area, S_m (m^2) gives filtrate flux, N_A ($L/m^2.h$). The solution flux was corrected with respect to water viscosity, μ_w (cp) at $25^\circ C$ as follows;

$$N_A = \frac{\mu_w(T)J_A}{\mu_w(25^\circ C)S_m} \quad (7.4)$$

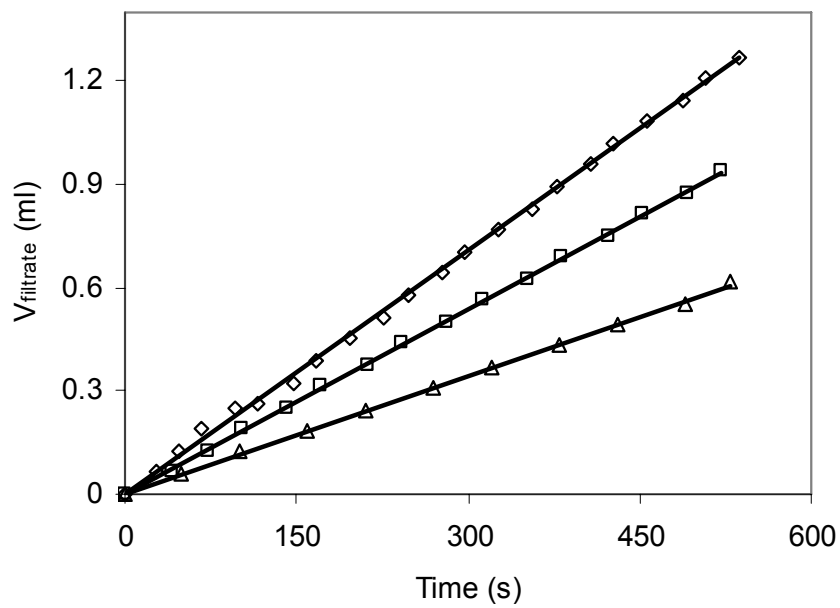


Figure 7.30. The change in permeate volume collected during water permeation through AN69-PEI membrane carried out at 0.5, 1.0 and 1.5 bar transmembrane pressure

When volumetric flux is plotted as a function of transmembrane pressure (Figure 7.31), the slope gives the hydraulic permeability of the filtrate, L_p ($L/m^2.h.bar$)

$$L_p = \frac{N_A}{\Delta P} \quad (7.5)$$

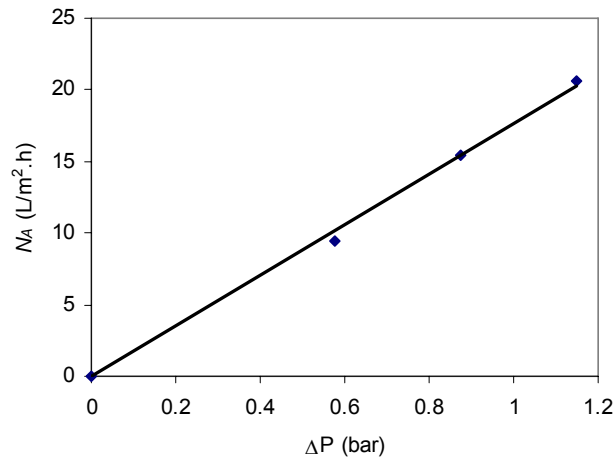


Figure 7.31. The change in water flux as a function of transmembrane pressure for AN69-PEI membrane.

Filtration studies of both catalytic and non-catalytic AN69-PEI ultrafiltration membrane against urea solutions with different concentrations show similar trends as shown in Figure 7.32. While there are no significant differences between hydraulic permeabilities obtained for the case of buffer and urea solutions, considerable reduction is observed when they are compared to hydraulic permeability of fresh water. This could be explained by the variation of solution chemistry, namely pH and ionic strength in which charged molecules could be linked to a compaction of the membrane matrix due to charge neutralization and double layer compression. The change in membrane structure or more precisely the double layer thickness can be quantified using the parameter of Debye length whose reduction effectively increases the cross-sectional area available for solution transport.

The results in Figure 7.32 indicate that neither permeabilities of buffer nor urea solutions differ from each other before and after enzyme immobilization. Although an addition of enzyme layer onto the surface of the membrane exerts a mass transfer resistance, this can be overwhelmed by the enzymatic reaction which leads to formation of smaller molecules that may facilitate the transport, hence no drop in the permeabilities due to enzyme immobilization was observed. Additionally, it was observed that the hydraulic permeabilities of urea solution through the membranes do not change with the urea concentration. This simply indicates that urea is not retained by these membranes. This is an expected result since urea is a small molecule with a diameter of 3.75Å and it has a very small dissociation constant in water so that ionic interaction with the membrane surface or its pores is not expected.

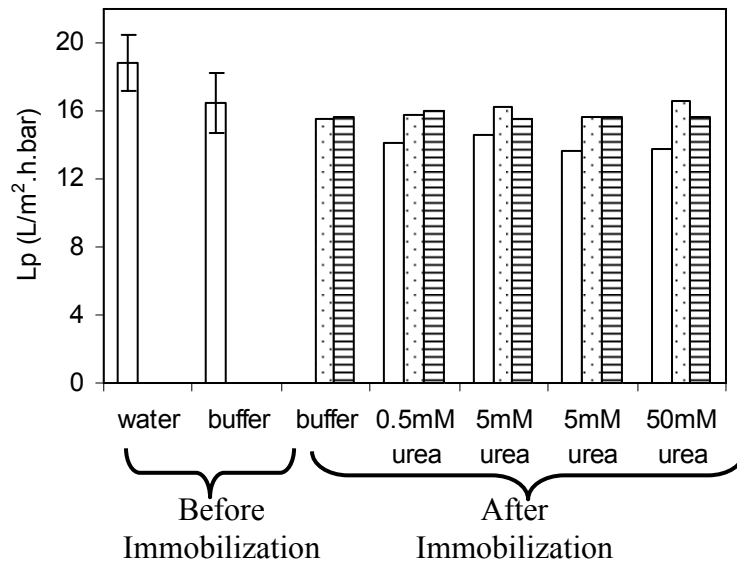


Figure 7.32. Hydraulic permeabilities of water, buffer and urea solutions through (□) AN69-PEI, (⋯)AN69-PEI-URE, (≡)AN69-PEI-URE-PEI

Hydraulic permeabilities of water, buffer and urea solutions through modified AN69 membrane on which urease was chemically immobilized are depicted in Figure 7.33. Compared with the hydraulic permeability of water, there is a considerable reduction in permeabilities for all buffer and urea filtrations. This could be again explained with the change in solution chemistry mentioned above.

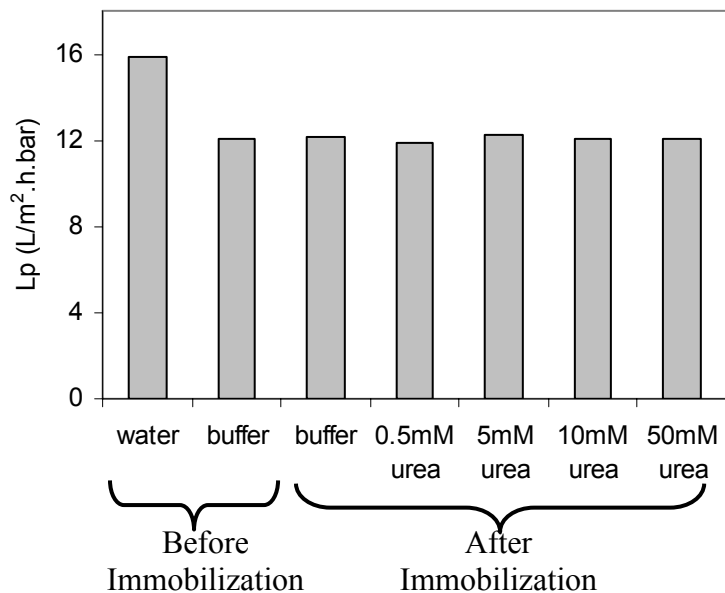


Figure 7.33. Hydraulic permeabilities of water, buffer and urea solutions through modified AN69 membrane on which urease was chemically immobilized.

7.3.2. Catalytic Activity Studies

At the end of the filtration processes, ammonia concentrations on each side of ultrafiltration cell (permeate and retentate) were determined and plotted with respect to their corresponding flux values. According to Figure 7.34, formation of ammonia increases with increasing its concentration in the feed solution up to a certain point where urea concentration is 5 mM. Above this limit, the catalytic membrane decomposes urea at the same rate which simply indicate that at the urea concentration of 5 mM, all catalytic active sides of urease are occupied by urea molecules, hence, further increase in urea concentration does not cause any change in the conversion. At high urea concentration ($\geq 5\text{mM}$), increasing the volumetric flux shortens the residence time for the urea molecules to contact with urease, consequently, the rate of ammonia formation decreases.

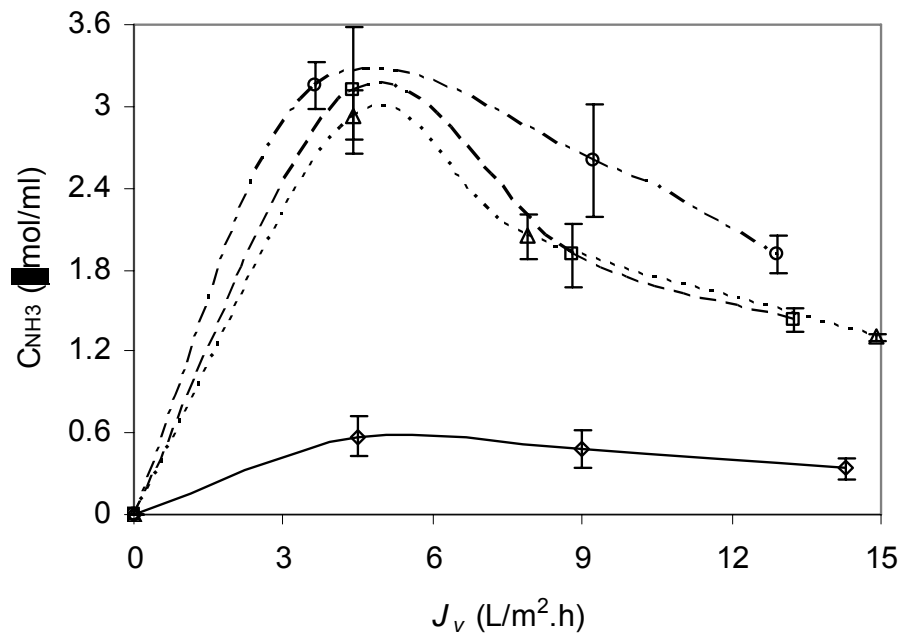


Figure 7.34. Ammonia formation through catalytic decomposition of urea by AN69-PEI-URE membrane. Feed solution concentrations are (\diamond) 0.5 mM, (\square) 5.0 mM, (Δ) 10 mM, (\circ) 50 mM.

Urease immobilized AN69-PEI membrane was coated again by the same cationic polyelectrolyte (PEI) in order to decrease desorption of enzyme molecules under pressure and hence to increase stability. Ammonia formation through catalytic decomposition of urea by this membrane as a function of solution fluxes are depicted in

Figure 7.35. The catalytic behaviour of sandwiched membrane, AN69-PEI-URE-PEI, was found to be different than that of AN69-PEI-URE membrane. This may be due to a change in the enzyme conformation, which may affect the enzyme kinetic parameters. The rate of ammonia formation increases as the urea concentration in the feed solution is increased from 0.5 to 50 mM. Even at the highest substrate concentration, urease is not fully saturated, consequently, flux is no longer being an effective parameter on the ammonia concentration.

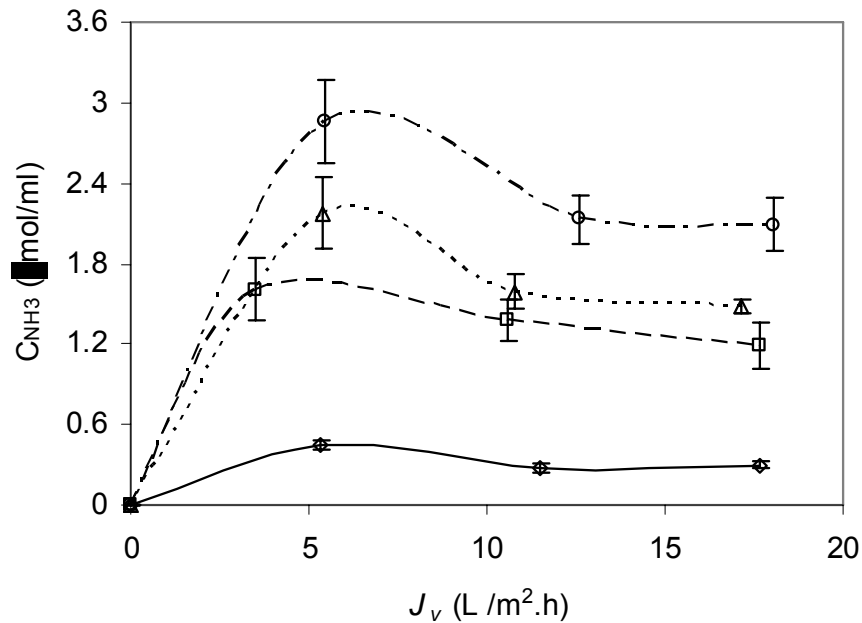


Figure 7.35. Ammonia formation through catalytic decomposition of urea by AN69-PEI-URE-PEI membrane. Feed solution concentrations are (\diamond) 0.5 mM, (\square) 5.0 mM, (Δ) 10 mM, (\circ) 50 mM.

The formation of ammonia by chemically immobilized URE as function of filtrate flux is shown in Figure 7.36. The lower ammonia formation especially at the lowest flux might be attributed to the kinetic parameters which are given in Table 7.2. Different immobilization method leads to different kinetic parameters. The efficiencies of catalytic membranes in terms of rate of ammonia formation is as follows AN69-PEI-URE > AN69-PEI-URE-PEI > AN69-URE.

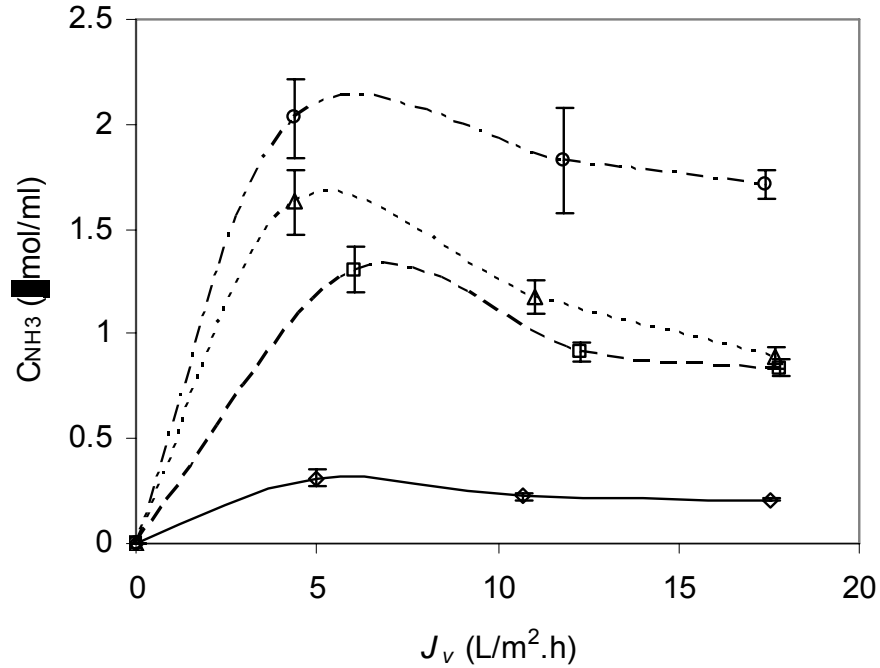


Figure 7.36. Ammonia formation through catalytic decomposition of urea by modified AN69 membrane on which urease was chemically immobilized. Feed solution concentrations are (\diamond) 0.5 mM, (\square) 5.0 mM, (Δ) 10 mM, (\circ) 50 mM.

To determine the influence of external mass transfer resistance on the observed reaction rates and the relative importance of mass transfer and enzymatic reactions; both effectiveness factors and Damköhler numbers were calculated as a function of urea concentration in the feed solution and the transmembrane pressures. As seen in Table 7.5, except the lowest urea concentration the effectiveness factors for all types of the membranes are close to one at three applied pressures. This indicates that stirring rate is not sufficient to eliminate external mass transfer resistance at the lowest urea concentration. Table 7.6 gives the changes in Da number with respect to substrate concentrations and transmembrane pressures. By combining the data in Table 7.5 and 7.6, it can be concluded that when D_a is less than unity, the effectiveness factor approaches almost one. This means that, when the transport of urea from feed side to the permeate side is controlled by enzymatic reaction, the data can be used to determine kinetic constants from Michaelis Menten equation. When D_a number is greater than 1, effectiveness parameters diverge from unity since transport in this case is controlled by the contribution of both diffusion and reaction.

Table 7.5. The change in effectiveness factors with respect to substrate concentrations under three different pressures (0.5, 1.0 and 1.5 bars) for the membranes on which urease is immobilized by means of covalent bonding (AN69-URE) and by means of electrostatic forces in the case of AN69-PEI-URE and AN69-PEI-URE-PEI.

Membrane	AN69-PEI-URE				AN69-PEI-URE-PEI				AN69-URE			
	Curea (mM)				Curea (mM)				Curea (mM)			
ΔP (bar)	0.50	5.00	10.00	50.00	0.50	5.00	10.00	50.00	0.50	5.00	10.00	50.00
0.50	0.69	0.93	0.97	1.00	0.70	0.92	0.97	1.00	0.70	0.92	0.97	1.00
1.00	0.73	0.90	0.96	1.00	0.70	0.89	0.95	1.00	0.70	0.89	0.95	1.00
1.50	0.74	0.91	0.96	1.00	0.67	0.88	0.95	1.00	0.67	0.88	0.95	1.00

Table 7.6. The change in Damköhler numbers with respect to substrate concentrations under three different pressures (0.5, 1.0 and 1.5 bars) for the membranes on which urease is immobilized by means of covalent bonding (AN69-URE) and by means of electrostatic forces in the case of AN69-PEI-URE and AN69-PEI-URE-PEI.

Membrane	AN69-PEI-URE				AN69-PEI-URE-PEI				AN69-URE			
	Curea (mM)				Curea (mM)				Curea (mM)			
ΔP (bar)	0.50	5.00	10.00	50.00	0.50	5.00	10.00	50.00	0.50	5.00	10.00	50.00
0.50	7.51	0.75	0.38	0.08	8.26	0.83	0.41	0.08	8.26	0.83	0.41	0.08
1.00	9.54	0.95	0.48	0.10	10.29	1.03	0.51	0.10	10.29	1.03	0.51	0.10
1.50	8.82	0.88	0.44	0.09	11.45	1.15	0.57	0.11	11.45	1.15	0.57	0.11

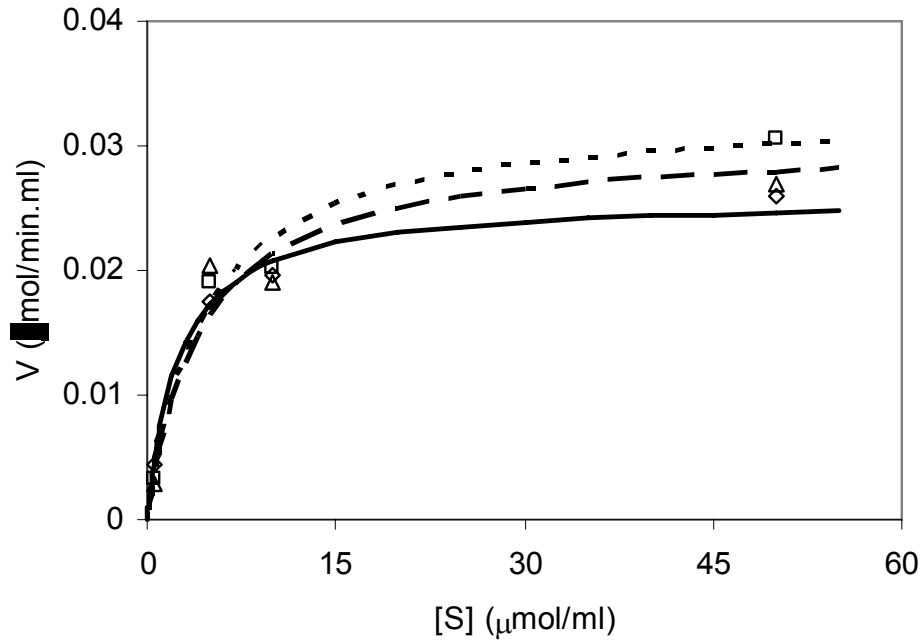


Figure 7.37. Reaction rate of AN69-PEI-URE membrane as a function of substrate concentration. Transmembrane pressures are, (◇) 0.5 bar, (□) 1.0 bar, (Δ) 1.5 bar.

The change in the reaction rates as a function of urea concentrations for the three types of membranes are depicted in Figure 7.37, 7.38 and 7.39. According to Figure 7.37, increasing pressure caused a decrease the reaction rate. This could be attributed to the loss of enzyme (release) during high pressure or conformational change occurred. In case of AN69-PEI-URE, urease is directly in contact with the solution and the only force that keep them on the surface of the membrane is ionic forces which are not as strong as covalent bonding as in the case of URE immobilized AN69 membrane by means of chemical attachment. However, in that case the reaction rate is the smallest and their kinetic parameters are given in Table 7.7. The transmembrane pressures for the other two membranes have no significant effect on their activities.

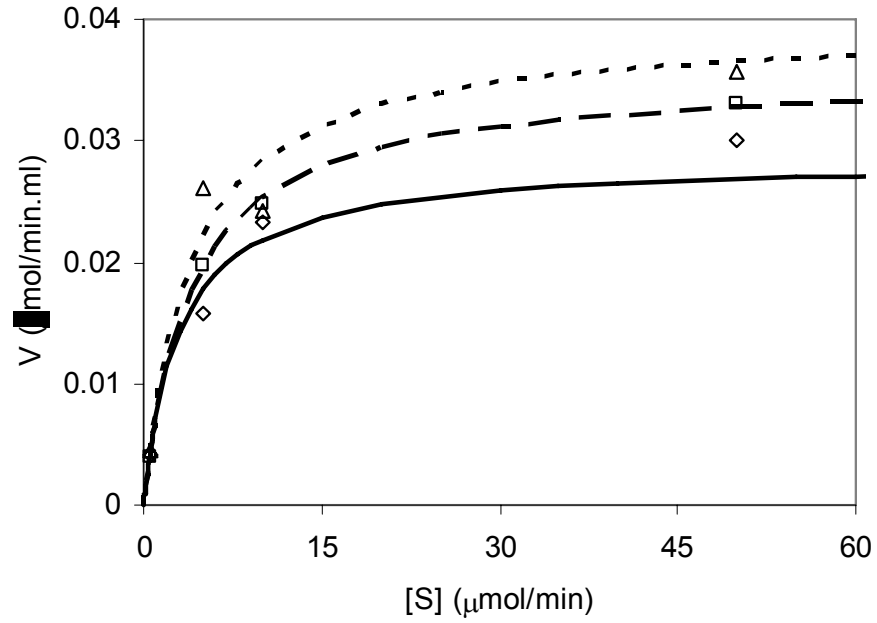


Figure 7.38. Reaction rate of AN69-PEI-URE-PEI membrane as a function of substrate concentration. Transmembrane pressures are, (◇) 0.5 bar, (□) 1.0 bar, (△) 1.5 bar.

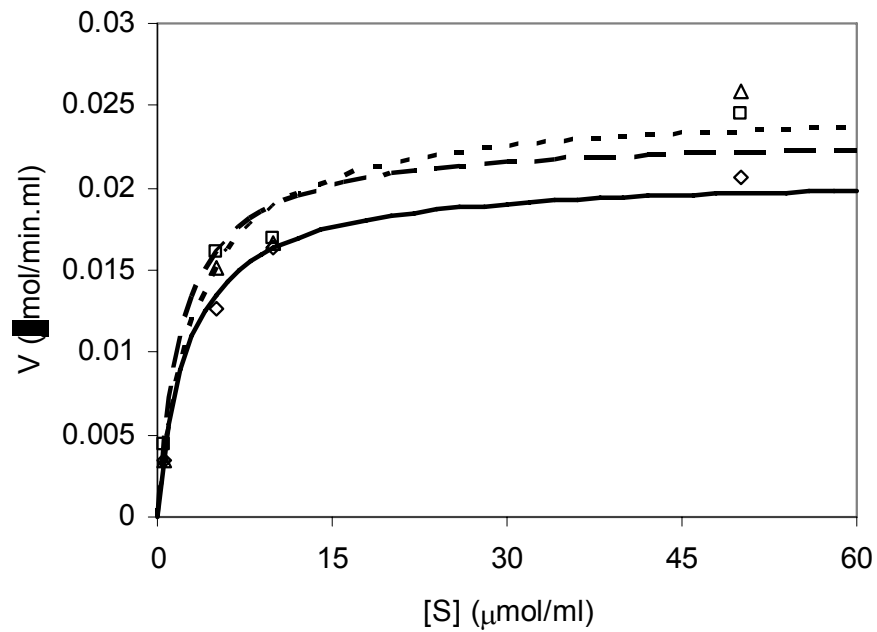


Figure 7.39. Reaction rate of chemically immobilized urease as a function of substrate concentration. Transmembrane pressures are, (◇) 0.5 bar, (□) 1.0 bar, (△) 1.5 bar.

Table 7.7. Kinetic parameters of urease immobilized AN69 membranes.

Membrane	$\Delta P(\text{bar})$	V_{\max}	K_m	k_{cat}
		$\mu\text{mol}/\text{min.mL}$	$\mu\text{mol}/\text{mL}$	$1/\text{min}$
AN69-PEI-URE*	0.45	0.0259	2.4617	0.0105
	0.85	0.0329	4.4766	0.0073
	1.30	0.0304	4.2931	0.0071
AN69-PEI-URE-PEI*	0.45	0.0285	3.0089	0.0095
	0.90	0.0354	4.0337	0.0088
	1.27	0.0394	3.9336	0.0100
AN69-URE**	0.45	0.0207	2.6383	0.0078
	1.00	0.0231	2.1774	0.0106
	1.45	0.0250	3.2490	0.0077

*, urease immobilized by means of ionic attachment

**, urease immobilized by means of covalent attachment

The results In Table 7.7 show that the maximum reaction rate of all membranes increases with the increase in pressure except AN69-PEI-URE where the reaction rate reduces at the highest transmembrane pressure.

In Figure 7.40, 7.41, and 7.42 the percentage of urea conversions as a function of filtrate fluxes are illustrated. Increasing substrate concentration decreases urea conversion. The catalytic ability of the membranes is not enough to decompose high urea concentration especially at higher fluxes.

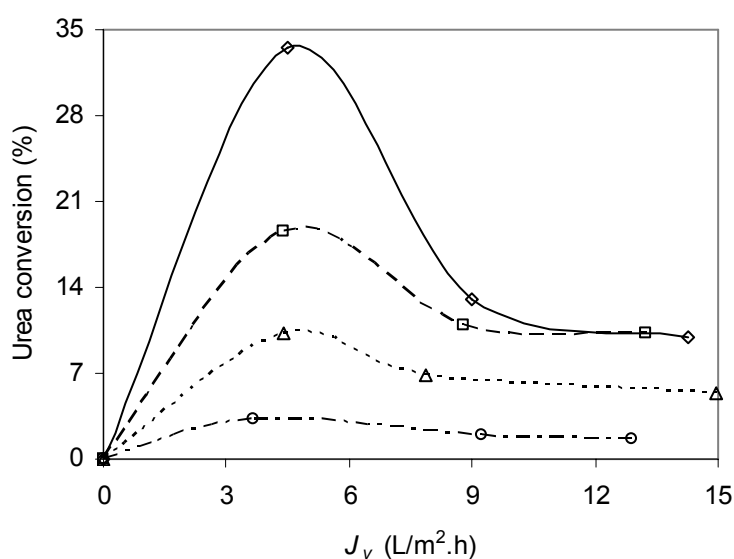


Figure 7.40. The change of urea conversion with the solution flux through AN69-PEI-URE membrane. Symbols are, (\diamond) 0.5, (\square) 5, (Δ) 10 and (\circ) 50 mM.

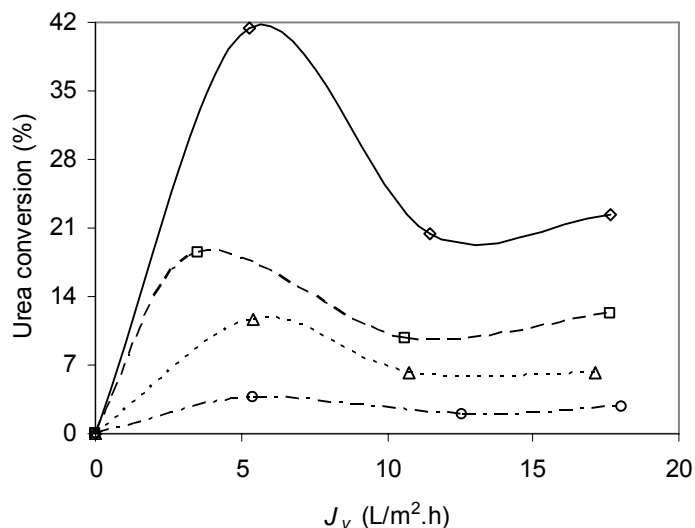


Figure 7.41. The change of urea conversion with the solution flux through AN69-PEI-URE-PEI membrane. Symbols are, (◇) 0.5, (□) 5, (△) 10 and (○) 50 mM.

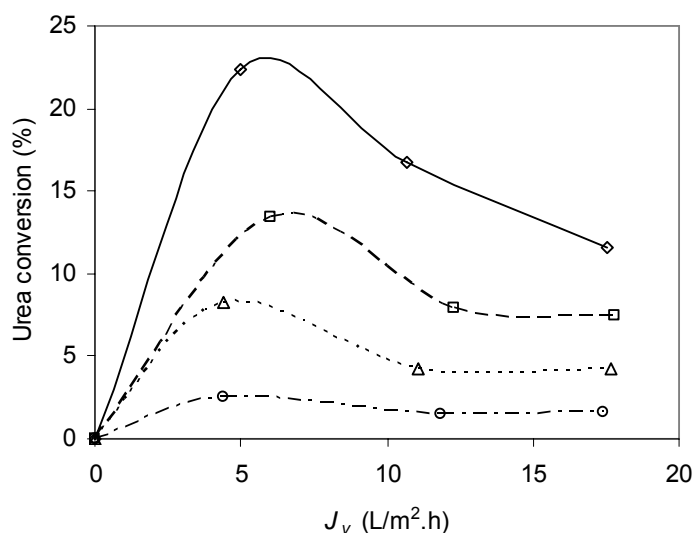


Figure 7.42. The change of urea conversion with the solution flux through modified AN69 membrane on which urease was chemically immobilized. Symbols are, (◇) 0.5, (□) 5, (△) 10 and (○) 50 mM.

The difference in urea conversions for the three types of membranes results from the difference in their kinetic parameters. The results in those three figures suggest that the catalytic membranes best work at the lowest filtrate flux.

In addition to conversion of urea, the retained activities at the end of the filtration experiments (~ 450 min) were determined and plotted in Figure 7.43 for the three types of catalytic membranes. Based on Figure 7.43, the activity lost with respect to initial value was 16% in the case of AN69-PEI-URE-PEI membrane while 50% of

initial activity lost was observed in the case of AN69-PEI-URE membrane and no activity change occurred in the case of chemically immobilized urease. The results suggest that under dynamic conditions urease in sandwiched form displayed the highest activity and permeability while urease immobilized AN69 membrane by means of covalent bonding showed the highest stability.

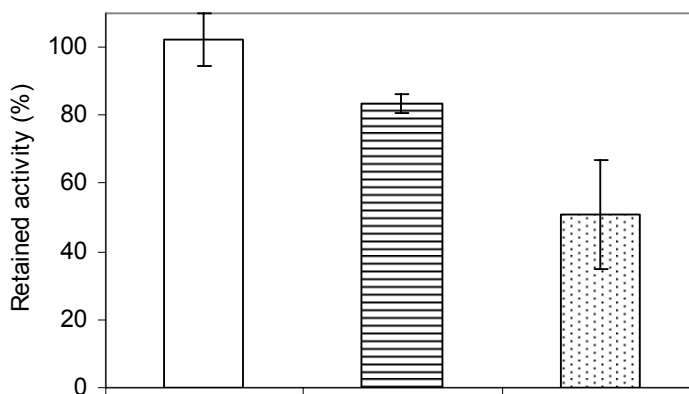


Figure 7.43. Percentage retained activity of the catalytic membranes at the end of 450 min of filtration process. (⊙) AN69-PEI-URE, (≡) AN69-PEI-URE-PEI, (□) AN69-URE

7.4. Model Results

7.4.1. Model Validation with the Experimental Filtration Data

Urea filtrations through catalytic AN69-PEI membrane were performed with different feed concentrations (1, 2.5, 5 and 10 mM) under different operating pressures (0.7, 1.1 and 1.4 bar) using dead-end stirred cell. The change in urea concentration during filtration was determined by sampling from the collected filtrate at each 10 min intervals. The data are represented in Figures 7.44a through 7.44c which correspond to operating pressures of 0.7, 1.1 and 1.4 bar, respectively. From all three figures, it can be concluded that urea concentrations decrease linearly with respect to time which is an indication that urease is catalytically active and proceeds to catalyze urea without suffering from deactivation.

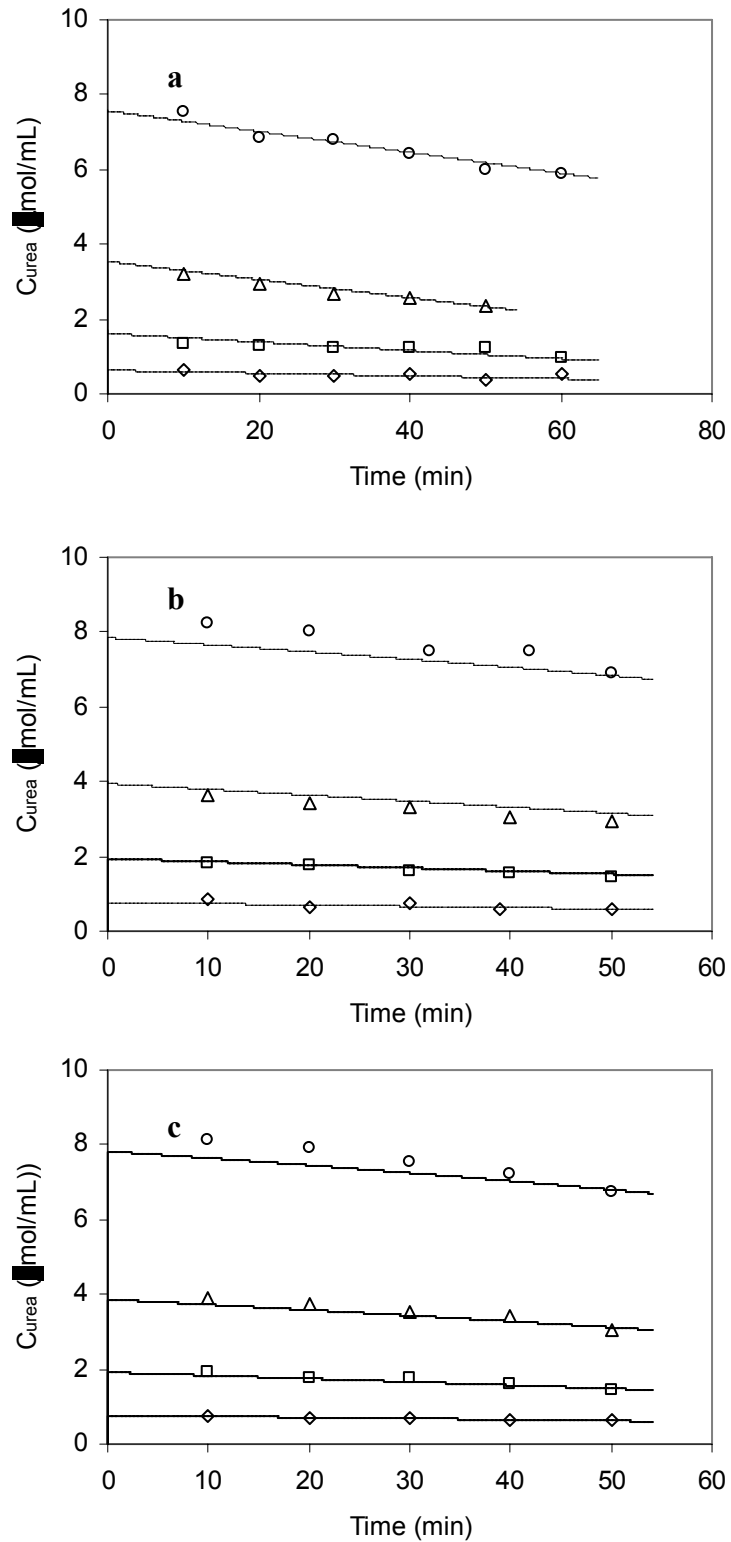


Figure 7.44. Comparison of experimental data with the model estimations. The data were collected at a) 0.7, b) 1.1 and c) 1.4 bar. Points represent experimental data and lines represent theoretical result. Symbols represent the feed concentrations: (\diamond) 1mM, (\square) 2.5mM, (Δ) 5mM and (\circ) 10 mM.

The experimental data were then used to correlate the model. The input data used for the solution of model equations are listed in Table 7.8. Due to lack of accurate theoretical approximations and the lack of experimental tools, it was not possible to calculate or determine thickness of the enzyme layers and the pore size of the enzyme layer as well. These values were estimated using the experimental data collected at 0.7 bar. The experimental data in Figure 7.44 as well as previous filtration data indicated that urea conversion changes with the applied pressure which points to the fact that the enzyme kinetic parameters depend on pressure. Since, classical Michaelis-Menten theory cannot take into account this fact; the enzyme kinetic parameters and solution flux values were also adjusted and the estimated values are listed in Table 7.9. For the correlation of the experimental data with the model, following error definition was used:

$$error = \sum_{i=1}^{N_{data}} \left(\ln C_{experimental} - \ln C_{theoretical} \right)^2 \quad (7.6)$$

The results shown in Figure 7.44 indicate that the model correlates the experimental data well.

Table 7.8. Parameters used for the correlation and prediction of the experimental data carried out at 0.7, 1.1 and 1.4 bar transmembrane pressures respectively.

$K_{c,m}$	Convective hindrance factor for membrane	1.019
$K_{D,m}$	Diffusive hindrance factor for membrane	0.98
$K_{c,e}$	Convective hindrance factor for enzyme layer	1.019
$K_{D,e}$	Diffusive hindrance factor for enzyme layer	0.98
$D_{i,\infty}$	Urea diffusion coefficient in solution, m ² /s	6.27x10 ⁻⁹
$D_{eff,m}$	Urea diffusion coefficient in membrane, m ² /s	4.82x10 ⁻⁹
$D_{eff,e}$	Urea diffusion coefficient in enzyme, m ² /s	2.87x10 ⁻⁹
N	Rotational speed, rate/s	5
$V_{f,0}$	Initial feed volume, m ³	50x10 ⁻⁶
μ_w	Viscosity of water, kg/m.s	8.937x10 ⁻⁴
δ_m, δ_e	Thickness of membrane and enzyme layer, m	25x10 ⁻⁶ 40x10 ⁻⁹
ϵ_m, ϵ_e	Porosity of membrane and enzyme layer	0.8 0.4765
λ_m, λ_e	Effective solute to pore size ratio for membrane and enzyme layer	0.0092 0.0093
Φ	Partition coefficient	0.98

According to the experimental data and model results, maximum conversion was attained at 2.5 mM feed concentrations for all transmembrane pressures, since the saturation concentration for the catalytic membrane is 2.5 mM. Above this limit no more urea is converted to ammonia, thus, urea conversion decreases with its increased concentration in the feed.

Table 7.9. Kinetic parameters estimated from the model correlation and predictions with the experimental data carried out at 0.7, 1.1 and 1.4 bar transmembrane pressures respectively.

Pressure (bar)	V_{max} (kmol/m ³ .s)	K_m kmol/m ³	J_v (m/s)
0.7	1	0.005	1.6×10^{-6}
1.1	2.5	0.025	2.0×10^{-6}
1.4	2.5	0.022	2.4×10^{-6}

7.4.2. Model Predictions

Theoretical analysis of an ultrafiltration process can be useful for predicting the effects of processing parameters such as transmembrane pressure and kinetic parameters of the immobilized membrane on the filtration efficiency. The mathematical model in this study predicts the urea concentrations through the enzyme and the membrane layers during filtration. The results are represented in terms of dimensionless numbers including Peclet number, Pe , and Thiele modulus, κ , in which the former is defined as the ratio of the mass transfer due to bulk motion to the molecular diffusion while the latter can be described as the ratio of reaction rate to the diffusional rate. Time is represented in dimensionless form with the multiplication of diffusion coefficient of urea in the membrane divided by the square of the membrane thickness and program calculates 5000 data point for each unit time which corresponds to 25 min.

Dimensionless urea concentrations through enzyme and membrane layers as a function of Pe number at the end of filtration process are illustrated in Figure 7.45. The plots were obtained by increasing the solution flux, while keeping κ^2 / θ constant as 9. To manipulate the change in urea concentration in enzyme layer more visible (250 times less than membrane thickness), 20 nodes were used to represent it and 30 nodes for the

membrane layer. In Figure 7.46, $z^*=0$ represents the feed side and $1+L_e/L_m$ corresponds to the permeate side.

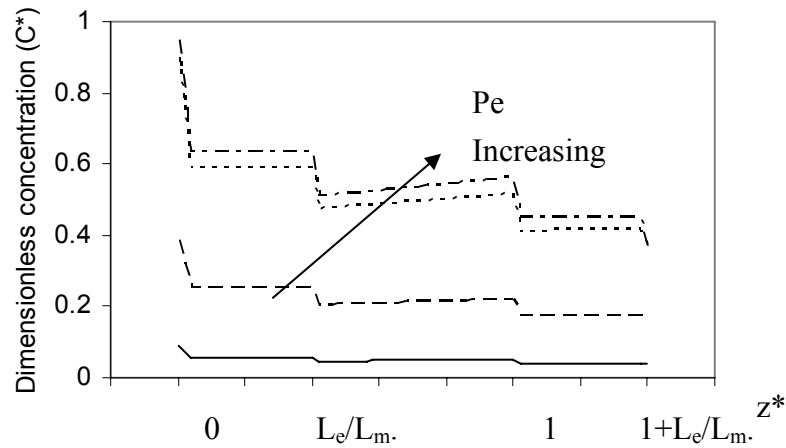


Figure 7.45. The change in dimensionless urea concentrations through enzymatic membrane layers as a function of Peclet numbers (0.006, 0.008, 0.013 and 0.026).

Sharp decreases in urea concentrations were observed at the boundaries due to partitioning effect which is related to the particle size of urea and pore size of the enzyme or membrane layer. The predictions in Figure 7.45 indicates that the urea concentrations along enzyme layers do not change since Thiele modulus was set to a high value which means that the enzymatic reaction is very fast compared to the mass transfer rate. On the other hand, a gradual increase in the urea concentrations through membrane layer is observed especially at higher Peclet numbers due to contribution of both convection and diffusion. This is due to the fact that higher mass transfer rates through the membrane and enzyme layers decrease the contact time between the enzyme and substrate layer, hence, decreases its conversion. The results suggest operating the ultrafiltration unit at low transmembrane pressures to maintain high urea conversion rates. Figure 7.46 shows the change in urea concentrations through the enzyme and membrane layers as a function of Thiele modulus, κ^2 / θ , while keeping the Pe number constant as 0.013. The increase in reaction rate, hence, the increase in Thiele modulus values increased the rate of urea conversion, consequently, lower urea concentrations were observed at higher Thiele modulus values.

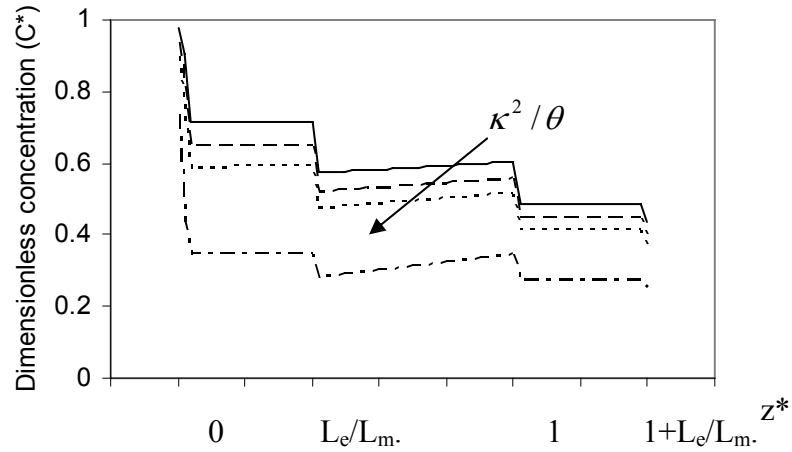


Figure 7.46. The change in urea concentrations through enzymatic membrane layers with respect to κ^2 / θ (3, 6, 9 and 30).

The comparison of urea conversions with respect to time at a constant κ^2 / θ value and different Pe numbers is depicted in Figure 7.47. The conversion of urea is calculated based on the expression given below;

$$Conversion = 1 - (C_F^* V_F^* - C_P^* V_P^*)_{t=t} \quad (7.7)$$

where, C_F^* and C_P^* is the dimensionless concentration of urea in the feed and permeate, V_F^* and V_P^* are dimensionless volume of feed and filtrate, respectively. Highest urea conversion was obtained at the smallest Pe, the conversion reaches to 90% almost at the beginning of the filtration. The lower flux increases the residence time of urea in the enzyme layer, hence, allows to achieve higher urea conversions. On the other hand, at high Pe numbers, conversion becomes lower and is not influenced by the increased values of Pe number.

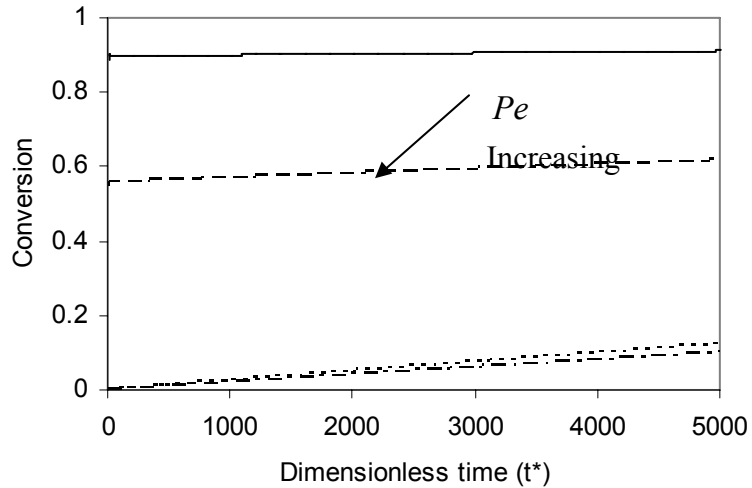


Figure 7.47. Urea conversions with respect to time. Lines represent Peclet numbers as 0.006, 0.008, 0.013 and 0.026.

In Figure 7.48, urea conversions as a function of Peclet number with Thiele modulus values are compared. At low Pe numbers, a linear reduction in urea conversion was observed regardless of the magnitude of Thiele modulus. However, at high Pe numbers, conversion increases with the increased values of Thiele modulus which corresponds to higher enzyme kinetic parameters. The results in Figure 7.48 also indicates that at high Pe numbers, conversion of urea does not change at all which suggests that above certain limit, there is no benefit of increasing the solution flux by increasing the transmembrane pressure.

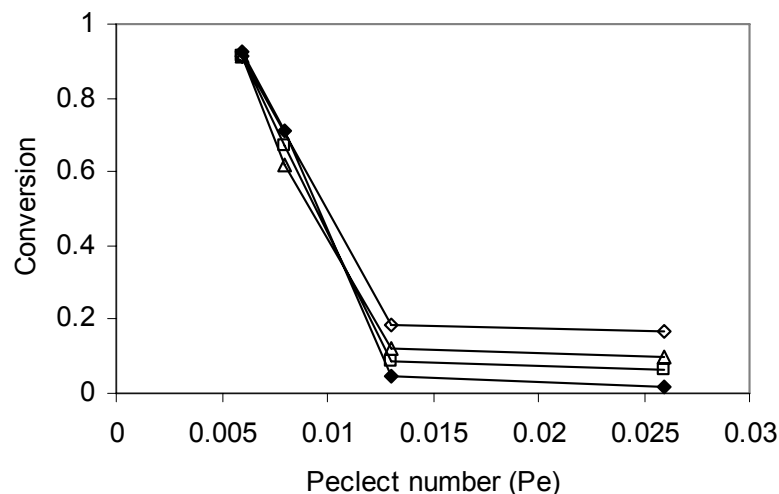


Figure 7.48. Comparison of the urea conversion with respect to Peclet number. Symbols denote κ^2 / θ as, (◆) 3, (□) 6, (Δ) 9 and (◇) 15.

Effectiveness factor is one of the important dimensionless parameter that describes the importance of external mass transfer resistance on the observed enzymatic reaction rates. The effectiveness factor close to one indicates the absence of external mass transfer resistance, hence, sufficient stirring rates both on the feed and permeate sides. Figure 7.49 illustrates the change in effectiveness factor as a function of Thiele modulus. At low Pe numbers, the effectiveness factor deviates significantly from one, decreases with the increased values of Thiele modulus. At these conditions, the reaction rate is high which causes high urea conversion to ammonia without its quick removal from the feed side due to low solution fluxes, consequently, development of concentration boundary layer near the enzyme boundary layer and increase in the external mass transfer resistance. At high Pe numbers, the effectiveness factor is close to one and it is not influenced by the increases in the kinetic parameters.

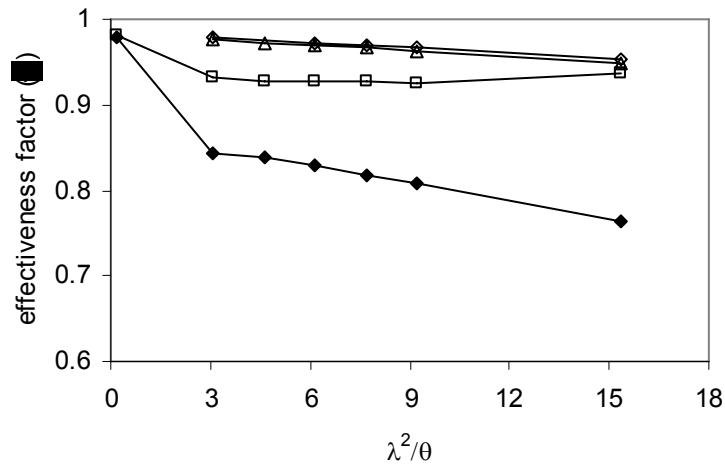


Figure 7.49. Effectiveness factor as a function of κ^2 / θ compared with the variation of Peclet number. Symbols denote as, (\blacklozenge) 0.006, (\square) 0.008, (\triangle) 0.013 and (\diamond) 0.026.

CHAPTER 8

CONCLUSION

The purpose of this thesis study was to prepare active and stable urease immobilized membranes for the efficient removal of urea and to predict the performances of these membranes under pressure. To achieve the first objective, two commercially available ultrafiltration membranes namely Poly (acrylonitrile-co-sodium methallyl sulfonate) copolymer (AN69) and polyethyleneimine (PEI) deposited AN69 membranes (AN69-PEI) were used as supporting materials on which urease was immobilized by means of physical adsorption using layer-by-layer self assembly method or chemical attachment using N-ethyl-N'-(3-dimethylaminopropyl) carbodiimide hydrochloride (EDC) and N-hydroxysuccinimide (NHS) coupling agents as a zero crosslinker. During physical immobilization (pH 7.4), the effect of type of polyelectrolytes on the activity of immobilized urease was compared between PEI and chitosan (CHI) cationic polyelectrolytes where urease was located either on top of the polyelectrolyte layer or between two polyelectrolyte layers in a sandwiched form. Physical immobilization results reveal that the amount of urease immobilized on AN69 or polyelectrolyte modified membranes are similar. The availability of polar and non-polar groups in the structure of urease allows its specific and non-specific adsorption on the membrane surface. Urease immobilization on AN69 membrane mainly takes place with non-specific adsorption, which results in clusters on certain areas of the membrane in a nucleation growth type of the process. Although urease amount adsorbed on AN69 or polyelectrolyte modified AN69 membranes were similar, significant differences in the maximum reaction rates were observed. The maximum reaction rates in the decreasing order were found as AN69-PEI-URE>AN69-CHI-URE>AN69-URE>AN69-PEI-URE-PEI>AN69-CHI-URE-CHI. Higher catalytic activity of AN69-PEI-URE membrane compared with that of AN69-CHI-URE was attributed to lower molecular weight of PEI and its linear structure which allows urease attachment in such a way that more active sites of the enzyme are available.

The amount of urease immobilized on the activated AN69 surface by chemical attachment and its maximum reaction rate were found lower than those values obtained

from physical immobilization. On the other hand, storage stability of chemically immobilized urease was found to be highest among all the membranes prepared. Urease immobilized on the unmodified AN69 membrane by non-specific adsorption has the lowest storage stability while urease sandwiched between two polyelectrolyte layers retained its activity for a longer period of time compared with the cases where urease is the last layer which is in contact with the environment. In the decreasing order, the storage stabilities of physically immobilized urease were determined as follows: AN69-PEI-URE-PEI>AN69-CHI-URE-CHI>AN69-PEI-URE>AN69-CHI-URE>AN69-URE.

The performances of the prepared membranes under dynamic conditions were also tested. The hydraulic permeabilities of the commercial and urease immobilized membranes were found similar due to addition of a thin layer with urease adsorption, hence, negligible resistance of this layer to flow. The highest urea conversion was achieved with the AN69-PEI-URE-PEI membrane. For all the membranes; the conversion decreased with the substrate concentration and the transmembrane pressure applied through the membrane. These results simply indicated that urea removal from the feed is controlled by enzymatic reaction rather than mass transfer. The maximum reaction rates increased with pressure in the case of AN69-PEI-URE-PEI membrane and AN69-URE membrane where urease was immobilized by means of covalent attachment. On the other hand, a decrease in the maximum reaction rate was observed with the AN69-PEI-URE membrane probably due to desorption of enzyme or its conformational change at high pressure.

The catalytic activity of the membrane prepared by the chemical attachment of urease was completely preserved at the end of 450 minutes. Even though the activity lost was observed for AN69-PEI-URE membrane, this has been significantly reduced by sandwiching urease between two polyelectrolyte layers. The performances of the urease immobilized membrane were also evaluated using a mathematical model developed. The model can predict the influences of operating conditions, enzyme kinetic parameters and the structural properties of the membrane on the conversion of the substrate.

In overall conclusion, it can be said that enzyme immobilization by layer-by-layer self assembly of polyelectrolytes is a simple and promising method as compared to complex conventional chemical attachment.

REFERENCES

- Krajewska B, Ureases II. Properties and their customizing by enzyme immobilizations: A review, *Journal of Molecular Catalysis B: Enzymatic*, 59, 22–40, 2009
- Organisation for Economic Co-operation and Development (OECD), 1994. Screening Information Data Sets of High Production Volume Chemicals Programme, Paris, France.
- Simka W., Piotrowski J., *Przem. Chem.*, 86, 841–845, 2007
- Lehmann H.D., Marten R., Gullberg C.A., *Artif. Organs.*, 5, 278–285, 1981
- Lefier D., *Bull. Int. Dairy Fed.*, 315, 35, 1996
- Kodama S., Suzuki T. J., *Food Sci.*, 60, 1097, 1995
- Woodly J.M, *Immobilized Biocatalysts, Solid Supports Catal. Org. Synth*, 254-271, 1992
- Tisher W, Wedekind F, *Immobilized Enzymes: Methods and Applications, Top Curr. Chem*, 200, 95-126, 1999
- Furuki S, In *Enzymes In Industry*, Aehle W. Ed., Wiley-VCH: Weinheim, Section 3.3, 2004
- Scouten W.H, In *Methods In Enzymology, Vol. 135: Immobilized Enzymes and Cells*, Mosbach K, Ed, Academic Press: New York, pp 30-65, 1987
- Yamada K, Iizawa Y, Yamada J, Hirata M, Retention of activity of urease immobilized on grafted polymer films, *Journal of Applied Polymer Science*, 102, 4886-4896, 2006
- Di Martino S., El-Sheriff H., Diano N., De Maio A., Grano V., Rossi S., Benchivenga U., Mattei A., Mita D.G., Urea removal from agricultural waste waters by means of urease immobilized on nylon membranes grafted with cyclohexyl-methacrylate, *Applied Catalysis B: Environmental*, 46, 613-629, 2003
- Ayhan F., Ayhan H, Piskin E, Tanyolac A, *Bioresou Technol.*, 81, 131, 2002

- Lin C.C., Yang M.C., Urea permeation and hydrolysis through hollow fiber dialyzer immobilized with urease: storage and operation properties, *Biomaterials*, 1989-1994, 2003
- Kuralay F, Özyörük H, Yıldız A, Potentiometric enzyme electrode for urea determination using immobilized urease in poly(vinylferrocene) film, *Sens.Actuat.B. Chem*, 109, 194-199, 2005
- Decher G., Hong J.D, Buildup of ultrathin multilayer films by a self-assembly process. I. Consecutive adsorption of anionic and cationic bipolar amphiphiles and polyelectrolytes on charged surfaces, *Ber. Buns. Phys. Chem.*, 95, 1430–1434, 1991
- Hoogeven N.G, Cohen-Stuart M.A., Fleer G.J., Böhner M.R., Formation and stability of multilayers of polyelectrolytes, *Langmuir*, 12, 3675–3681, 1996
- Ladam G., Schaad P., Voegel J.-C., Schaaf P, Deche G.r, Cuisinier F., In situ determination of the structural properties of initially deposited polyelectrolyte multilayers, *Langmuir*, 16, 1249–1255, 2000
- Balabushevitch N.G., Sukhorukov G.B., Moroz N.A, Volodkin D.V., Larionova N.I., Donath E., Moehwald H., Encapsulation of proteins by layer-by-layer adsorption of polyelectrolytes onto protein aggregates: factors regulating the protein release, *Biotechnol. Bioeng.*, 76, 207–213, 2001
- Crespilho F.N., Ghica M.E., Florescu M., Nart F.C., Oliveira Jr. O.N., Brett C.M.A., A strategy for enzyme immobilization on layer-by-layer dendrimer–gold nanoparticle electrocatalytic membrane incorporating redox mediator, *Electrochem. Commun.*, 8, 1665–1670, 2006
- Caseli L., Santos Jr. D.S.D., Foschini M., Goncalves D., Oliveira Jr. O.N., The effect of the layer structure on the activity of immobilized enzymes in ultrathin films, *J. Colloid Interface Sci.*, 303, 326–331, 2006
- Garbers E., Mitlöhner R., Georgieva R., Bäuml H., Activity of immobilized trypsin in layer structure of polyelectrolyte microcapsules (PEMC), *Macromol. Biosci.*, 7, 1243–1249, 2007
- Wachem P.B. van, Lyun M.J.A van, Olde Damink L.H.H, Dijkstra P.J, Feijen J, Nieuwenhuis P, Tissue regenerating capacity of carbodiimide crosslinked dermal

- sheep collagen during repair of the abdominal wall, *Biomaterials*, 17, 230-239, 1994
- Alcock H.R, Lampe F.R., *Contemporary polymer chemistry*, 2nd Ed, Engelwood Cliffs, N.J, Prentice Hall, 1990
- Holmes-Farley S.R, Reamey R.H, McCarthy T.J, Deutch J, Whitesides G.M, Acid-base behavior of carboxylic groups covalently attached at the surface of polyethylene- the usefulness of contact-angle in following the ionization of the surface functionality, *Langmiur*, 1, 725-40, 1985
- Gabrovska K, Georgieva A, Godjevargova T, Stoilova O, Manolova N, Poly(acrylonitrile) chitosan composite membranes for urease immobilization, *Journal of Biotechnology*, 129, 674-680, 2007
- Pozniak G, Krajewska B, Trochimczuk W, Urease immobilized on modified polysulfone membrane: preparation and properties, *Biomaterials*, 16, 129-134, 1995
- Uragami T, Ueguchi K, Watanabe M, Miyata T, Preparation of urease immobilized polymeric membranes and their function, *Catalysis Today*, 118, 158-165, 2006
- Akay G, Erhan E, Keskinler B, Algur O.F, Removal of phenol from wastewater using membrane-immobilized enzymes Part II. Cross-flow filtration, *J.M.S*, 206, 61-68, 2002
- Hicke H.G, Böhme P, Becker M, Shulze H, Ulbright M, Immobilization of enzymes onto modified polyacrylonitrile membranes: Application of the acyl azide method, *J. Applied Polymer Science*, 60, 1147-1161, 1996
- Ulbright M, Papra A, Polyacrylonitrile enzyme ultrafiltration membranes prepared by adsorption, cross-linking, and covalent binding, *Enzyme and Microbial Technology*, 20, 61-68, 1997
- Hu Y, Wang Y, Luo G, Dai Y, Modeling of a biphasic membrane reactor catalyzed by lipase immobilized in a hydrophilic/hydrophobic composite membrane, *Journal of Membrane Science* 308, 242–249, 2008
- Honti G.D., “Urea” IN *The Nitrogen Industry*, Academia Kiado, Budapest, Hungary, 1976

- Dallet P., Labat L., Kummer E., Dubost J.P., *J. Chromatogr. B: Biomed. Sci. Appl.*, 742, 447, 2000
- Lemmen W. The Environmental Impact of a Stamicarbon 2000 MTD Urea plant. In: *AIChE Ammonia Safety Symposium*; 1994
- United Nation Industrial Development Organization (UNIDO) and International Fertilizer Development Center (IFDC), “Fertilizer Manual”, Chapter 9, page 258, 3rd ed, Kluwer Academic Publishers, 1998
- Ljubica M. , Igor D., Hrvoje L., Treatment of wastewater generated by urea production, *Resources, Conservation and Recycling*, 54, 149–154, 2010
- Mehnen J., Verweel C., Experience to date with the Stamicarbon desorber–hydrolyser system, in: *Proceedings of Stamicarbon’s Seventh Urea Symposium*, Maastricht, The Netherlands, Paper 9, pp. 1–15, 1987
- Taylor A.J., Vadgama P., *Ann. Clin. Biochem.*, 29, 245, 1992
- Schimidt DF, Schniepp BJ, Kurz SB, McCharty JT, Inaccurate blood flow rate during rapid hemodialysis, *Am.J.Kidney Dis*, 17, 34-7, 1991
- Krivitski NM, Theory and validation of Access flow measurement by dilution technique during hemodialysis, *Kidney Int*, 48, 244-50, 1995
- Della Ciana L., Caputo G., *Clin. Chem.*, 42, 1079, 1996
- Gordon A., Better O.S., Greenbaum M.A, Marantz L.B., Gral T., Maxwell M.H., *Trans. ASAIO*, 17, 253–258, 1971
- Krajewska B., Zaborska W., *Biocyb. Biomed. Eng.*, 9, 91–102, 1989
- Y. Nos’e, Artificial kidney research, is it really not necessary? *Artif. Organs*, 14, 254–256, 1990
- Larsen T A, Peters I, Alder A, Eggen R, Maurer M, Muncke J, Re-engineering the toilet for sustainable wastewater management. *Environ Sci Technol*, 35, (9): 192A–197A, 2001
- Hammer, D.A., *Constructed wetlands for wastewater treatment*, Lewis Publishers, Chelsea, Mich., 1989
- Crites R. W., Tchobanoglous, G., *Small and Decentralized Wastewater Management Systems*. United States of America. McGraw-Hill Companies, Inc., 1998

- Buisson H., Cote P., Praderie M., Paillard H., The use of immersed membranes for upgrading wastewater treatment plants. *Water Science and Technology*, 37(9): 89-95, 1998
- Rosenberger S., Kruger U., Witzig R., Manz W., Szewzyk U., Kraume M., Performance of a bioreactor with submerged membranes for aerobic treatment of municipal waste water. *Water Research*, 36(2): 413-420, 2002
- Berube P.R., Hall E.R., Fate and removal kinetics of contaminants contained in evaporator condensate during treatment for reuse using a high-temperature membrane bioreactor. *Journal of Pulp and Paper Science*, 27(2): 41-45, 2001
- Fan Y.B., Wang J.S., Jiang Z.C., Test of membrane bioreactor for wastewater treatment of a petrochemical complex, *Journal of Environmental Sciences*, 10(3): 269- 275, 1998
- Cicek, N., Franco J.P., Suidan M.T., Urbain V., Manem J., Characterization and comparison of a membrane bioreactor and a conventional activated-sludge system in the treatment of wastewater containing high-molecular-weight compounds. *Water Environment Research* 71(1): 64-70, 1999
- Bugg T.D.H, "Introduction to Enzyme and Coenzyme Chemistry", 2nd Ed, Blackwell Pub, p 19-22, 2004
- Ratner B.D, Hoffman A.S, Schoen F.J, Lemons J.E, "Biomaterials Science: An Introduction to Materials in Medicine", Academic Press, p 135, 1996
- Bull H.B, Breese K, Surface tension of amino acid solutions: A hydrophobicity scale of the amino acid residues. *Arch. Biochem. Biophys*, 161, 665-670, 1974
- Sumner J.B., *J. Biol. Chem.*, 69, 435–441, 1926
- Dixon N.E., Gazzola C., Blakeley R.L., Zerner B., *J. Am. Chem. Soc.*, 97, 4131–4133, 1975
- Mobley H.L.T., Hausinger R.P., *Microbiol. Rev.*, 53, 85–108, 1989
- Krajewska B., *Wiad. Chem.*, 56, 223–253, 2002
- Takishima K., Suga T., Mamiya G., *Eur. J. Biochem.*, 175, 151–165, 1988
- Polacco J.C., Havir E.A., *J. Biol. Chem.*, 254, 1707–1715, 1979
- Das N., Kayastha A.M., Srivastava P.K., *Phytochemistry*, 61, 513–521, 2002

- Krajewska B., Ureases. I. Functional, kinetic and catalytic properties: a review, *J. Mol. Catal. B: Enzym.*, 59: 9-21, 2009
- Jabri E., Carr M.B., Hausinger R.P., Karplus P.A., *Science*, 268, 998–1004, 1995
- Jabri E., Karplus P.A., *Biochemistry*, 35, 10616–10626, 1996
- Benini S., Rypniewski W.R., Wilson K.S., Miletto S., Ciurli S., Mangani S., A new proposal for urease mechanism based on the crystal structures of the native and inhibited enzyme from *Bacillus pasteurii*: why urea hydrolysis costs two nickels, *Structure*, 7, 205–216, 1999
- Riddles P.W., Andrews R.K., Blakeley R.L., Zerner B., *Biochim. Biophys. Acta* 743, 115–120, 1983
- Karplus P.A., Pearson M.A., Hausinger R.P., *Acc. Chem. Res.* 30, 330–337, 1997
- Dixon N.E., Riddles P.W., Gazzola C., Blakeley R.L., Zerner B., *Can. J. Biochem.*, 58, 1335–1344, 1980
- Cabral J.M.S., Kennedy J.F., Immobilization techniques for altering thermal stability of enzymes. In: Gupta MN, ed. *Thermostability of enzymes*. Berlin: Springer-Verlag, 162-179, 1993
- Zhao X.S, Bao X.Y, Guo W.P, Lee F.Y., Immobilizing catalysts on porous materials, *Materials Today*. Mar, 9(3),32-39, 2006
- Kara F., Demirel G., Tümtürk H., *Bioprocess Biosyst. Eng.*, 29, 207–211, 2006
- Shah Y., Shah D., Kothari R.M., Trivedi B.M., *Res. Ind.*, 39, 184–190, 1994
- Kurokawa Y., Sano T., Ohta H., Nakagawa Y., *Biotechnol. Bioeng.*, 42, 394–397, 1993
- Hatayama H., Swabe T., Kurokawa Y., *J. Sol-Gel Sci. Technol.*, 7, 13–17, 1996
- Kobayashi T., Miyama H., Kawata S., Nosaka Y., Furii N., *J. Appl. Polym. Sci.*, 46, 2183–2188, 1992
- Miyama H., Kawata M., Nosaka Y., *Biotechnol. Bioeng.*, 27, 1403–1410, 1985
- Godjevargova T.S., Dimov A., Immobilization of urease onto membranes of modified acrylonitrile copolymer, *Journal of Membrane Science*, 135, 93-98, 1997
- M. Vassilev, Laboratory diagnostics. Express tests, *Medicina I fizkultura*, Sofia, 1990

- Zhao H., Ju H., Multilayer membranes for glucose biosensing via layer-by-layer assembly of multiwall carbon nanotubes and glucose oxidase, *Anal. Biochem.* 350, 138-144, 2006
- Decher G., Hong J.D., *Macromol. Chem. Macromol. Symp.*, 46, 321-327, 1991
- Vipavee P., Thomas J.M, Stepwise polymer surface modification: Chemistry-Layer-by-Layer deposition, *Macromolecules*, 31, 1906-1914, 1998
- Lajimi R.H., Abdallah A.B., Ferjani E., Roudesli M.S., Deratani A., Change of the performance properties of nanofiltration cellulose acetate membranes by surface adsorption of polyelectrolyte multilayers, *Desalination*, 163, 193-202, 2004
- Nguyen Q.T., Ping Z., Nguyen T., Rigal P., Simple method for immobilization of biomacromolecules onto membranes of different types, *J. Membr. Sci.*, 213, 85-95, 2003
- Smuleac V., Butterfield D.A., Bhattacharyya D., Layer-by-layer-assembled microfiltration membranes for biomolecule immobilization and enzymatic catalysis, *Langmuir*, 22, 10118-10124, 2006
- Datta S., Cecil C., Bhattacharyya D., Functionalized membranes by layer-by-layer assembly of polyelectrolytes and in situ polymerization of acrylic acid for applications in enzymatic catalysis, *Ind. Eng. Chem. Res.*, 47, 4586-4597, 2008
- Wang Y., Caruso F., Macroporous zeolitic membrane bioreactors, *Adv. Funct. Mater.*, 14, 1012–1018, 2004
- Yu A., Liang Z., Caruso F., Enzyme multilayer-modified porous membranes as biocatalysts, *Chem. Mater.*, 17, 171–175, 2005
- Godjevargova T, Gabrovska K, Immobilization of urease onto chemically modified acrylonitrile copolymer membranes, *Journal of Biotechnology*, 103, 107-111, 2003
- Yang M.C., Lin C.C., Urea permeation and hydrolysis through hollow fiber dialyzer immobilized with urease, *Biomaterials*, 22, 891-896, 2001
- Gendler E, Gendler S, Nimmi M.E, Toxic reaction evoked by glutaraldehyde fixed pericardium and cardiac valve tissue bioprosthesis, *J. Biomed. Mater. Res.*, 18, 727-736, 1984

- Eyble E, Griesmacher A, Grimm M, Wolner E, Toxic effects of aldehydes released from fixed pericardium on bovine aortic endothelial cells, *J. Biomed. Mater. Res*, 23, 1355-1369, 1989
- Huang Lee L.L.H, Cheung D.T, Nimmi M.E, Biochemical changes and cytotoxicity associated with the degradation of polymeric glutaraldehyde derived crosslinks, *J. Biomed. Mater. Res*, 24, 1185-1201, 1990
- Lyun M.J.A van, Wachem P.B. van, Olde Damink L.H.H, Dijkstra P.J, Feijen J, Relation between in vitro cytotoxicity and crosslinked dermal ship collagens, *J. Biomed. Mater. Res*, 26, 1091-1110, 1992
- Wissink M.J.B, Beernink R, Pieper J.S, Poot A.A, Engbers G.H.M, Beugeling T, Aken W.G van, Feijen J, Immobilization of heparin to EDC/NHS-crosslinked collagen. Characterization and in vitro evaluation, *Biomaterials*, 22, 151-163, 2001
- Ye P, Xu Z.K, Wu J, Innocent C, Seta P, Nanofibrous poly(acrylonitrile-co-maleic acid) membranes functionalized with gelatin and chitosan for lipase immobilization, *Biomaterials*, 27, 4169-4176, 2006
- Li D, He Q, Cui Y, Duan L, Li J, Immobilization of glucaose oxidase onto gold nanoparticles with enhanced thermostability, *Biochemical and Biophysical research Communications*, 355, 488-493, 2007
- Unuma H., Hiroya M., Ito A., *J. Mater. Sci. Mater. Med*, 18, 987-990, 2007
- Stollner D, Scheller FW, Warsinke A (2002) Activation of cellulose membranes with 1,1' carbonyldiimidazole or 1-cyano-4-dimethylaminopyridinium tetrafluoroborate as a basis for the development of immunosensors. *Anal Biochem* 304:157-165
- Zhao Z.P., Wang Z., Wang S.C., *J.Membr.Sci*, 217, 151-158, 2003
- Jones K.L., O'Melia C.R., *J.Membr.Sci*, 165, 31-46, 2000
- Smith K.A., Colton C.K., Merril E.W., Evans L.B., *Chem.Eng.Progr.Symp.Ser.*, 64, 45, 1968
- Komiyama H., Smith J.M., *AIChE J.*, 20, 1110-1117, 1974
- Deen W.M., *AIChE J.* 33, 1409-1425, 1987
- Bowen W.R., Mohammad A.W., Hilal N., *J.Membr.Sci.*, 126, 91-105, 1997

- Toh Y.H.S., Ferreira F.C., Livingstone A.G., The influence of membrane formation parameters on the functional performance of organic solvent nanofiltration membranes, *Journal of Membrane Science*, 299, 236-250, 2007
- Holownia A.T., A catalytic membrane for hydrolysis reaction carried out in the two-liquid phase system-Membrane preparation and characterization, mathematical model of the process, *Journal of Membrane Science*, 259, 74-84, 2005
- Nakao S.I., Models of membrane transport phenomena and their applications for ultrafiltration data, *J.Chem.Eng.Jpn.*, 15, 200, 1982
- Bradford M.M., A rapid and sensitive method for the quantification of microgram quantities of protein utilizing the principle of protein-dye binding, *Analytical Biochemistry*, 72, 248-254, 1976
- Weatherburn M.W., Phenol-hypochlorite reaction for determination of ammonia, *Anal. Chem.*, 39, 971-974, 1967
- Krajewska B., Zaborska W., The effect of phosphate buffer in the range of pH 5.80-8.07 on jack bean urease activity, *Journal of Molecular Catalysis B: Enzymatic*, 6, 75-81, 1999
- Ravi C.R.K., Punit K.S., Prakash M.D., Arvind M.K., Immobilization of pigeonpea (*Cajanus cajan*) urease on DEAE-cellulose paper strips for urea estimation, *Biotech. Appl. Biochem.*, 39, 323-327, 2004
- Ingmar H.H., Pedro P. Antonia H., The effect of protein- protein and protein-membrane interactions on membrane fouling in ultrafiltration, *J. Membr. Sci.*, 179, 79-90, 2000
- Ladam G., Shaaf P., Decher G., Voegel J.C., Cuisinier F.J.G., Protein adsorption onto auto-assembled polyelectrolyte films, *Biomolecular Engineering*, 19, 273-280, 2002
- Chen J.P., Chiu S.H., A poly(N-isopropylacrylamide-co-N-acryloxysuccinimide-co-2-hydroxyethyl methacrylate) composite hydrogel membrane for urease immobilization to enhance urea hydrolysis rate by temperature swing, *Enzyme and Microbial Technology*, 26, 359-367, 2000
- Goldstein L., Kinetic behavior of immobilized enzyme systems In: Mosbach K (ed). *Methods in enzymology*, vol. 44. Academic Press, New York, pp 397-443, 1976

Liang JF, Li YT, Yang C, "Biomedical application of immobilized enzymes," Journal of Pharmaceuticals Sciences, vol. 89, pp. 979-990, 2000

Ahmad F, "Measuring the conformational stability of enzymes," In: Thermostability of Enzymes, editor: Gupta MN, (Berlin: Springer-Verlag, pp. 96-112, 1993

APPENDIX A

DIMENSIONALIZED MODEL EQUATIONS

1. Dimensionless Parameters

$$C_e^* = \frac{C_e}{C_{Feed}} \quad C_m^* = \frac{C_m}{C_{Feed}} \quad C_F^* = \frac{C_F}{C_{Feed}} \quad C_P^* = \frac{C_P}{C_{Feed}}$$

$$V_F^* = \frac{V_F}{V_{Feed}} \quad V_R^* = \frac{V_R}{V_{Feed}} \quad \delta = \frac{V_{Feed}}{V_m} \quad V_m = AL_m$$

$$z^* = \frac{z}{L_m} \quad t^* = \frac{D_{\infty m} t}{L_m^2} \quad \theta = \frac{K_m}{C_{Feed}} \quad Pe = \frac{J_v L_m}{D_{\infty m}}$$

$$K^2 = \frac{V_{\max} L_m^2}{D_{\infty m} C_{Feed}} \quad Bi_F = \frac{k_{mF} L_m}{D_{\infty m}} \quad Bi_P = \frac{k_{mP} L_m}{D_{\infty m}} \quad D_{Re} = \frac{D_{\infty e}}{D_{\infty m}}$$

2. Dimensionalized the Transport Equations

Species continuity equation for the feed side is written below

$$\frac{d(C_F V_F)}{dt} = -k_{mF} (C_F - C_{Fi})$$

$$C_F \frac{dV_F}{dt} + V_F \frac{dC_F}{dt} = -k_{mF} (C_F - C_{Fi})$$

where, $\frac{dV_F}{dt} = -J_v A$. Then, apply chain rule for the transformation of $\frac{dC_F}{dt}$.

$$\frac{dC_F}{dt} = \frac{d(C_F^* C_{Feed})}{dt^*} \cdot \frac{dt^*}{dt}, \text{ where } \frac{dt^*}{dt} = \frac{D_{\infty m}}{L_m^2}$$

since, those parameters are constants and put out of the differential equation we obtained the dimensionless concentration changed with respect time as follows;

$$\frac{dC_F}{dt} = \frac{D_{\infty m} C_{Feed}}{L_m^2} \frac{dC_F^*}{dt^*}$$

similarly, when the other dimensionless parameters are displaced with appropriately we get following equation,

$$-C_F^* C_{Feed} J_v A + V_F^* V_{Feed} \frac{D_{\infty m} C_{Feed}}{L_m^2} \frac{dC_F^*}{dt^*} = -k_{mF} C_{Feed} (C_F^* - C_{Fi}^*)$$

C_{Feed} in both side of the equation are canceled out, then if we multiply each side of equation by $\frac{L_m}{AD_{\infty m}}$, we obtained

$$\frac{J_v L_m}{D_{\infty m}} C_F^* + \frac{V_{Feed}}{AL_m} V_F^* \frac{dC_F^*}{dt^*} = -\frac{k_{mF} L_m}{D_{\infty m}} (C_F^* - C_{Fi}^*)$$

when we put the appropriate dimensionless parameters into above equation, we obtained the final form of species continuity equation for the feed side completely dimensionless.

$$-(Pe)C_F^* + \delta V_F^* \frac{dC_F^*}{dt^*} = -Bi_F [C_F^* - C_{Fi}^*]$$

Similarly boundary equations can be converted into dimensionless form as given below,

$$\text{B.C.I, at } z=a \quad K_{Ce} Pe C_e^* - (K_{De} \varepsilon_e D_{Re}) \frac{dC_e^*}{dz^*} = -Bi_F (C_e^* - C_{ei}^*)$$

$$\text{B.C.II, at } z=b \quad K_{Ce} Pe C_e^* - (K_{De} \varepsilon_e D_{Re}) \frac{dC_e^*}{dz^*} = K_{Cm} Pe C_e^* - (K_{Dm} \varepsilon_m) \frac{dC_e^*}{dz^*}$$

$$\text{B.C.III, at } z=c \quad K_{Cm} Pe C_e^* - (K_{Dm} \varepsilon_m) \frac{dC_e^*}{dz^*} = K_{Ce} Pe C_e^* - (K_{De} \varepsilon_e D_{Re}) \frac{dC_e^*}{dz^*}$$

$$\text{B. C.IV, at } z=d \quad K_{Ce} Pe C_e^* - (K_{De} \varepsilon_e D_{Re}) \frac{dC_e^*}{dz^*} = Bi_P (C_{ei}^* - C_e^*)$$

VITA

PERSONALITY

Date of Birth :May 3, 1974

Place of Birth:Nevşehir

EDUCATION

2010 **Philosophy of Doctorate (Ph.D.)** İzmir Institute of Technology, Department of Chemical Engineering

2003 **Master of Science (M.S.)** İzmir Institute of Technology, Department of Chemical Engineering

2000 **Bachelor of Science (B.S.)** Ege University, Department of Chemical Engineering

PUBLICATIONS

Guedidi S, Yurekli Y, Deratani A, Déjardin P, Innocent C, Altinkaya S.A, Roudesli S, Yemenicioğlu A, Effect of enzyme location on activity and stability of trypsin and urease immobilized on porous membranes by using layer-by-layer self-assembly of polyelectrolyte, Journal of Membrane Science, 365, 59-67, 2010

PRESENTATIONS

Yürekli Y, Guedidi S, Altinkaya S.A, Yemenicioğlu A, Innocent C, Deratani A, Roudesli S, “Modeling the Performance of Enzyme Immobilized Membranes”, Euromembrane 2009, September 6-10, 2009, Montpellier, France

Yürekli Y, Guedidi S, Altinkaya S.A, Yemenicioğlu A, Innocent C, Deratani A, Roudesli S, “Preparation and ,Characterization of Urease Immobilized Ultrafiltration membranes”, Euromembrane 2009, September 6-10, 2009, Montpellier, France

MEMBERSHIP

Chamber of Chemical Engineers, Aegean Branch Management Department Member